INVESTIGATION OF EXTENDABLE NOZZLE CONCEPTS

Charles N. Scott

Robert W. Nordlie

William W. Sowa

Goodyear Aerospace Corporation
Akron, Ohio

Final Report GER 15240

November 1972

NATIONAL AERONAUTICS AND SPACE ADMINISTRATION

George C. Marshall Space Flight Center

Huntsville, Alabama

INVESTIGATION OF EXTENDABLE NOZZLE CONCEPTS

Charles N. Scott

Robert W. Nordlie

William W. Sowa

Goodyear Aerospace Corporation

Akron, Ohio

FOREWORD

This Final Technical Report covers work performed under Contract NAS 8-21476. This contract was initiated 1 October 1968. The design and fabrication portion of the contract was completed 30 June 1971. The testing portion was completed 3 August 1972. This manuscript was released by the authors in November 1972 for publication as a Goodyear Engineering Report.

This contract with Goodyear Aerospace Corporation, Akron, Ohio was initiated by the National Aeronautics and Space Administration, George C. Marshall Space Flight Center, Huntsville, Alabama, 35812. It was accomplished under the technical direction of Mr. D. E. Pryor, S & E-ASTN-PPB.

Mr. C. N. Scott of Goodyear Aerospace Corporation acted as project engineer on this program. He was assisted by Mr. R. W. Nordlie. Mr. J. T. Harris was responsible for the Airmat weaving operations, Mr. W. W. Sowa was responsible for the thermal and Flow Analysis, and Mr. N. C. Costakos was responsible for the Structural Analysis.

ABSTRACT

This report summarizes the work performed on Contract NAS 8-21476. The objective of this program was to perform preliminary research and technology toward the development of a transpiration cooled inflatable nozzle extension. The J-2 engine of the Saturn-Apollo launch vehicle was selected as a design application test-bed to provide realistic operational parameters and a possible hot firing demonstration. The nozzle extension attached at the 27.5 to 1 area ratio of the basic J-2 nozzle exit and extended to an area ratio of 48 to 1. The final nozzle extension design as evolved during this effort utilized conically woven stainless steel Airmat* as the major construction material. Model and full-scale nozzle extensions were fabricated and tested although an actual J-2 hot firing demonstration was not possible due to the lack of a proper altitude test opportunity.

*T.M., Goodyear Aerospace Corporation, Akron, Ohio

TABLE OF CONTENTS

LIST OF ILLUSTRATIONS

LIST OF TABLES

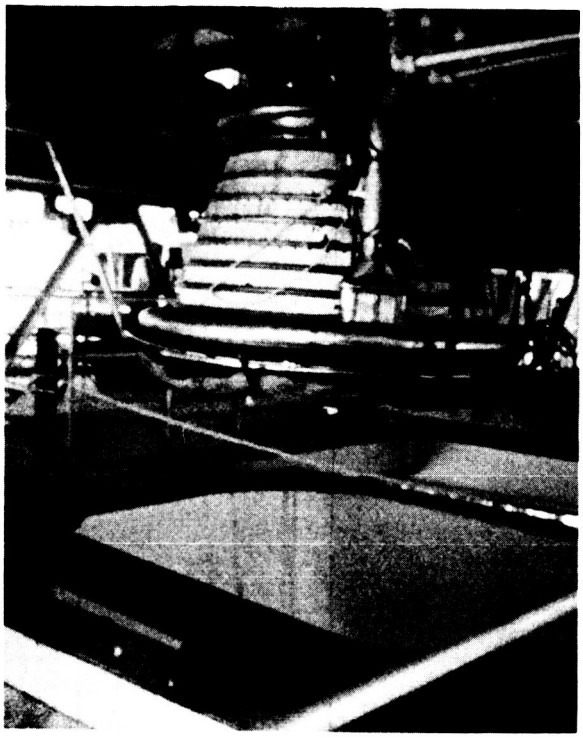

RETRACTED POSITION

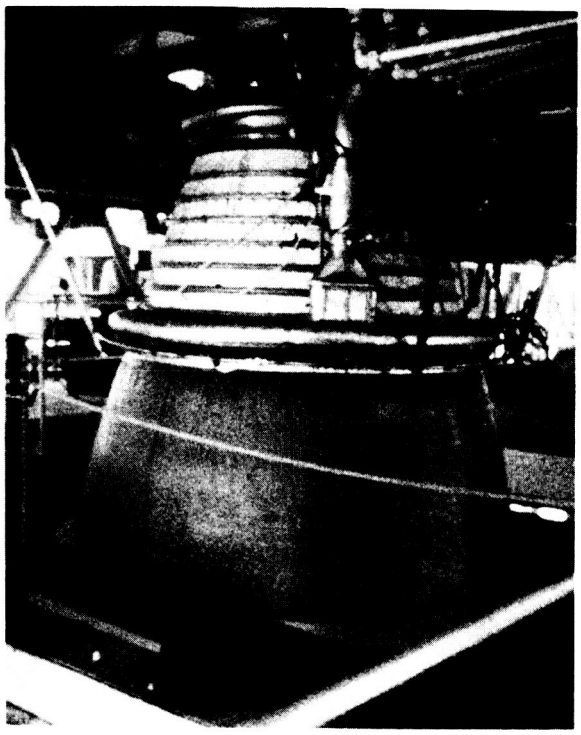

EXTENDED POSITION

Airmat Extendable Nozzle - J-2 Rocket Engine Application

SECTION I

SUMMARY

Goodyear Aerospace Corporation (GAC) designed, developed, and fabricated an extendable transpiration cooled nozzle extension applicable to the J-2 Rocket Engine. Cold Flow and deployment tests were performed by NASA, at the George C. Marshall Space Flight Center, with the nozzle extension installed on a J-2 Engine test facility.

The nozzle extension was fabricated using a woven stainless steel Airmat* material. The Airmat was fabricated into a conical shape and the outer surface was coated with a silicone elastomer to make it gas tight. The inner surface which had been woven to a controlled porosity was not coated.

The design concept was to pressurize the Airmat nozzle extension utilizing the exhaust gas from the rocket engine pump drive turbine. The gas would flow through the inner surface of the Airmat and cool this surface from the hot rocket engine exhaust gases.

The nozzle extension was designed to be mounted to the existing J-2 nozzle. After installation it can be packaged by rolling up the nozzle extension around the lower extremes of the existing fixed nozzle as shown in Figure 61. During space flight the nozzle extension would be automatically deployed during the engine start as the turbine exhaust pressurant enters the rolled up extension package and unfurls it as shown in Figure 61, Views B, C, D, and E. The efficiency of the rocket engine in space flight will be increased by virtue of the higher expansion ratio.

The present J-2 nozzle has an expansion ratio of 27.5 to 1 at its exit. The nozzle extension fabricated increased the exit expansion ratio to 48 to 1. Studies were also conducted showing that the expansion ratio can be increased to 55 to 1 or more.

The factors that limit the nozzle extension length are the supply of pressurizing gas and the technology of weaving conical Airmat. The pressurizing gas flow rate for the J-2 Rocket Engine was 5.22 pounds per second. Increasing the flow rate would allow longer nozzle extensions to be operated. Development of an Airmat loom capable of weaving wider conical Airmat with a tighter inner face porosity would also make longer nozzle extensions practical.

The basic design involved control of the Airmat inner face porosity so that the required Airmat internal pressure could be achieved with the available gas supply. The Airmat nozzle extension carries the thrust loads from the rocket engine exhaust gases forward to the existing nozzle. To eliminate any compression stresses in the Airmat, the nozzle extension must be pressurized so that the combined stresses are tension stresses. The pressure actually achieved for the specified gas supply is a function of the Airmat inner face porosity.

*T.M., Goodyear Aerospace Corporation, Akron, Ohio

The desired porosity requirement was 1.0 percent or lower and a development weaving program was conducted. Laboratory tests indicated that porosities of 1.10 percent at 10 psi pressure and 0.95 percent at 7 psi pressure were achieved. It was concluded that tighter weaves could be achieved by refining the weaving techniques and equipment.

The development weaving program included the development of the techniques for weaving of conical Airmat. With this technique, the nozzle extension can be fabricated from one piece of Airmat. This advanced the state-of-the-art in fabrication as previous nozzle extensions have been fabricated by tailoring flat Airmat to form a cone.

The technical achievements performed on this program are reported in detail in this report. The program plan included preliminary design, laboratory testing, testing of a sub-scale model, development weaving, final design, fabrication, and testing of a full-scale nozzle extension. Several supplemental investigations were also conducted and are summarized in this report.

The deployment testing of the full-scale nozzle extension was quite successful. The nozzle extension was installed on the J-2 nozzle and rolled-up over the nozzle. The nozzle extension deployed satisfactorily from this position. A total of eleven deployment tests were conducted.

SECTION II

INTRODUCTION

Goodyear Aerospace Corporation has, for several years, conducted a continuing research, development and fabrication program for high expansion ratio, packageable nozzle extensions for both liquid and solid rocket engines. Extensions have been fabricated and tested for the Titan II second-stage engine, the Aerobee Rocket Engine, and the Genie and Skybolt solid propellant rocket motors. All of these nozzle extensions used an ablative elastomeric liner supported by an internally pressurized textile Airmat supporting structure. These nozzle extensions had expansion ratios ranging from 40 to 1 for the Aerobee engine to 100 to 1 for the Titan II second-stage engine.

The test of these extensions showed that the concept was feasible with the three problem areas requiring further development; (1) a more effective elastomeric ablative material, (2) nozzle extension attachment development, and (3) weight reduction.

Recognizing the potentials of an effective high expansion ratio nozzle extension for space applications, the National Aeronautics and Space Administration, Marshall Space Flight Center, Huntsville, Alabama and Goodyear Aerospace Corporation met to discuss nozzle extensions that did not employ an insulation liner on the inner wall. These discussions resulted in the evolution of a concept in which a nozzle extension would be fabricated from stainless steel Airmat. By using the gas exhausted from the rocket engine propellant pump drive turbine, the nozzle extension would be pressurized. The inner wall of the nozzle extension would be cooled by the mass transfer of the pressurizing gas through the porous inner wall of the nozzle extension. Before embarking on a full-scale nozzle extension development program, it was necessary to ascertain the feasibility of the concept.

A program was initiated with the North American Rockwell Corporation, Rocketdyne Division, Canoga Park, California for the first step in establishing feasibility of the transpiration cooling concept. The program was divided into two phases. The first phase was a design phase and the second was a full-scale nozzle extension fabrication phase in which a full-scale extension having a 55 to 1 expansion ratio was to be fabricated and demonstration tested on the J-2X rocket engine. Phase I was authorized and started on 19 October 1967 and completed on 31 December 1967. Phase II was deleted in favor of Contract NAS 8-21476.

During the Phase I Program, a preliminary design of the nozzle extension along with supporting design testing, stress analysis and thermal analysis was completed. A major part of this effort was a weaving investigation in which the Goodyear Aerospace development loom was set up and sample material of various weave patterns woven for testing. These samples were then tested under cold flow conditions to establish the porosity of the woven material. The samples were then hot fire tested using a small oxygen-hydrogen rocket engine to establish the thermal characteristics of the woven material and to verify the flow and thermal analysis predictions. These tests proved the

feasibility of pursuing the development of the full-scale extensions. For a complete discussion of this effort, see Reference 1.

Subsequent to this effort, the National Aeronautics and Space Administration, George C. Marshall Space Flight Center, Huntsville, Alabama prepared a request for proposal for a 13-month, two-phase program. Phase I was a design and design testing phase and Phase II was a fabrication phase for two full-scale nozzle extensions for the J-2S engine. One of these nozzle extensions was to be a half length and the other a full length one. The full length nozzle was to attach to the J-2S engine at an expansion ratio of 40 to 1 and extend to an expansion ratio of 80 to 1. A proposal, Reference 2, was submitted by and a contract, NAS8-21476, awarded to Goodyear Aerospace to proceed with the program.

A scale model nozzle extension was fabricated and tested on a hydrogen-oxygen engine. This testing further proved the feasibility of the packageable, transpiration cooled nozzle extension. This test was scaled and conducted at conditions matching the operating conditions of the full scale J-2S engine.

The results of the effort expended on the Phase I program pointed up certain areas for product improvement and the need to conduct certain tests to substantiate theory used in the thermal analysis and additional effort to complete the extension design. As a result, Phase II was restructured and implemented to add the additional tasks.

Midway through the program the extendable nozzle application was changed from the J-2S to the J-2 rocket engine by NASA direction.

Two nozzle extension assemblies and one manifold assembly were fabricated and delivered to NASA for testing. Cold flow tests and deployment tests were subsequently performed.

This report summarizes the program effort and results for the program. A complete bibliography is furnished for use should the reader wish detail information on the specific tasks. This report summarizes all contract effort during the period from 3 October 1968 through completion.

SECTION III

EXTENDABLE NOZZLE DESIGN

A. J-2S NOZZLE EXTENSION DESIGN

1. General

During an initial effort performed under contract with North American Rockwell Corporation, Rocketdyne Division, a design of a 55 to 1 expansion ratio nozzle extension for the J-2X Rocket Engine was evaluated. This effort included drawings, structural analysis and thermal analysis. A complete description of this effort was included in Reference 1.

In the interim between the conclusion of this original evaluation and the establishment of this contract, the J-2X engine effort evolved into the preliminary development of an advanced version of the J-2 basic engine known as the J-2S.

The basic concept was maintained for the J-2S Rocket Engine; but, due to differences in configuration and operating parameters between the J-2X and J-2S engines, certain changes in the basic design were required. These changes are described in the following paragraphs.

2. J-2S Nozzle Design Data

The basis for the J-2S nozzle extension design was data supplied by NASA and shown in Table I. Included with this data were plots of nozzle exhaust gas heat transfer coefficient versus axial distance from the J-2S exit plane and engine exhaust pressure versus axial distance from the J-2S exit plane. These plots are shown in Figurs 1 and 2 respectively.

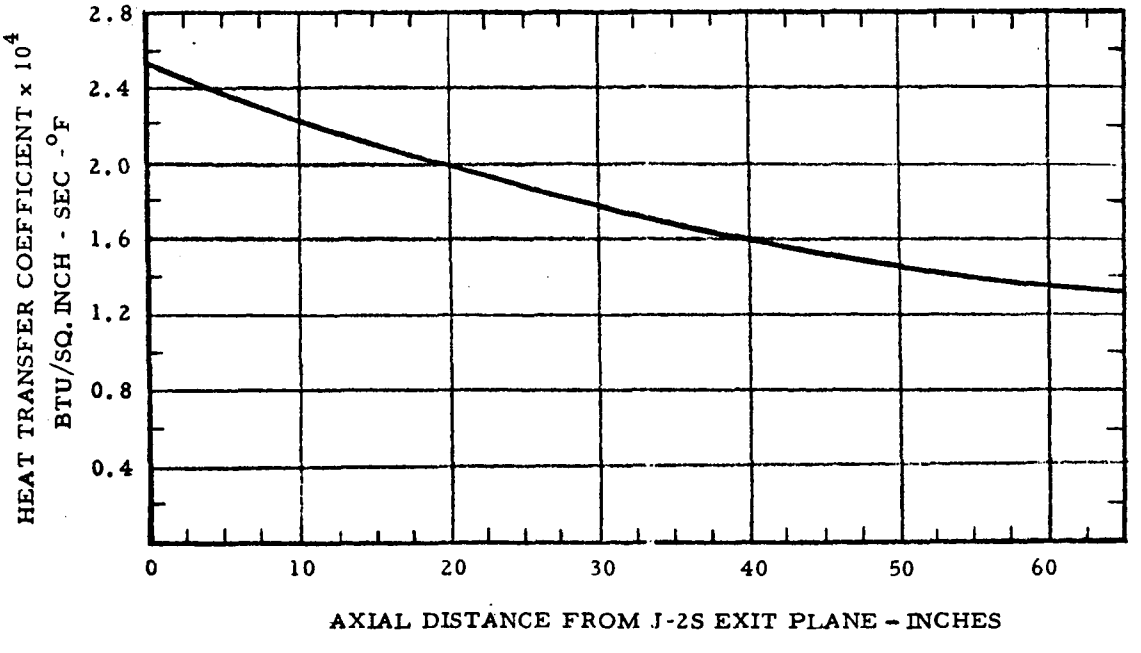

Figure 1. J-2S Nozzle Exhaust Gas Heat Transfer Coefficients (Without transpiration cooling)

Table I. J-2S Nozzle Design Criteria

Item	Description
1. Cooling Method	Transpiration Cooling
2. Coolant and Nozzle Pressurant for Mainstage Operation	Turbine Exhaust Gas
3. Turbine Exhaust Gas Characteristics:	
Composition	50% (wt) H_2 - 50% (wt) H_2O
Molecular Weight	3.74 LBM/LB-MOLE
Specific Heat @ Constant Pressure	2.02 BTU/LBM-°F
Specific Heat Ratio	1.37
Flowrate	9.0 LBM/SEC *
Total Temperature	600°F
Total Pressure (Maximum)	20 PSIA
4. Thrust Chamber Combustion Gas:	
Composition **	4% (wt) H_2 - 96% (wt) H_2O
Molecular Weight **	13.507 LBM/LB-MOLE
Specific Heat @ Constant Pressure ***	0.95 BTU/LBM-°F
Specific Heat Ratio (Effective)	1.17
Flowrate	602 LBM/SEC
Adiabatic Wall Temperature (Effective)	5700°F
5. Nozzle Exhaust Heat Transfer Coefficients	Figure 1
6. Thrust Chamber Combustion Gas Pressure Distribution on Nozzle Inner Wall Surface	Figure 2
7. Nozzle Deployment Gas:	
Composition	GH_e or Turbine Exhaust Gas
Temperature	-300°F (GH_e) or 600°F (Turbine Exhaust Gas)
Maximum Allowable Deployment Pressure Inside Nozzle	50 PSIA
8. Nozzle Minimum Temperature Before Deployment and Prior to Engine Restarts	-60°F
9. Nozzle Maximum Deployment Time	2 seconds
10. Maximum Allowable Loads on Engine Due to Nozzle Deployment	
Total Longitudinal (Direct Aft)	7500 LB_f
11. Engine Gimbaling Requirements:	
Maximum Angular Acceleration	24.5 RAD/SEC^2
Maximum Angular Velocity	$\pi/6$ RAD/SEC
Gimbal Arm Length	9.7 Feet (From Gimbal Point to J-2S Thrust Chamber Exit Plane)
12. Nozzle Instrumentation	
Thermocouples	2 Rows (90° Apart) of 10 Chromel/Alumel T/C's uniformly spaced along length of nozzle for measuring porous inner wall hot surface temperatures
Pressure Taps	2 Rows (90° Apart and Opposite T/C Rows) of 10 pressure taps uniformly spaced along length of nozzle outer wall for measuring internal (turbine exhaust gas) pressures

*LOX Turbine Bypass Flow (3.7 LBM/SEC) is not included as part of this Flowrate

**Evaluated at the thrust chamber combustion gas static temperatures and pressures within the nozzle

***Effective value to be used in heat transfer analysis.

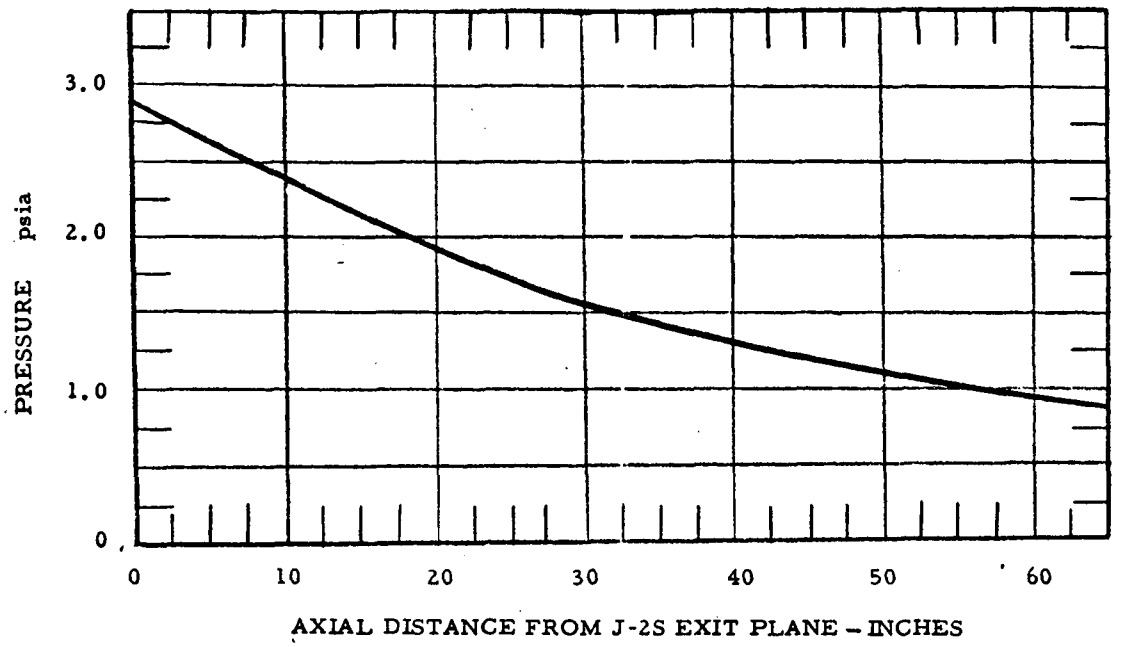

Figure 2. J-2S Nozzle Exhaust Gas Static Pressure Distribution

3. J-2S Nozzle Extension Design Description

a. Geometry. The J-2S nozzle extension is basically the same as that described in Reference 1 for the J-2X extension with certain exceptions. These changes affect the extension configuration only. The extension attachments to the engine and manifold remain the same.

The extension is a right-truncated cone having a minor diameter of 78.44 inches, a major diameter of 109 inches, and a length of 61 inches. The J-2S nozzle extension half-angle is 13°54' (the J-2X extension half angle was 14° 03'). The extension attaches to the J-2S thrust chamber at an expansion ratio of 40 to 1 (27.5 to 1 for the J-2X extension) and extends to an exit expansion ratio of 80 to 1 (55 to 1 for the J-2X extension).

b. Design. The Airmat cone wall thickness is 4 inches. Since the above dimensions are for the inner nozzle face, the outer face dimensions will be correspondingly larger.

Flat Airmat was used in the design. This required that the nozzle extension be fabricated utilizing eight gores. Each gore was slit on it's outer face at six locations to allow for the larger outer surface circumference and the slits closed by tape cut from the woven parent material.

c. Airmat Description. The Airmat configuration for the J-2S nozzle extension design is as follows:

Warp: 90 filament yarn, 112 ends per inch

Fill: 300 filament yarn, 80 ends per inch

Drops: 300 filament yarn, 41 ends per square inch

Airmat Depth: 4 inches

The weight of the Airmat material is dependent on the yarn size, the number of yarns woven per inch in the warp and fill directions, the drop yarn density, and the Airmat depth.

The individual stainless steel filaments are approximately one-half mil in diameter. Calculating the yarn volume per unit length and using 0.28 lbs/in^3 as the weight of stainless steel, the following data results.

90 filament yarn = 16,900 feet/pound

300 filament yarn = 5,050 feet/pound

The following Airmat weight results.

$$\text{One face} = \frac{12 \times 112}{16{,}900} + \frac{12 \times 80}{5050}$$

$$= 0.08 + 0.19$$

$$= 0.27 \text{ pounds per square foot}$$

$$\text{Drop Yarns} = \frac{12 \times 12 \times 41 \times 4}{5050}$$

$$= 0.46 \text{ pounds per square foot}$$

$$\text{Total} = 0.27 + 0.46 + 0.27$$

$$= 1.00 \text{ pound per square foot}$$

Thus the Airmat weight is approximately one (1) pound per square foot.

4. J-2S Nozzle Extension Design Modifications

The design of the J-2S nozzle extension was later modified. Two major design changes were incorporated.

The first modification involved the design and fabrication of a nonrigid manifold for distribution of the pressurizing gas to the nozzle extension. The design of the nozzle extension mounting rings was also affected by this modification.

The second modification involved weaving of conical Airmat instead of flat Airmat. Conical woven Airmat allowed fabrication of the nozzle extension from one piece of Airmat. This change required initiation of a conical Airmat weaving task.

a. Pressurization Gas Distribution Manifold. During the design effort on the J-2S nozzle extension, it was planned to use a manifold that had been designed and fabricated for the J-2X engine. In order to use this manifold on the J-2S engine, it was found that extensive modification would be required to adapt it to the J-2S engine and the nozzle extension. As a result of this finding, a task to design and fabricate a manifold for the J-2S engine and nozzle extension was added to the program.

The manifold consisted of a woven stainless steel cloth formed into a torus. The cloth torus was attached to a supporting structure which also provided for the attachment of the torus to the J-2S engine thrust chamber and provided an attachment of the nozzle extension to the manifold. The outer face of the nozzle extension attached to the manifold through a stainless steel angle bolted to the mounting structure. The inner face of the extension attached to the thrust chamber by means of a stainless steel angle ring bolted to the thrust chamber exit flange. Figure 3 shows the extension and manifold attachment to the J-2S thrust chamber.

b. Conical Weaving of J-2S Nozzle Extension. The normal method of producing Airmat is to weave it in a flat configuration to the width and thickness desired. To fabricate a conical shape using flat Airmat requires that gores be cut to

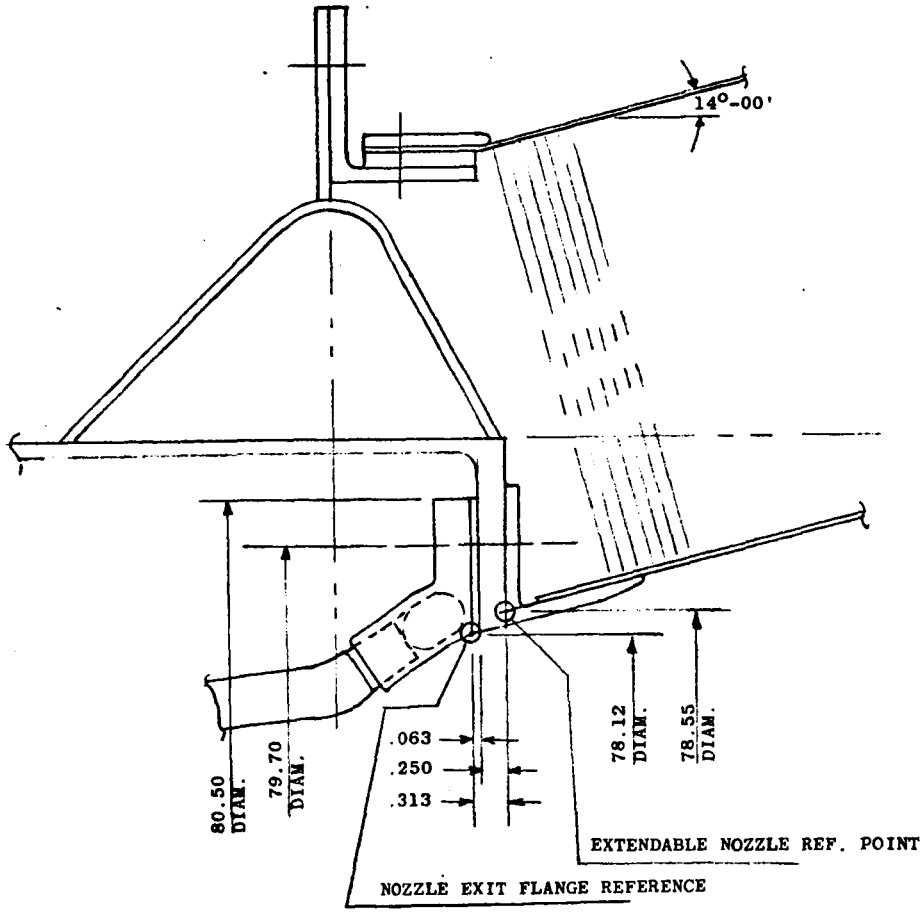

Figure 3. J-2 Nozzle Reference Point Location

form the cone. To adjust the inner and outer Airmat faces for the difference in circumference requires a number of slits in the outer face, which when the slit width is established, must be closed with tape cut from the Airmat face material. In addition, an inner and outer joint is required at the juncture of the gores.

To reduce fabrication complexity and increase operational reliability, the GAC Development Loom was modified to provide the capability to weave the nozzle extension Airmat conically in one piece. This eliminated all joints except one inner and one outer joint where the ends of the Airmat were joined.

5. Design Support Test Data

During the design of the J-2S nozzle extension,several test programs were conducted to substantiate the design and the structural analysis. The test programs were as follows:

a. Yarn Tensile Tests

b. Airmat Tensile Tests

c. Coating Material Tests

d. Airmat Porosity Tests

e. Welding Investigation

a. Yarn Tensile Tests. Three types of yarn were used to weave the Airmat. These types are identified as follows:

Warp: Number 19: 12/90/2Z Type 304 Stainless Steel with 1% PVA Coating

Fill: Number 20: 12/300/2Z Type 304 Stainless Steel Uncoated

Drops: Number 21: 12/300/2Z Type 304 Stainless Steel with 1% PVA Coating

Yarn was taken from five spools selected at random and fifteen tests were performed on each of the above three types of yarn. Three tensile and three loop tensile specimens were tested from each spool.

The tests were conducted at ambient temperature on an Instron tensile test facility. The specimen gage length was six inches and the strain rate was 10 percent per minute. The results of the tests are summarized in Table II.

Loop tensile tests are performed using two pieces of yarn. Both ends of one piece of yarn are inserted in one jaw of the Instron tester. The second piece of yarn is looped through the first piece and both ends are inserted in the other jaw. The total load in pounds to fail the test setup is reported. Failures occur at the loop of one yarn to the other.

b. Airmat Tensile Tests. Tensile tests were conducted to determine the Airmat face cloth strengths. After weaving, six specimens were prepared for warp tensile tests and six specimens were prepared for fill tensile tests. The warp yarns were 12/90/2Z with 112 yarns per inch. The fill yarns were 12/300/2Z with 80 yarns per inch.

Table II. Yarn Tensile Tests

Yarn No.	Ult. Tensile Load, lbs.	Ult. Loop Tensile Load, lbs.	Elongation At Failure, %
19	5.60	2.51	1.27
20	11.08	7.75	1.08
21	12.00	4.33	1.18

NOTE: Values are averages of fifteen tests

Ravelled test specimens, one-inch wide, were prepared. The tests were conducted using the Instron Tensile Test Facility. The specimen gage length was four inches and the strain rate was 15 percent per minute. Test results are reported as pounds per inch of width.

An average ultimate strength of 225 pounds per inch was obtained in the warp direction, and 943 pounds per inch was obtained in the fill direction.

c. Coating Material Tests. The exterior surface of the J-2S nozzle extension requires an elastomeric coating to act as a gas barrier for prevention of leakage of the coolant gas through the exterior face of the extension. The elastomer requirements were that it would satisfactorily perform under operating conditions of 20 PSI pressure in a 625°F temperature environment.

It must remain flexible after exposure to this pressure,and temperature, and must have good adhesion to the Airmat surface. The elastomer must be capable of being applied by brushing or similar methods.

A survey of available coatings was made. Based upon manufacturers data and discussions with manufacturers' representatives, a silicone elastomer designated as S-2288 and manufactured by Dow-Corning Corporation, Midland, Michigan was selected for test.

Two specimens were tested. The test specimens were placed in a fixture which allowed the specimen to be pressurized on the uncoated side. A flowrater was installed in the pressurization line to measure leakage should it occur. The test fixture was placed in an oven and the specimen pressurized to 10 PSI. The oven was then turned on and the temperature increased to 625°F. Stabilization of the temperature required 45 minutes. The pressure was then increased to 20 PSI and held for 2 minutes. After 2 minutes the pressure was increased to 25 PSI and held for 5 minutes. The test was thus concluded and the specimen was removed for visual inspection.

Two specimens were tested as described. Neither specimen leaked or delaminated. Visual inspection after testing showed that the coating remained rubbery and had no visual degradation.

As a result of these tests, the S-2288 elastomer was adopted as the coating material to be specified in the J-2S nozzle extension design.

d. Porosity Tests. Previous tests to determine the porosity of GAC woven metal fabric for use in the Airmat nozzle extension program were conducted using nitrogen gas. These tests were reported in Reference 1. Similar tests were conducted in this program using hydrogen gas and the same Airmat material.

The actual testing was conducted at GAC's Wingfoot Lake Hydrogen Test Facility. The hydrogen gas supply was a trailer-tank having a capacity of 3000 cubic feet. The transpiration gas flow was measured by two flowraters each equipped with a shut-off valve. The gas supply to the flowraters was regulated with a two-inch throttle valve. Gas pressure was read on two pressure gages, one installed forward of the flowraters and one connected to the specimen test fixture. Gas temperature was also monitored at the flowraters and at the test fixture.

The test specimen, Specimen No. 85 as described in Reference 1, was placed in the test fixture which had a four-inch square opening. An airtight seal was achieved by coating the clamping surfaces with an RTV silicone rubber sealant material. The entire system was checked for leaks prior to testing.

The actual test readings are presented in Table III. These readings are converted from SCFM, flowrater reading, to cubic feet per minute of hydrogen in this table. Two runs were conducted. The first run measurements were recorded at 3.2, 7.4 and 12.2 PSIG chamber pressures. The second run recordings were at 13.7, 17, and 20 PSIG. On the second run, measurements at 13.8 PSIG were recorded as the pressure was being reduced.

The flow rate through the test specimen was calculated using the following equation when the flow through the test specimen is subsonic.

$$\dot{W} = \frac{A P_1 \sqrt{2 g J}}{R} \left\{ \frac{C_P}{T_1} \left[\left(\frac{P}{P_1}\right)^{2/K} - \left(\frac{P}{P_1}\right)^{\frac{K+1}{K}} \right] \right\}^{1/2}$$

and by the following equation when the flow through the test specimen is sonic.

$$\dot{W} = A P_1 g \sqrt{\frac{K \left(\frac{2}{K+1}\right)^{\frac{K+1}{K-1}}}{\sqrt{K g R T_1}}}$$

Dividing both sides of the equations by the surface area A_s establishes a relationship by which gas flow rate per unit surface area is a function of the Airmat pressure (P_1), the back pressure (P), the Airmat gas temperature (T_1),

Table III. Porosity Test Data

PSIG Spec.	Temp. °F At Spec.	PSIG At Flowrater	Temp. °F At Flowrater	PSIG At Trailer	SCFM Air	X_p	X_t	$X_{sp\ gr}$	SCFM H_2	R	CFM H_2
3.2	23	5.0	25	125	18.0	0.903	0.955	0.264	107.61	0.744	80.06
7.4	25	11.5	28	125	28.6	0.815	0.957	0.264	186.98	0.607	113.49
12.4	17	13.5	19	125	51.0	0.738	0.949	0.264	275.83	0.488	134.61
13.7	14	15.0	17	125	53.5	0.722	0.946	0.264	296.70	0.462	137.08
17.0	11	17.0	14	125	59.0	0.684	0.943	0.264	346.48	0.412	142.75
20.0	8	22.5	11	125	64.5	0.651	0.940	0.264	399.25	0.374	149.32
13.8	7	15.0	10	125	53.5	0.722	0.939	0.264	298.91	0.454	135.71

Conversion from SCFM Air to CFM Hydrogen

$$(1)\quad SCFM_{H_2} = \frac{SCFM\ (Air)}{X_p\ X_t\ X_{sp\ gr}\ X_F}$$

$$(2)\quad CFM_{H_2} = SCFM_{H_2}\ \frac{(14.7)\ (460^\circ + F^\circ)}{530\ (14.7 + PSIG)} = SCFM_{H_2}\ X\ R$$

and the porosity (A/A_s). The porosity ratio (A/A_s) is defined as the open area in the fabric divided by the surface area of the fabric and is unknown. During the test, the Airmat pressure, the back pressure, and temperature were measured as was the gas flow rate. Therefore, evaluating the above equations as a function of the gas properties and upstream conditions and then superimposing the measured test data points permits one to estimate the effective porosity of the test specimen. The calculated and measured data is presented in Figure 4. The calculations were based on a gas temperature of 70°F.

Six test points were obtained, three points under subsonic flow conditions and three test points at sonic flow conditions. The back pressure in each case was the ambient surface pressure. Thus the gage pressure along the abscissa is the pressure differential across the test specimen. The range chosen encompasses the pressure range expected in the actual J-2S nozzle application.

The test data when plotted in Figure 4 indicates that the effective porosity varied from approximately 0.007 at a pressure differential of 3 psig to 0.010 at 20 psig. The correlation between theoretical calculations and the test data is considered to be quite good.

The effective porosity appears to increase with the test pressure. The theoretical porosity curves were developed using the term C_dA as a constant over the range of pressures. Apparently the physical value of C_dA increases with pressure. Theoretical calculations do not compensate for this consideration.

An objective of this test program was to compare the flow data reported in Reference [1] for nitrogen gas with flow data obtained in this test program

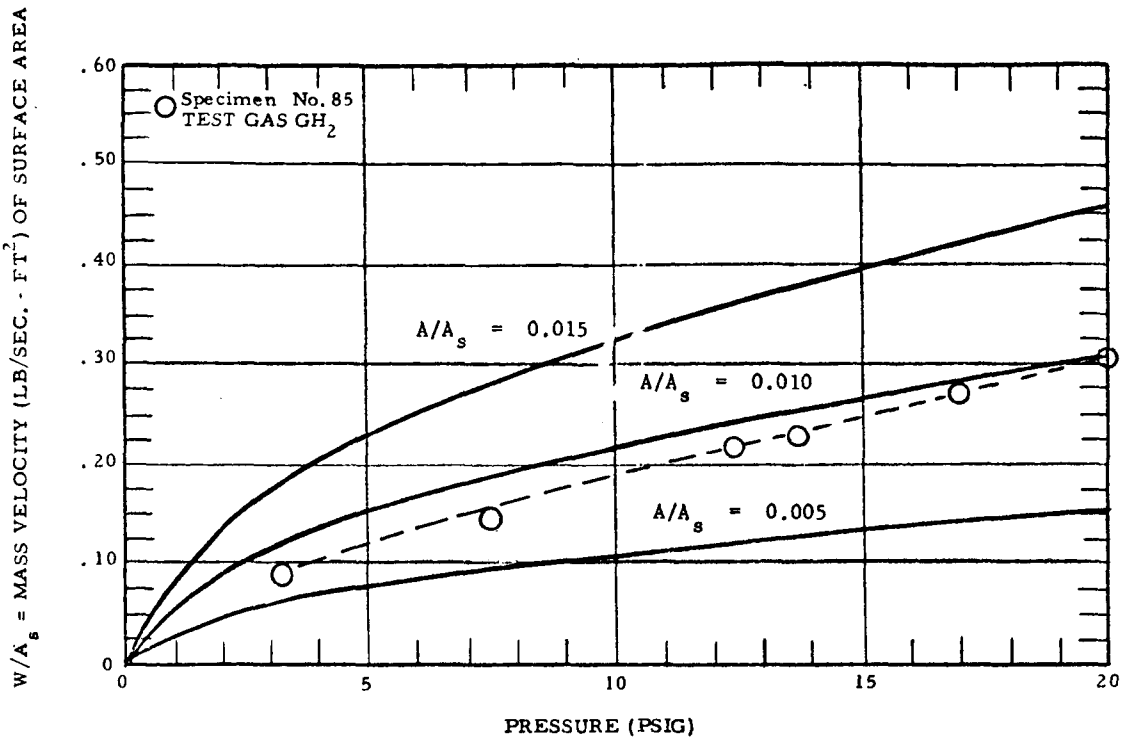

Figure 4. Mass Velocity vs Airmat Pressure

for hydrogen gas. In both cases the test specimens were of the same material. Only sonic flow data was recorded during the nitrogen gas test series. The test data also indicated a linear increase in the porosity as the pressure increased. The porosity in the nitrogen test series varied from 0.012 to 0.014 in the 13 to 20 PSI range. The test data of the two test series correlate quite well with the theoretical calculations. This information was used in the thermal analysis of the J-2S nozzle extension and for the sub-scale test model.

e. Welding Investigation. In connection with the design of the J-2S Nozzle Extension, a resistance welding investigation was conducted to establish the joining details applicable to the nozzle design. A welding schedule was established that provides joint strengths that satisfy nozzle structural strength requirements.

The design of the J-2S nozzle extension is such that welding equipment that could be used is generally limited to the type capable of making welds from one side of the material. This limits available equipment to two types of Weldmatic capacitor-discharge power supplies, 45 and 160 watt-second, used in conjunction with either a light-duty or heavy-duty hand probe. It was determined that either of the two power supplies would perform satisfactorily. The heavy-duty hand probe was preferred over the light-duty probe.

Butt and lap type joints were compared. The strength of the welded butt joint was in general higher than the strength of the welded lap joints. Butt type joints were adapted.

Prior to establishing the details of the weld joint, control strength data was obtained. The material for testing was obtained from Airmat woven during a previous program. Ten specimens, five in the warp direction and five in the fill direction, were tested in the GAC Instron test facility. One-inch wide ravelled strip tensile specimens were prepared. The warp specimens were tested using a six-inch gage length and a strain rate of ten percent per minute. The fill specimens were tested using a four-inch gage length and a strain rate of fifteen percent per minute. The following average test results were obtained.

Warp Specimens:	Ultimate tensile strength	=	260 lbs/inch
	Elongation at failure	=	9.2%
	Tangent Modulus	=	5700 lbs/inch
Fill Specimens:	Ultimate tensile strength	=	731 lbs/inch
	Elongation at failure	=	2.4%
	Tangent modulus	=	35,900 lbs/inch

The strength requirements of the welded joints were calculated and established from the structural analysis data of Reference 8. The weld strength requirements were 47 pounds per inch in the warp direction and 127 pounds per inch in the fill direction. The fill direction applies to the circumferential direction of the J-2S nozzle extension. A load factor of safety requirement of 1.5 was applied to the strength requirement resulting in the following strength requirements.

Warp Direction	61 pounds per inch
Fill Direction	191 pounds per inch

Several criteria were investigated to establish the weld details. They included welding force, welding energy, number of weld rows, and number of spots per inch per row. It was first established that two rows of welds provided the most efficient joint. After a series of tests involving the other three variables, it was concluded that a weld force of nine pounds and a weld energy of 15 watt-seconds resulted in the best strength. Forty spots per inch per row was determined to be the most efficient weld spacing.

The weld specimens were all tested using a Detroit Bench Tester. The following room temperature weld joint strengths were obtained.

Warp Direction	148 pounds per inch
Fill Direction	312 pounds per inch

These weld strengths were corrected for the elevated temperature strength ratio with the following elevated temperature joint strength resulting.

Warp Direction	97 pounds per inch
Fill Direction	205 pounds per inch

These values are higher than the required values which have a 1.5 load safety factor included.

This investigation concluded that satisfactory weld strengths were achievable. It also established the joint details adopted on the design drawings.

During fabrication of the full-sized nozzles, the actual weld strengths obtained were checked during the welding process and the weld schedule was adjusted accordingly.

B. SUBSCALE NOZZLE DESIGN

1. General

During the effort on the J-2X engine extension design, thermal tests of the woven stainless steel Airmat specimen were conducted. These tests were designed to prove feasibility of the transpiration cooling concept (see Reference 1 for details of this effort). It was concluded from these test results that the concept was feasible but additional testing should be conducted on a rocket facility that more closely duplicated the J-2S engine operating conditions. It was further recommended that a smaller scale nozzle extension than that proposed for the J-2S engine be fabricated and tested. This action would allow substantiation of all design objectives before fabrication of a full-scale extension for the J-2S engine. Based upon these recommendations, NASA made available a test facility at the George C. Marshall Space Flight Center employing a hydrogen-oxygen rocket engine.

2. Design Data

The operating parameters of the test engine, designated as the 4-K engine, were furnished by NASA and are tabulated in Table IV.

Table IV. 4-K Engine Design Criteria

Item	Parameter
Nozzle Throat Diameter	1.75 inches
Nozzle Exit Diameter	5.15 inches
Propellant	Oxygen-Hydrogen
Combustion Chamber Pressure	600 to 1000 PSIA
Combustion Chamber Temperature	6200°R
Mixture Ratio (O/F)	5
Ratio of Specific Heats	1.25
Weight Flow Rate	10.7 lbs/sec at 1000 PSIA

In addition to the operating data, NASA supplied a complete set of 4-K engine design drawings. Using these data, a scale model nozzle extension was designed.

3. Nozzle Extension Geometry

The scale model extension was a right circular truncated cone having a half angle of thirteen degrees fifty-four minutes. It was decided that the scale extension would cover the range of expansion ratios for both the J-2X and J-2S engines. This then dictated that the scale extension sould attach to the 4-K engine nozzle at an expansion ratio of 27.5 to 1 (J-2X design) and extend to an exit expansion ratio of 80 to 1 (J-2S design).

From the geometry of the 4-K engine, the exit of the thrust chamber was at an expansion ratio of 8.72 to 1 (exit diameter - 5.15 inches). It was, therefore, necessary to fabricate an adapter section which extended the thrust chamber exit from 8.72 to 1 to 27.5 to 1. This adapter was fabricated by NASA. See Figure 5.

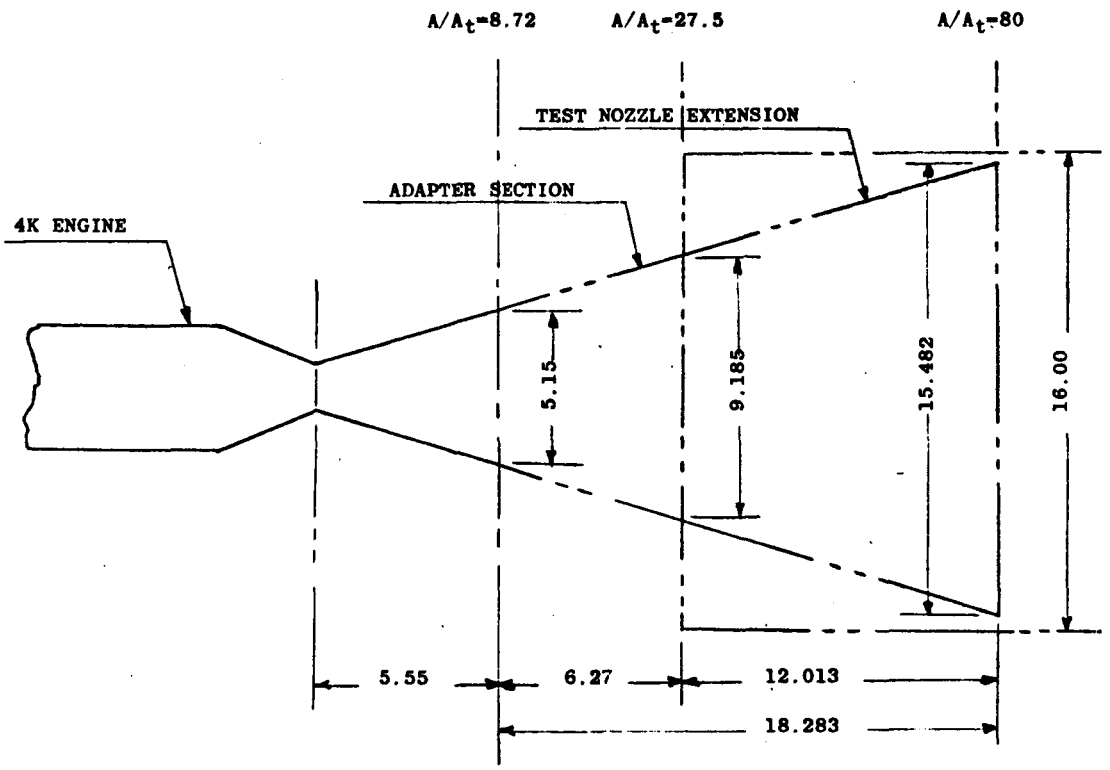

Figure 5. Schematic Drawing of 4-K Engine Test Arrangement

The scale model extension consisted of three main sections:

(1) the attachment rings

(2) the Airmat extension

(3) instrumentation.

Figure 6 is a drawing of the extension. The following paragraphs decribe the pertinent details of the design.

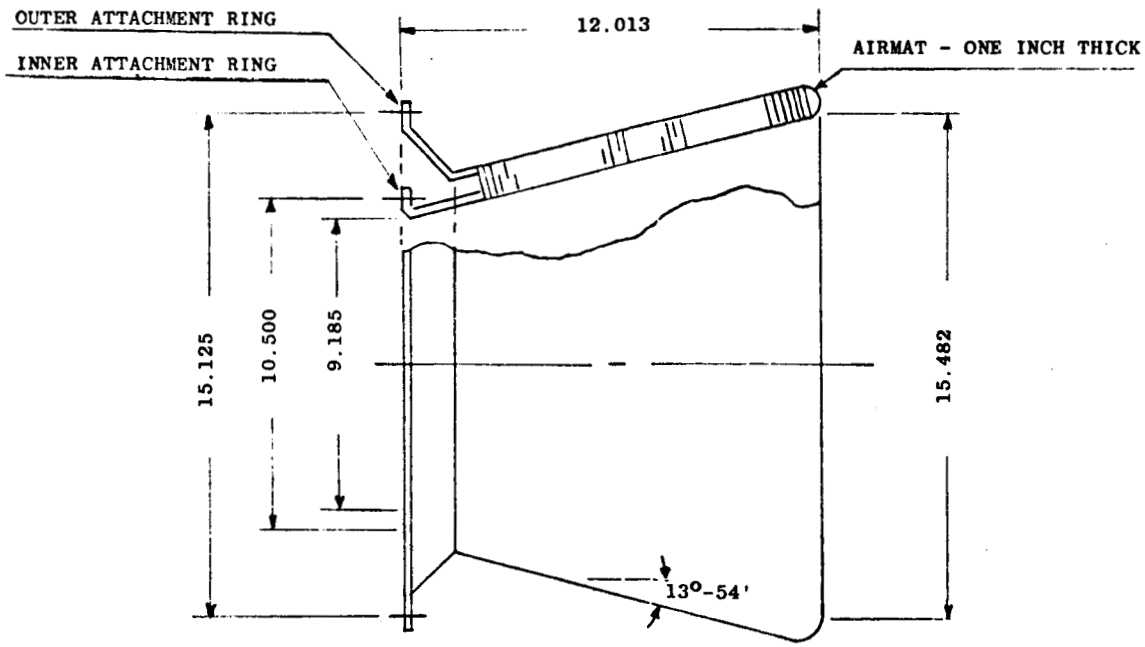

Figure 6. Test Nozzle Extension Configuration

a. Attachment Rings. To provide an attachment method for the test extension to the 4-K engine, two stainless steel rings, an outer and an inner ring, were designed. The outer attachment ring was a double flanged, conical spinning using type 304 stainless steel. The outer flange was designed to attach to the backwall of the diffuser provided in the 4-K engine test facility. A bolted attachment was used with a gasket between the ring flange and the diffuser wall. The inner attachment ring was a formed angle ring. As in the outer ring, type 304 stainless steel was used. This angle ring attached to the nozzle adapter by means of a bolted connection. A gasket was provided between the ring and the nozzle adapter. The outer and inner faces of the Airmat cone were welded to the attachment rings as shown in Figure 6. Coolant and pressurization ports were provided in the backwall of the diffuser.

b. Airmat Extension. The Airmat extension was a right circular truncated cone having a half angle of 13 degrees 54 minutes. The minor diameter was 9.185 inches, the major diameter was 15.482 inches and the length was 12.013 inches. The extension used one-inch thick Airmat and the entrance ends of the outer and inner faces were welded to the attachment rings. The Airmat was

woven using a 3 by 3 basket weave. It was woven with 112 yarns per inch of 12/90/2Z type 304 stainless steel multifilament yarns in the warp direction, 80 yarns per inch of 12/300/2Z type 304 stainless steel multifilament yarn in the fill direction, and 42 yarns per square inch of 12/300/2Z type 304 stainless steel multifilament yarn for the drop yarns. This Airmat construction was chosen to yield a porosity of one percent or less. The outer face of the Airmat was brush coated with Dow Corning S-2288 silicone. As stated above, the extension attached to the 4-K engine at an expansion ratio of 27.5 to 1 and extended to an exit expansion ratio of 80 to 1.

c. Model Extension Instrumentation. The instrumentation provided on the model extension was designed to obtain Airmat inner and outer face temperatures and Airmat wall pressure. To accomplish this, two rows of chromel alumel thermocouples, three thermocouples per row were attached to the extension. The two rows were located 90 degrees apart. These thermocouples were attached to the extension inner face. In addition, two thermocouples were attached to the extension outer face and located 90 degrees apart and positioned near the entrance end of the Airmat extension.

To measure Airmat extension wall pressure, two rows of pressure taps, two taps per row and 90 degrees apart, were provided. These taps were installed in the outer face of the extension.

4. Subscale Nozzle Extension Fabrication

The outer attachment ring was fabricated from 0.032-inch thick, type 304 stainless steel sheet stock. It was spun into a conical shaped ring having a vertical flange and a lower flange spun at an angle of 13 degrees 54 minutes from the horizontal. The vertical flange was drilled to match drilled holes in the back face of the diffuser wall. The lower flange was used to provide a welded attachment for the outer face of the Airmat.

The inner attachment ring was a machine angle fabricated from type 304 stainless steel. The ring thickness was 0.250 inch with one leg vertical, and the other 13 degrees 54 minutes from the horizontal or the angle between legs was 76 degrees 6 minutes. A notch was machined in the lower leg which provided a smooth transition at the ring to Airmat face interface when the inner face of the Airmat was welded to the ring.

The Airmat cone was fabricated from woven type 304 stainless steel, multifilament yarn. The Airmat was one-inch thick and woven in a flat configuration. The nozzle Airmat was cut into four gores, each representing one fourth of the nozzle extension. Each gore was slit at two places on the outer face and opened up a distance to correct for the difference in the inner and outer face circumferences. The joints, 4 places on the inner face and 12 places on the outer face, were closed using stainless steel tape cut from the Airmat. The tapes were attached to the Airmat by spot resistance welding. The exit end of the extension was closed in a similar manner.

Final assembly of the extension consisted of spot resistance welding the inner and outer Airmat faces to the attachment rings, installing the pressure taps and thermocouples and coating the outer surface with the S-2288 silicone to seal the outerface of the Airmat against coolant gas flow.

C. J-2 NOZZLE EXTENSION DESIGN

1. Introduction

Due to a redirection in the J-2S engine development program, NASA modified the contract scope of work changing the application of the nozzle extension from the J-2S engine to the J-2 engine. This change occurred midway through the program.

The design criteria for the J-2 engine as supplied by NASA is presented in Subsection 2 that follows.

The major design effort required to change from the J-2S engine to the J-2 engine involved establishment of the nozzle extension geometry which was dictated by the differences in the coolant supply availability from the propellant pump drive turbine. The J-2S engine had a coolant supply flow rate of 9 pounds per second and the J-2 engine has a coolant supply flow rate of 5.22 pounds per second. The design of the J-2 nozzle extension is the most critical because of the lower coolant flow rate available.

2. J-2 Nozzle Extension Design Data

The basis for the J-2 nozzle extension design was data supplied by NASA and shown in Table V. Included with this data are plots of nozzle exhaust gas heat transfer coefficient versus axial distance from the J-2 exit plane and engine exhaust pressure versus distance from the J-2 exit plane. These plots are shown in Figures 7 and 8.

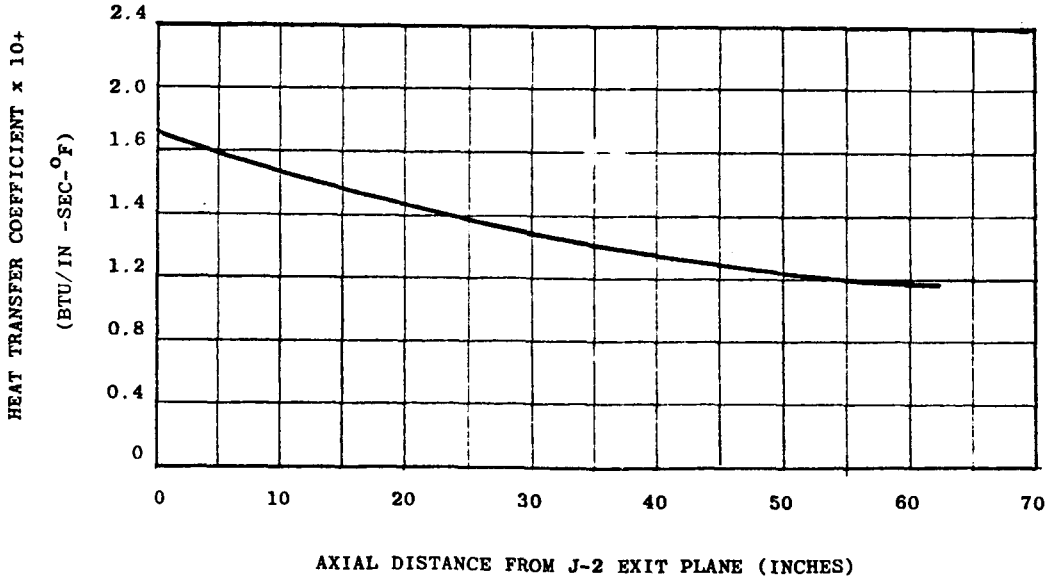

Figure 7. J-2 Nozzle Exhaust Gas Heat Transfer Coefficients

Table V. J-2 Nozzle Design Criteria

Item	Parameter
1. Cooling Method - Transpiration Cooling	
2. Coolant Gas - Turbine Exhaust Gas	
Composition	49% (Wt) H_2O - 50% (Wt) H_2
Molecular Weight	3.57 lbm/lb-mole
Specific Heat @ Constant Pressure	2.035 BTU/lbm-°F
Specific Heat Ratio	1.377
Flowrate	5.22 lbm/sec
Supply Pressure (to Manifold)	20.9 psia
Inlet Temperature	524°F
3. Thrust Chamber Combustion Gas	
Composition *	4% (Wt) H_2 - 96% (Wt) H_2O
Molecular Weight *	13.507 lbm/lb-mole
Specific Heat @ Constant Pressure+	0.92 BTU/lbm-°F
Specific Heat Ratio *	1.26
Flowrate	534 lbm/sec
Adiabatic Wall Temperature	5700°F
4. Nozzle Extension Exhaust Heat Transfer Coefficients (Zero Coolant Flow)	Figure 1
5. Thrust Chamber Combustion Gas Pressure Distribution on Nozzle Extension Inner Wall	Figure 2

*Evaluated at the thrust chamber combustion gas static temperatures and pressures within the nozzle.

+Effective value to be used in heat transfer analyses.

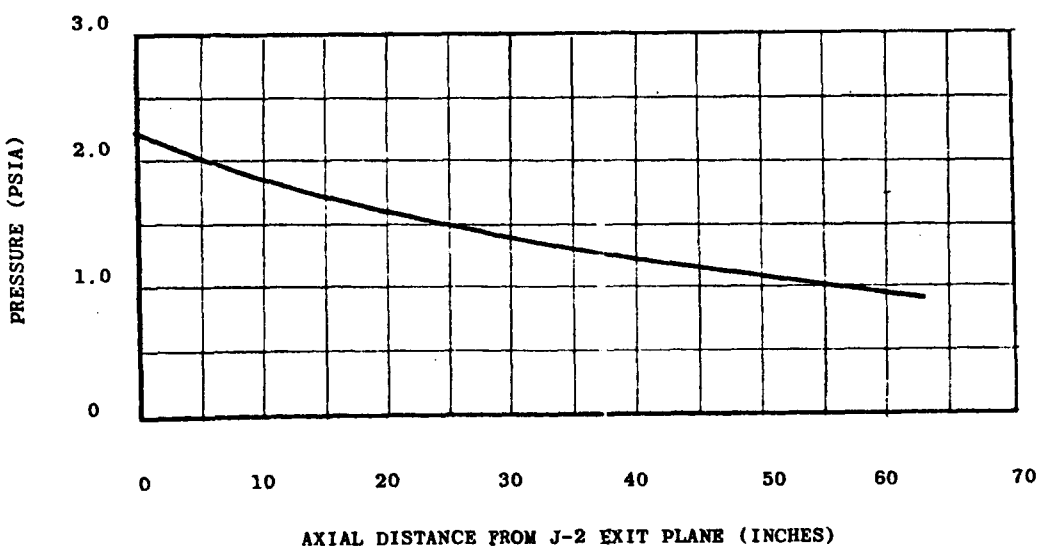

Figure 8. J-2 Nozzle Exhaust Gas Static Pressure Distribution

3. J-2 Nozzle Extension Design Analysis

a. Geometry. The basic design criteria used in establishing the J-2 nozzle extension geometry was as follows:

(1) Forward end expansion ratio = 27.5 to 1

(2) Aft end expansion ratio = 55 to 1

(3) Throat diameter = 14.7 inches

(4) Slope angle = 14°

The above data, by calculation, results in a diameter of 77.09 inches at 27.5 to 1 expansion ratio and a diameter of 109.02 inches at the 55 to 1 expansion ratio.

The North American Rockwell Corporation, Rocketdyne Division drawings gave the diameter of the inner aft edge of the J-2X engine nozzle exit flange to be 78.12 inches. When compared to the J-2 engine nozzle throat diameter of 14.7 inches, the actual 27.5 to 1 expansion ratio point falls forward of the aft edge of the J-2X nozzle.

Discussions with NASA established that for design purposes,the 55 to 1 expansion ratio diameter would be honored as well as the 14° slope angle. Thus the 27.5 to 1 expansion ratio becomes theoretical only.

To establish the basic design geometry at the forward end of the nozzle extension, GAC chose to locate a reference point on the forward edge of the attachment angle from which all nozzle geometry could be correlated. This reference point would also be in line with the inner Airmat surface. The point was located 0.313 inch aft of the existing nozzle exit flange allowing 0.063 inch for a shim and 0.250 inch for the thickness of the manifold attaching ring. The diameter at this point was calculated to be 78.55 inches.

The nozzle length was then established using the 78.55-inch forward diameter, the 109.02-inch aft diameter, and the 14° slope angle.

The result of the geometry calculations is that actually the forward edge of the nozzle extension has an expansion ratio of 28.46 to 1 although it is considered for practical purposes to be at 27.5 to 1.

Actually, four nozzle extensions of different lengths and exit expansion ratios were involved in the design. They are described as follows:

Nozzle Extension (ϵ = 55 to 1). This nozzle extension represents the original arbitrary decision to double the J-2X nozzle exit expansion ratio and was used to establish the extension geometry.

Nozzle Extension (ϵ = 50.71 to 1). The GAC experimental loom was chosen for the Airmat weaving on this program due to cost considerations. This loom had a capability of weaving Airmat up to 54 inches wide. This width capability limits the slope length of the nozzle extension that can be fabricated from the Airmat. Since an extension having an expansion ratio

of 50.71 to 1 has a slope length of 54 inches, this was the largest nozzle that could be fabricated utilizing this loom. GAC has other looms with the largest having a capability of weaving Airmat up to 20 feet in width. For purposes other than development, this loom could be utilized.

Nozzle Extension (ϵ = 48 to 1). The design criteria for the J-2 nozzle extension limits the coolant gas supply to 5.22 pounds per second. In order to maintain the required Airmat design pressures with the present Airmat porosity the porous inner surface area is limited to 94.8 square feet. This is the surface area of a 27.5 to 48 expansion ratio nozzle.

In future designs the nozzle length could be increased by increasing the gas supply flow rate criteria or by obtaining a tighter weave of the Airmat.

Nozzle Extension (ϵ = 41.33 to 1). The program plan was to fabricate both a full-length and a one-half length nozzle extension. This nozzle is approximately one half the length of the full length 27.5 to 55 expansion ratio nozzle.

This nozzle extension has the same coolant gas supply as the longer nozzle. The intent of the program was to fabricate one nozzle to a more conservative design to be used in case the performance of the longer nozzle was unsatisfactory.

All four nozzle extensions were included in the design studies although only two nozzles were planned to be fabricated. The two nozzle extensions selected for fabrication were the ϵ = 48 to 1 and the ϵ = 41.33 to 1 designs. The ϵ = 41.33 to 1 nozzle extension is subsequently referred to as the Number 1 or the short nozzle. The ϵ = 48 to 1 nozzle extension is subsequently referred to as the Number 2 or long nozzle.

The location of the nozzle extension reference joint is shown in Figure 3. The different length nozzles considered in the design are shown in Figures 9, 10, 11, and 12. Table VI is a compilation of nozzle extension geometry for different lengths and Figure 13 is a plot of nozzle extension length and surface areas versus expansion ratio.

b. Structural Analysis. The pressure requirements inside the Airmat nozzle extension are a function of the axial or thrust loads applied to the nozzle extension by the engine exhaust gases. The pressure requirements are based on the criteria that the compression stresses caused by the thrust loads cannot exceed the tension stresses caused by the nozzle extension inflation pressure. Otherwise, the nozzle extension would buckle due to compression instability.

The change in application of the nozzle extension from the J-2S engine to the J-2 engine established this criteria as a critical design consideration. This was caused by the lower pressurizing gas supply and the resulting lower Airmat pressure. The J-2 nozzle extension structural analysis is presented as follows.

The thrust loading was calculated in three parts; first the engine exhaust pressure over the nozzle extension length, second the engine exhaust pressure on the aft toroidal end of the nozzle extension, and third a skin friction effect.

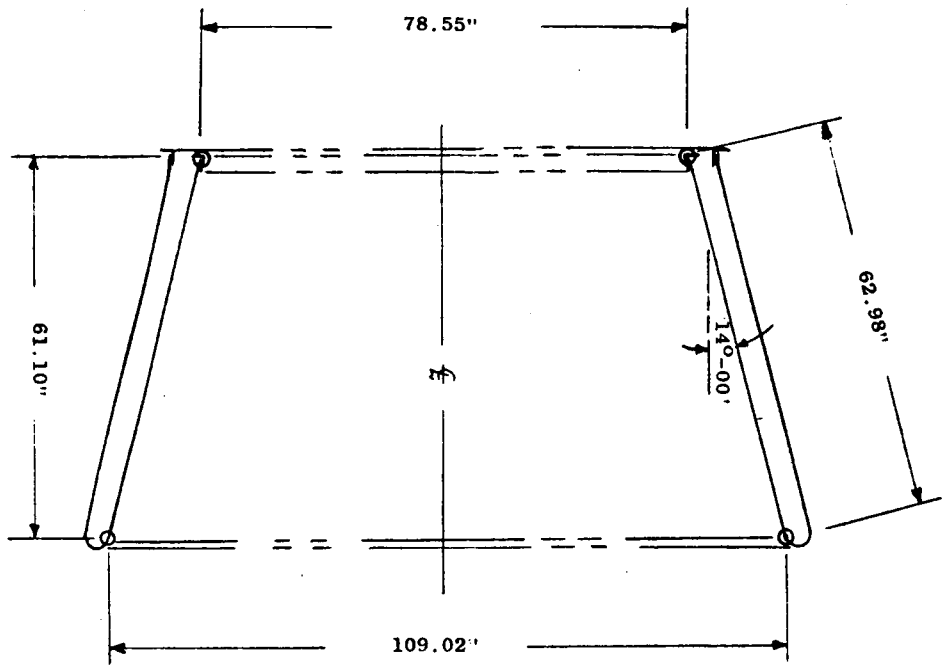

Figure 9. J-2 Nozzle Extension Geometry - 55 to 1 Expansion Ratio

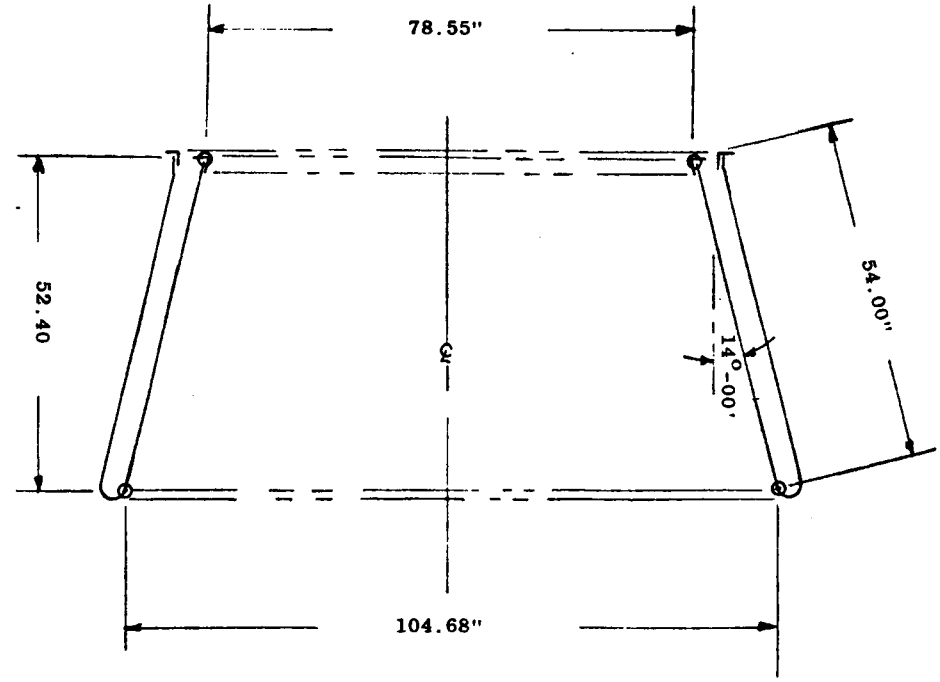

Figure 10. J-2 Nozzle Extension Geometry - 50.71 to 1 Expansion Ratio

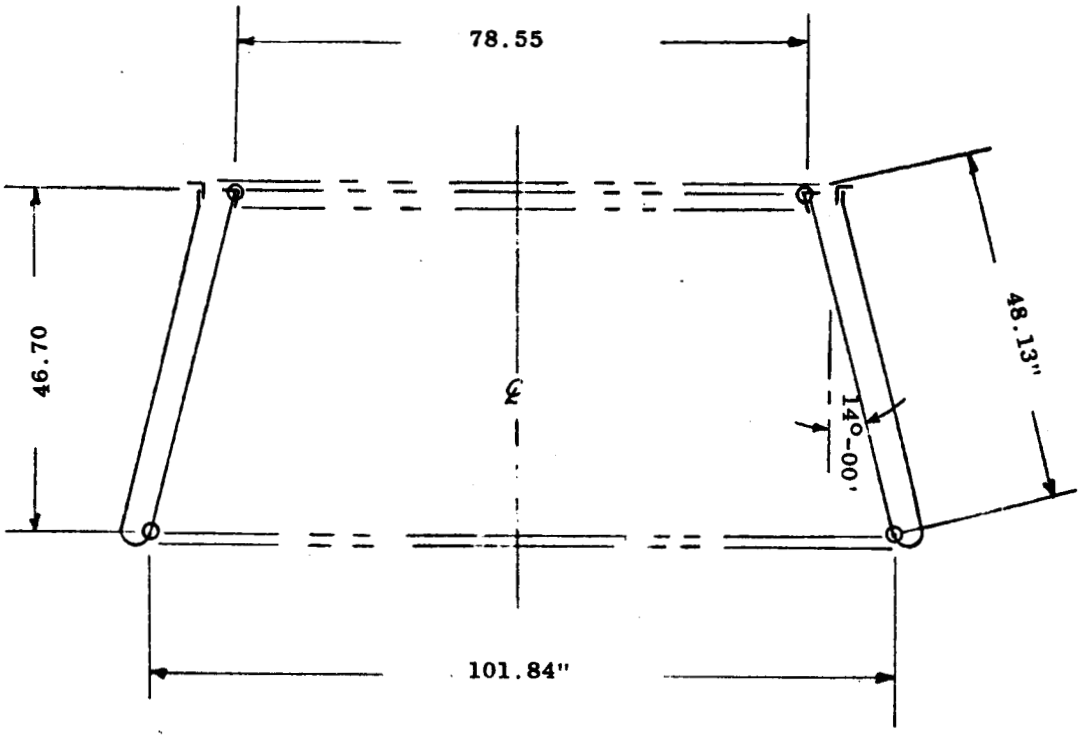

Figure 11. J-2 Nozzle Extension Geometry - 48 to 1 Expansion Ratio

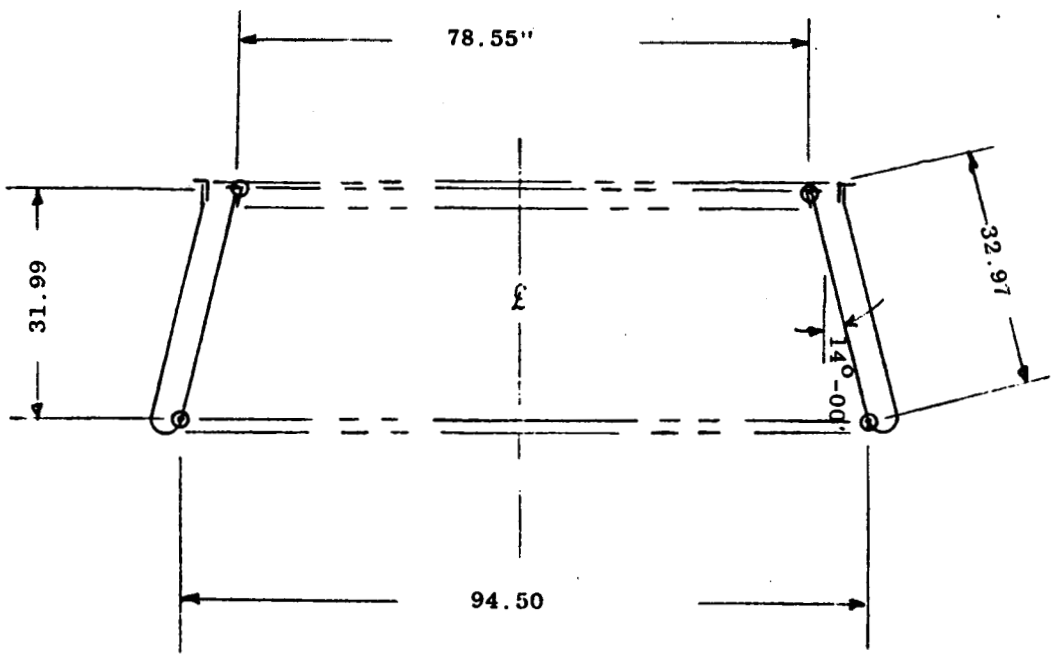

Figure 12. J-2 Nozzle Extension Geometry - 41.33 to 1 Expansion Ratio

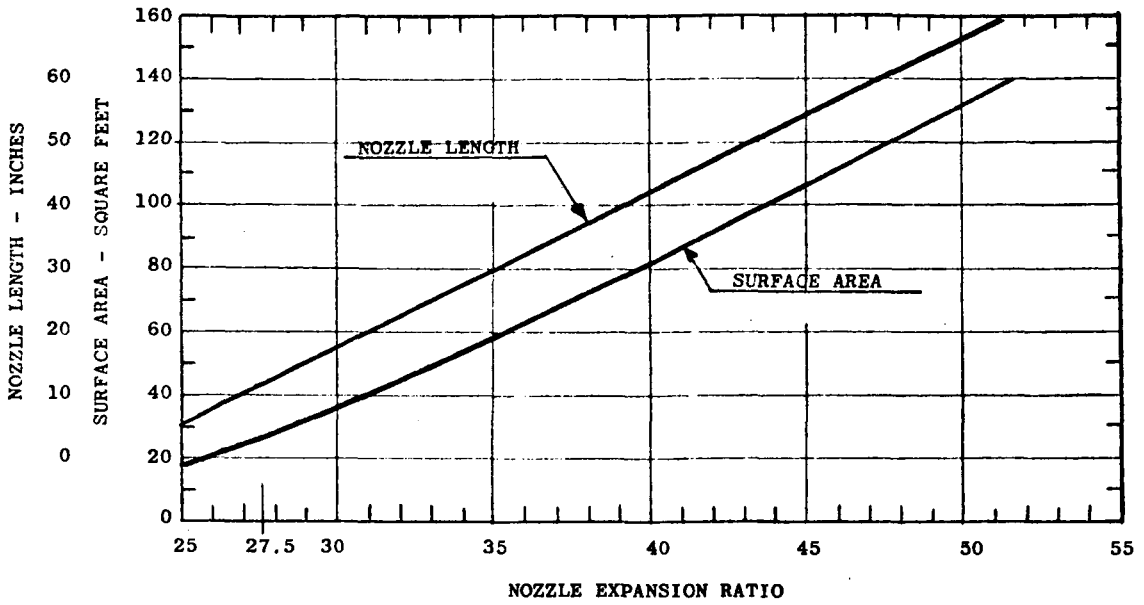

Figure 13. J-2 Nozzle Extension Length and Surface Area

Table VI. J-2 Nozzle Extension Geometry at Various Expansion Ratios

Expansion Ratio	Diameter Inches	Circum-ference Inches	Length Inches	Slope Length Inches	Surface Area Square Feet
27.5	77.09	242.19	--	--	--
28.46	78.55	246.77	0	0	0
30	80.52	252.96	3.91	4.07	7.0
35	86.97	273.22	16.88	17.40	31.4
40	92.97	292.07	28.92	29.80	55.7
41.33	94.50	296.88	31.99	32.97	62.2
45	98.59	309.73	40.19	41.42	80.0
48	101.84	319.94	46.70	48.13	94.8
50	103.95	326.57	51.34	52.48	104.3
50.71	104.68	328.24	52.40	54.00	107.6
55	109.02	342.48	61.10	62.98	128.8

The J-2 nozzle extension pressure distribution versus length is plotted in Figure 14. This data was derived from Figure 8. The loads on the aft end of the nozzle extension were calculated using the pressure and area criteria shown in Figure 14. The negative skin friction effect was calculated using an arbitrary value of 0.02 pounds per square inch of surface area.

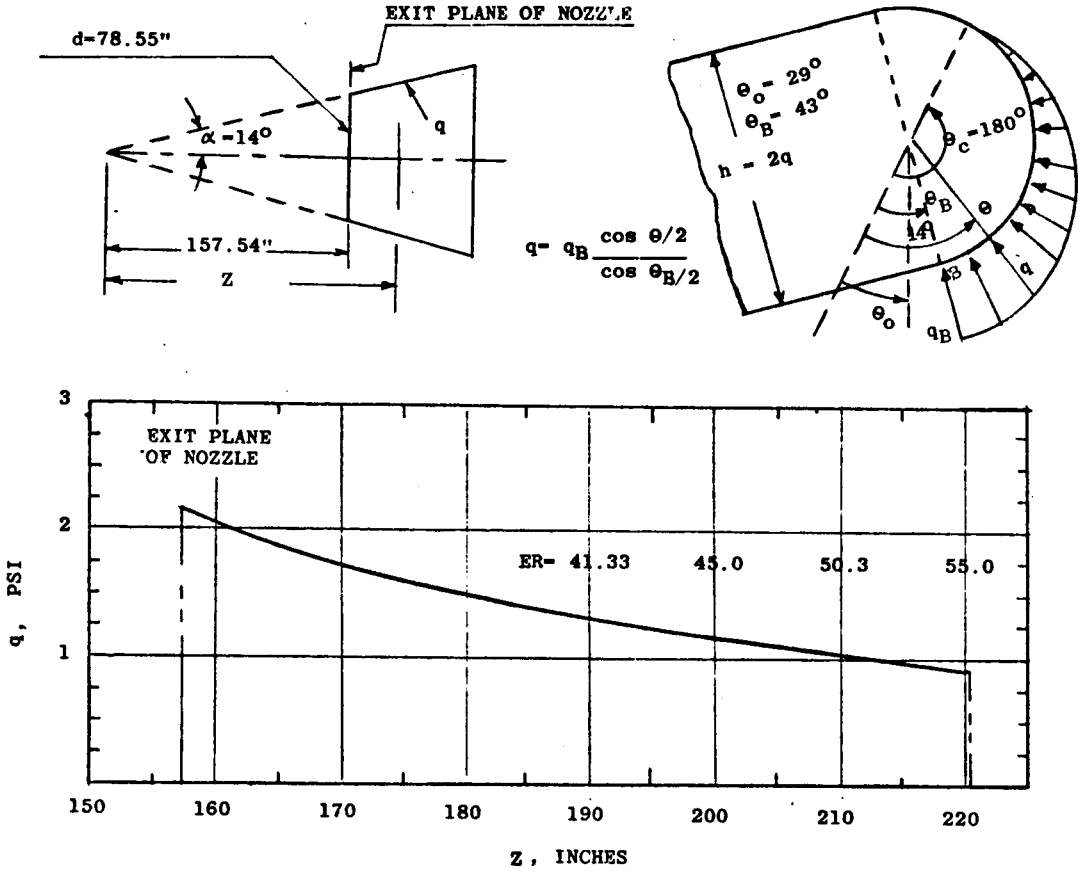

Figure 14. J-2 Nozzle Extension Pressure Distribution

(1) Axial Load on Conical Portion. The geometry and loading for the J-2 nozzle extension is shown in Figure 14. The internal pressure as a function of Z is given in Table VII. The axial thrust is given by

$$F_c = 2 \pi \tan^2 \alpha \int_{Z_1}^{Z} q \, z \, d z$$

and is evaluated for increments of Z in Table VIII. Summation of the incremental forces gives the total thrust as a function of Z with Z_1 fixed at 157.54 inches.

Table VII. J-2 Nozzle Extension Internal Pressure and Thrust

Z In.	q PSI	ΔF Lb.	F Lb.
157.54	2.19	0	0
162.78	1.98	683	683
168.02	1.82	643	1326
173.26	1.67	609	1935
178.50	1.54	577	2512
183.74	1.45	554	3066
188.97	1.35	534	3600
194.21	1.26	511	4111
199.45	1.18	491	4602
204.69	1.10	471	5073
209.63	1.03	452	5525
215.71	0.96	433	5958
220.41	0.90	414	6372

Table VIII. J-2 Nozzle Extension Axial Thrust vs Expansion Ratio

E.R.	$Z = 29.47 \sqrt{E.R.}$ In.	F_c Lb.
41.33	189.54	3650
45.0	197.94	4420
50.3	209.94	5525
55.0	219.30	6300

(2) Axial Load on Toroidal Portion. The load distribution acting on the toroidal closure is shown in Figure 14. The axial load is given by

$$F_{TOR} = \frac{2\pi q_B a R}{\cos \frac{\theta B}{2}} \int_{\theta_B}^{\theta_c} \cos \frac{\theta}{2} \sin(\theta - \theta_o) \left[1 - \frac{a}{R} \cos(\theta - \theta_o) \right] d\theta$$

$$= \frac{2 \pi (2) q_B R}{0.93042} \quad I \left(\frac{a}{R}\right)$$

Values are given in Table IX.

Table IX. J-2 Axial Load on Toroidal Portion

ER	q_B PSI	R In.	$I\left(\frac{a}{R}\right)$	F_{TOR} Lb.
41.33	1.33	49.19	0.92644	819
45.0	1.18	51.24	0.92856	758
50.71	1.03	54.28	0.92906	702
55.0	0.90	56.45	0.93043	640

(3) Friction Load on Conical Portion. Skin friction drag is estimated to be 0.02 lbs/in^2. The friction load tending to decrease the thrust is

$$F_F = 0.02 \; A_{cone} \cos 14^\circ$$

$$= 0.0194 \; A_{cone}$$

Table X gives values of skin friction force.

Table X. J-2 Nozzle Extension Skin Friction vs Expansion Ratio

E.R.	A_{cone} In.^{2}	F_F Lb.
41.33	8,560	171
45	11,520	230
50.71	15,490	310
55	18,550	371

(4) Total Axial Thrust and Pressure Requirement. The total axial thrust is

$$P_{axial} = F_C + F_{TOR} - F_F$$

The pressure requirement is given by

$$p\ \pi\ (d_1 + h \cos\ \alpha)\ h \cos \alpha = (F.S.)\ P_{axial}$$

where d_1 = 78.55 inches

h = 4" = Airmat thickness

α = 14° = angle of cone

Thus

$$p = \frac{(F.S.)\ P_{axial}}{1005}$$

Values of p and P_{axial} are given in the Summary Table XI and plotted in Figure 15.

Table XI. J-2 Nozzle Extension Summary of Loads and Pressure Requirements

Expansion Ratio E.R.	Loads				Pressure Requirement	
	F_c Load on Conical Part Lb	F_{TOR} Load on Aft End Toroid Lb	F_F Friction Load Lb	P_{axial} Axial Thrust Lb	p F.S.=1.0 psi	p F.S. = 1.5 psi
41.33	3650	819	171	4300	4.28	6.42
45.0	4420	758	230	4950	4.93	7.40
50.71	5525	702	310	5920	5.89	8.84
55.0	6300	640	371	6570	6.55	9.83

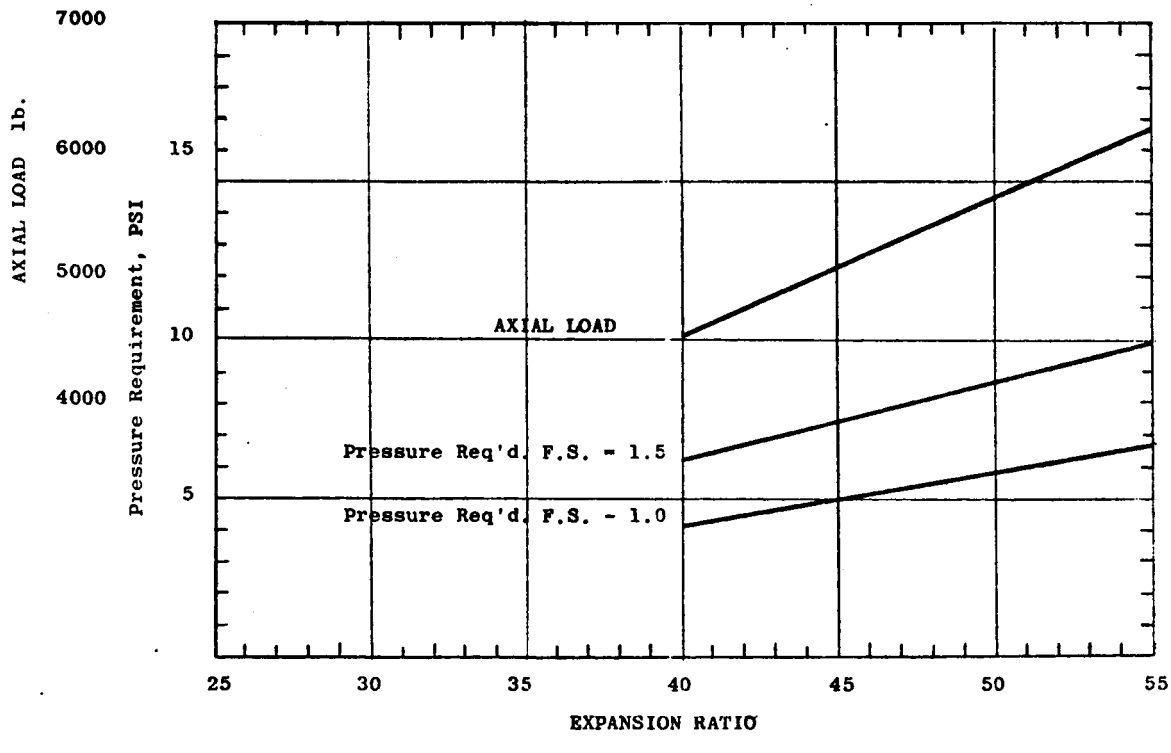

Figure 15. J-2 Nozzle Extension Axial Load and Pressure Requirement

c. Nozzle Extension Geometry Selection

(1) Introduction. The nozzle extension Airmat internal pressure must be sufficient to support the thrust loads from the engine exhaust. The actual nozzle extension Airmat internal pressure that will be achieved in operation is a function of the properties and the supply flow rate of the pressurizing gas, and the porosity of the inner face of the Airmat material. Both the internal pressure requirement and the actual internal pressure are functions of the inner surface area or the length of the nozzle extension.

Thus to determine the longest practical nozzle extension length for the J-2 engine criteria, an analysis of all contributing factors was conducted. Figure 16 was the basic tool used in this analysis.

(2) Internal Pressure Requirement. The internal pressure requirement as a function of nozzle extension length was determined in Section III-C-3 and plotted in Figure 15. These pressure requirements versus nozzle extension expansion ratios for four different load safety factors were in turn plotted on Figure 16.

(3) Pressure Determination. Airmat pressure expected in the nozzle extension for the range of expansion ratios considered are also plotted on Figure 16. Plots are shown for seven different porosity values. This data was abstracted from Section IV of this report.

The expected pressure calculations are based on the J-2 engine coolant gas flow rate of 5.22 pounds per second and actual nozzle extension operating conditions.

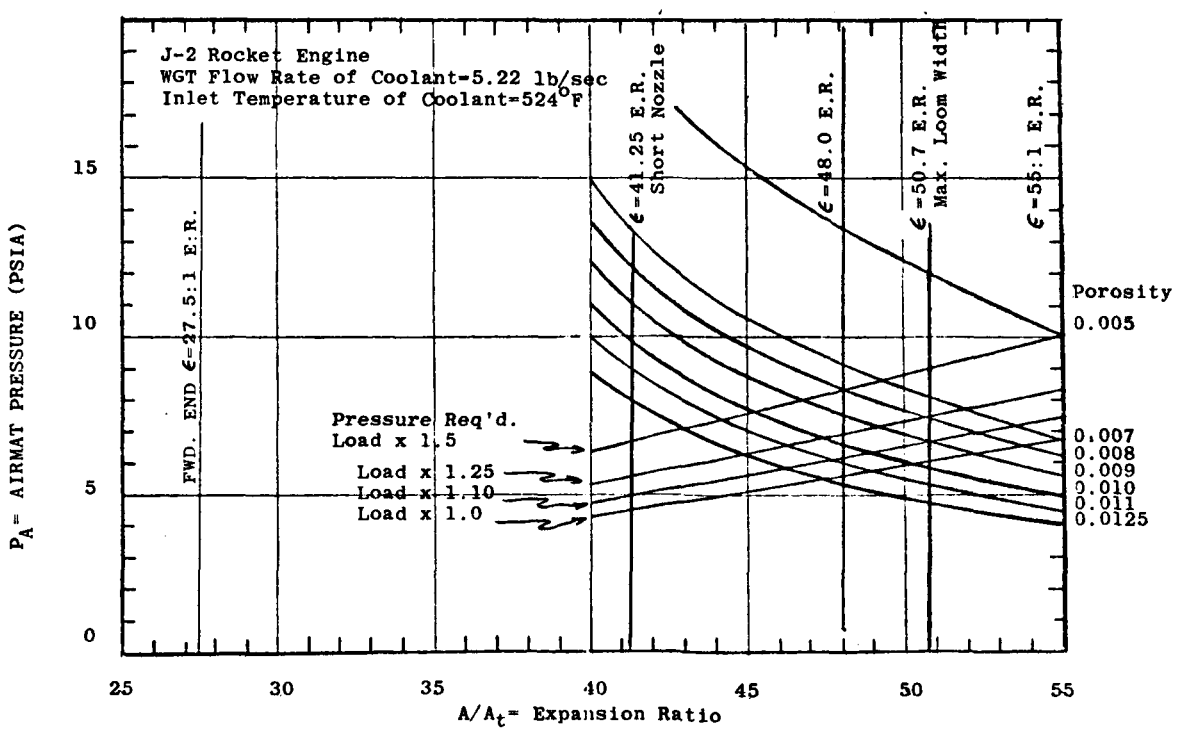

Figure 16. J-2 Nozzle Extension - Expansion Ratio Determination Curves

The preliminary Airmat porosity determination was 1.10 percent at 10 PSI internal pressure which is obtained from Figure 50.

(4) Requirements, ϵ = 55 to 1, Nozzle Extension. Figure 16 shows that for a 55 to 1 expansion ratio nozzle extension using a load safety factor of 1.50 that an Airmat porosity of 0.5 percent would be required. An Airmat internal pressure of 10 PSI would result. Using a load safety factor of 1.25 the Airmat porosity requirement would be 0.6 percent with a resulting Airmat pressure of 8.3 PSI.

Since the development weaving task showed that the lowest Airmat porosities obtained were in the 1.0 percent range, it would not be practical with the present state-of-the-art of conical Airmat weaving to obtain the required porosities for this full length nozzle extension. An increase in the coolant gas flow rate could, however, allow using a longer nozzle.

(5) Requirements, ϵ = 50.71 to 1, Nozzle Extension. This nozzle extension represented the longest nozzle extension that can be conically woven on the present experimental loom.

Using a 1.25 load safety factor, the Airmat pressure requirements would be 7.5 PSI and the porosity requirement would be 0.8 percent. This porosity was again considered to be unrealistic at this time.

(6) Requirements, ϵ = 48 to 1, Nozzle Extension. It was thus required that the longest practical nozzle extension for a 1.25 load safety factor, the allowable gas flow rate, and the present conical weaving porosity criteria, be determined. From previous analysis and from inspection of Figure 16, it was determined that the pressure requirement limit would be approximately 7.0 PSI. The porosity values previously considered in the 10 PSI range were re-evaluated in the 7 PSI range. This decreased the porosity expected to 0.95 percent rather than 1.10 percent at 10 PSI. This data is presented in Figure 51 . From Figure 16 it is determined that the pressure required curve crosses an extrapolated 0.95 percent porosity curve at an expansion ratio of 48 to 1.

(7) Summary - Geometry Selection. The maximum expansion ratio recommended for the nozzle extension was 48 to 1. This was based on pressure requirements, the available gas supply, and the present state-of-the-art of conical Airmat weaving as regards porosity. The criteria for the 48 to 1 expansion ratio nozzle is summarized as follows.

(a)	Airmat pressure requirement - Load x 1.25 safety factor	= 7.0 PSI
(b)	Airmat gas supply	= 5.22 lbs/sec
(c)	Airmat porosity	= 0.95 percent

4. J-2 Nozzle Extension Design Description

The basic J-2 nozzle extension assembly drawings are

EA 2211-013-101 Expansion ratio 48 to 1

EA 2211-013-103 Expansion ratio 41.33 to 1

Complete detail, assembly, and installation drawings were prepared for each nozzle extension.

The basic change in the nozzle extension design was the development of conically woven Airmat. This greatly reduced the number of seams required in fabricating the Airmat assembly.

The Airmat construction for the conical Airmat was also different than that for the flat Airmat. When flat Airmat was used the gores were cut from the Airmat so that the fill direction of the Airmat became the hoop direction of the nozzle extension. The flat Airmat makeup was as follows:

Warp yarns	90 filament yarn at 112 yarns per inch
Fill yarns	300 filament yarn at 80 yarns per inch
Drop yarns	300 filament yarn at 41 yarns per square inch
Depth	4 inches

When using conical woven Airmat, it is necessary to use the Airmat warp yarns in the nozzle extension hoop direction. The makeup of the conical Airmat was as follows:

Warp yarns	300 filament yarns at 84 yarns per inch at the forward end of the nozzle extension tapering to 92 yarns per inch at the exit end of the nozzle extension
Fill yarns	90 filament yarns at 70 yarns per inch
Drop yarns	300 filament yarn at 41 yarns per square inch
Depth	4 inches

SECTION IV

THERMAL AND FLOW ANALYSIS

A. INTRODUCTION

A preliminary thermal and flow analysis was conducted by Goodyear Aerospace Corporation to determine the feasibility of using Airmat material as a medium for applying a transpiration cooling technique on an extendable rocket nozzle extension. This preliminary analysis was based on requirements furnished by the North American Rockwell Corp., Rocketdyne Div. for the J-2X liquid fueled rocket engine. The details of this were published in Ref. (1). The objectives of the referenced study and analysis were: (1) to develop Airmat material porosity requirements for using a transpiration cooling technique, (2) establish a simple test program for evaluating the effectiveness of transpiration cooling using the porous Airmat material and finally, (3) develop a means of extrapolating the test results to full scale conditions as would exist on the J-2X rocket engine.

The results of this preliminary program proved to be very encouraging. The results of the flow analysis indicated that Airmat porosities on the order of 1% were required for the range of possible turbine exhaust gas flow rates and pressure available. Parallel efforts in Airmat weaving techniques resulted in attaining of Airmat porosity levels of about 1%. Simple transpiration cooling tests were then conducted on developed Airmat specimen material. The tests showed that the transpiration cooling when applied to low porosity Airmat material could be very effective when employed as an active cooling system at coolant flow rates simulating turbine exhaust gas flow rates.

On the basis of the positive results obtained during the preliminary study program, it was recommended that a more broadened approach be taken to develop the transpiration cooling technique using Airmat material. In particular, a more realistic approach for determining the efficiency of the transpiration cooling technique in terms of the available system parameters was required. These are discussed in the following sections.

B. THERMAL ANALYSIS

The approach to determining the transpiration cooling gas flow rate requirements and the resulting surface temperature of the inner wall of the Airmat material during the preliminary study was based on a very simple steady state heat balance procedure. This procedure simply equated the heat transferred by convection to the inner wall from the engine exhaust gas to the sensible heat rise of the cooling gas. The resulting cooling gas flow rate requirement and inner wall temperature predictions

using this approach proved to be unsatisfactory primarily due to the high coolant gas flow rates required. Similarly, the approach used by Friedman in Reference (3) was utilized and led to a conservative prediction of the cooling gas flow rate requirement and Airmat material temperature. An approach developed by Bartle and Leadon was then investigated. Preliminary calculations showed that this approach represented the effectiveness of transpiration cooling closely resembling the results obtained during the simple test program conducted during the preliminary phase of the nozzle extension program and reported in Ref. 1. The summary details of this approach are presented herein.

The effectiveness of Airmat material as a heat exchanger can be obtained using the Bartle and Leadon approach as presented in Reference (4). Consider a portion of the Airmat nozzle extension wall as shown in Figure 17 . A simple heat balance at a position within the nozzle extension equates the heat into the surface to the heat removed by the coolant or:

$$h_g\ (T_{aw} - T_w) = \rho\ v\ c_{pc}\ (T_{co} - T_{ci}) \qquad (1)$$

where

c_{pc} = specific heat of the coolant, Btu/lb-°F

h_g = convective heat transfer coefficient, Btu/hr-ft^2 - °F

T_{aw} = adiabatic wall temperature, °F

T_w = surface temperature, °F

T_{ci} = coolant inlet temperature, °F

T_{co} = coolant outlet temperature

v = injection velocity of coolant, ft/sec.

ρ = density of coolant, lb/ft^3

If one assumes that the coolant outlet temperature is equal to the surface temperature of the porous material, then equation (1) can be written as:

$$h_g\ (T_{aw} - T_w) = \rho\ v\ c_{pc}\ (T_w - T_{ci}) \qquad (2)$$

Substituting the relationship between the Stanton number and the convective heat transfer coefficient in equation (2), results in the following heat balance equation:

$$St\ (\rho\ u\ c_{pg})\ (T_{aw} - T_w) = (\rho\ v\ c_{pc})\ (T_w - T_{ci}) \qquad (3)$$

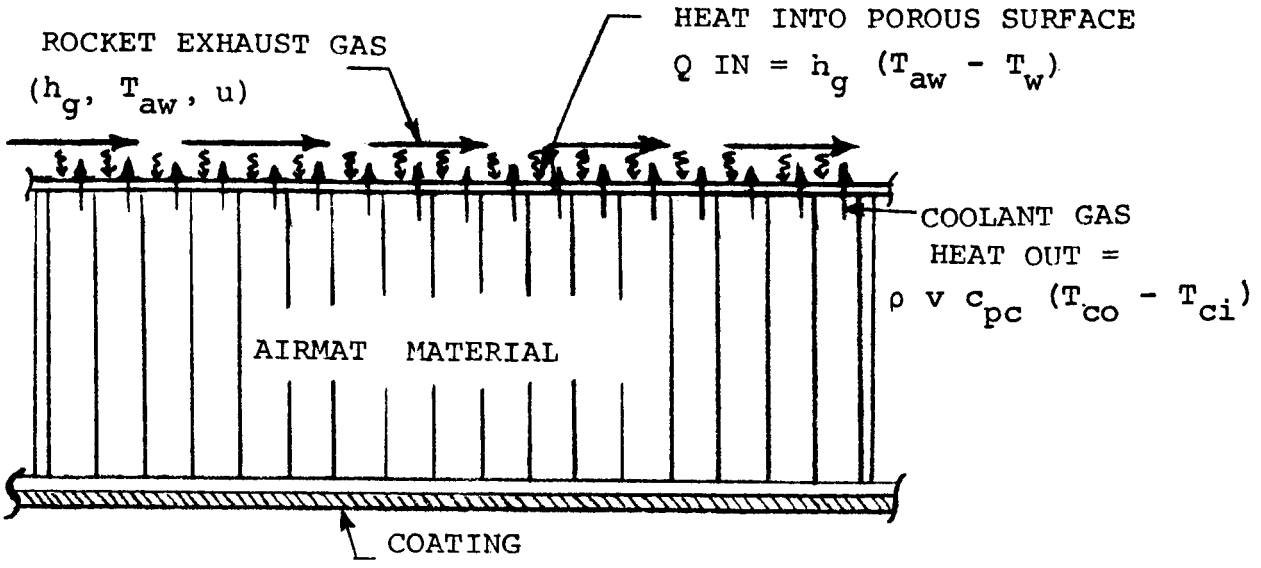

Figure 17. Airmat Transpiration Cooling Heat Balance Model

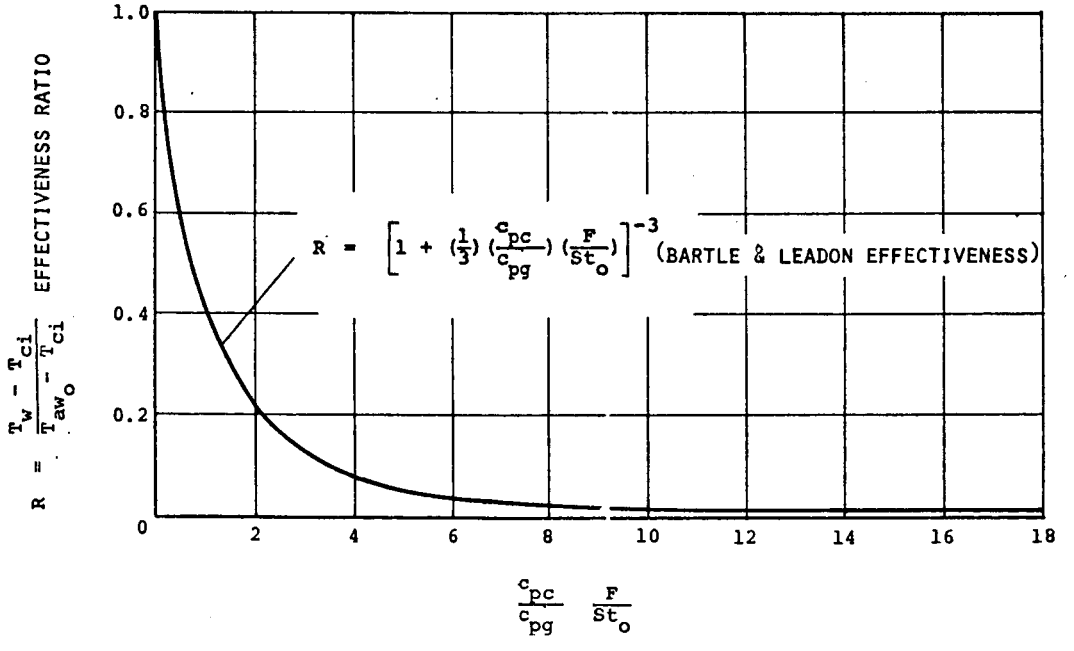

Figure 18. Effectiveness Ratio vs Flow Rate

where St = Stanton number, dimensionless

ρ_g = density of rocket exhaust gas, lb/ft^3

u = velocity of rocket exhaust gas, ft/sec.

c_{pg} = specific heat of rocket exhaust gas, Btu/lb-°F

Since it is required to find the temperature of the porous surface in terms of the overall heat exchange effectiveness of the transpiration cooling mechanism, equation (3) must be re-defined in terms of the zero injection rate convective heat transfer coefficient and the unaltered adiabatic wall temperature. By substituting these parameters into equation (3), the effectiveness ratio can be shown to be:

$$R = \frac{T_w - T_{ci}}{T_{aw_o} - T_{ci}} = \left[1 + \left(\frac{c_{pc}}{c_{pg}}\right)\left(\frac{F}{St_o}\right)\left(\frac{q_o}{q}\right)\right]^{-1} \qquad (4)$$

This effectiveness ratio is shown in Figure 18 as a function of the dimensionless flow rates

$$\left(\frac{c_{pc}}{c_{pg}}\right)\left(\frac{F}{St_o}\right).$$

Where: c_{pc} = Specific heat of the coolant gas, Btu/lb-°F

c_{pg} = Specific heat of the rocket exhaust gas, Btu/lb.-°F

$F = \frac{(\rho v)_c}{(\rho u)_g}$ = Mass velocity ratio

St_o = Zero injection rate Stanton number

q = Modified heat flux rate into the porous surface, Btu/ft^2-sec.

q_o = Zero injection rate heat flux rate, Btu/ft^2-sec.

T_{aw_o} = Adiabatic wall temperature at zero injection rate, °R

This effectiveness ratio has been shown to be practically independent of Reynolds number and Mach number. As a consequence, it can easily be evaluated for a surface exposed to constant heat-conditions. A curve fit of Bartle and Leadon test data has shown that the effectiveness ratio could be represented by the following equation:

$$R = \frac{T_w - T_{ci}}{T_{aw_o} - T_{ci}} = \left[1 + \left(\frac{1}{3}\right)\left(\frac{c_{pc}}{c_{pg}}\right)\left(\frac{F}{St_o}\right)\right]^{-3} \qquad (5)$$

The sharp reduction in the effectiveness ratio as the flow rate parameter increases illustrates the potential of the transpiration cooling system for decreasing the porous wall temperature. For example, the effectiveness ratio will decrease if the wall temperature decreases for a constant coolant gas inlet temperature and an unvarying adiabatic wall temperature. Physically, the wall temperature reduction can be accomplished by increasing the mass flow of the coolant gas transpiring through the porous wall. The effectiveness ratio also dramatizes the fact that an overabundance of coolant gas flow will be very effective. An efficient design, where coolant gas availability is limited, must operate where the surface temperature is not minimal, but rather compatible with the materials available and can accommodate the design requirements.

C. FLOW ANALYSIS

The expandable nozzle extension will be transpiration cooled by turbine exhaust gas flowing through the inside surface of the Airmat material forming the nozzle extension. The pressure acting on the inside surface of the Airmat nozzle extension can be considered small compared to the internal pressure of the Airmat extension. Thus, the ratio of external pressure to

internal pressure across the inside surface where the coolant gas transpires can be assumed to be always less than the critical pressure ratio for the turbine exhaust coolant gas. Therefore, sonic flow can be assumed to exist across the inner surface of the Airmat, provided this surface offers enough constriction at the available pressure or less to keep the internal pressure from falling off.

Where sonic flow exists in the open cross-sectional areas of the Airmat nozzle extension, the maximum turbine exhaust gas flow rate that can pass through this flow constriction is related by the following flow relationship:

$$\dot{w} = \frac{p_1 C_d A_t g k \sqrt{\left(\frac{2}{k+1}\right)^{\frac{k+1}{k-1}}}}{\sqrt{g\ k\ R\ T_1}} \qquad (6)$$

where $\dot{w}$ = turbine exhaust gas flow rate (lb/sec),

p_1 = Airmat pressure (lb/sq ft),

A_t = exit area (sq ft),

C_d = flow coefficient, dimensionless

g = gravitational acceleration (32.2 ft/sec^2),

k = specific heat ratio,

R = gas constant per unit weight (ft lb/lb-°R), and

T_1 = temperature of gas at p_1 (°R).

If both sides of equation (6) are divided by the surface area (A_s) to be cooled by the transpiring gas, then the mass flow per unit of cooled surface area can be written as follows:

$$\frac{\dot{w}}{A_s} = \frac{p_1 g k\ C_d \sqrt{\left(\frac{2}{k+1}\right)^{\frac{k+1}{k-1}}}}{\sqrt{g\ R\ k\ T_1}} \left(\frac{A_t}{A_s}\right) \qquad (7)$$

Thus the mass flow rate of coolant gas per unit of cooled surface area is a function of the upstream pressure, the type of gas and its properties as well as the porosity of the Airmat inner wall.

This equation can be used in various ways. For example, assuming a fixed level of porosity, the mass velocity per unit surface area of the transpiration medium can be determined for a range of pressures and different coolant gas mediums. In the present case, the cooling gas medium and flow rate is specified and it is required to develop a transpiration medium which satisfies the prescribed conditions under which it must operate. Thus, equation (7), is a valuable relationship which must be used to define porosity requirements as well as Airmat operating pressures. The latter two parameters along with the surface temperature correlation presented as equation (5) are the basic tools required to study parametrically an active transpiration cooling system employing a thin porous surface.

D. J-2S NOZZLE EXTENSION ANALYSIS

The J-2S rocket engine nozzle extension was investigated to determine primarily its porosity requirement for transpiring the coolant gas, its operating temperature and its internal pressure characteristics. The rocket engine gas and turbine exhaust gas design criteria data for the J-2S engine are presented in Table I, while the heat transfer coefficient and static pressure acting on the inside surface of the expandable nozzle section are shown in Figures 1 and 2 as a function of axial length.

The porosity requirements for the inner surface of the expandable nozzle extension were calculated using equation (7) and the gas data presented in Table I. The results are shown in Figure 19 where the internal Airmat pressure is shown versus the Airmat porosity requirement for three different mass velocity values. The upper value of mass velocity (0.075 lb/sec per sq. ft. of surface area) was obtained by dividing the turbine exhaust gas flow rate of 9.0 lb/sec by the approximate inside surface area of the expandable nozzle extension. This surface area was estimated to be 120 ft^2. The other values were obtained by decreasing the mass flow of the exhaust gas while keeping the nozzle extension area constant.

The purpose of the data shown in Figure 19 was primarily directed at estimating the coolant mass velocity effect on Airmat pressure and porosity. Design data for the J-2S Nozzle extension limited the upper pressure to 20 psia, the supply pressure of the turbine exhaust gas, and a lower pressure of 3 psia. The latter pressure is the maximum static pressure acting on the inside surface of the nozzle extension. Thus, a fabric having a porosity of 1.5%, transpiring the turbine exhaust gas at 0.075 $lb/sec\text{-}ft^2$ of surface area, will establish an Airmat pressure of about 6 psia. At this pressure, decreasing the mass velocity requires a decreasing fabric porosity. However, a fixed porosity offers the possibility of varying the mass velocity over an Airmat internal pressure range. The widest latitude for varying

the mass velocity can apparently be achieved at fabric porosity levels less than 1%. This porosity level would assure an internal Airmat pressure of a magnitude necessary to sustain sonic flow. The effectiveness ratio was evaluated using the design data presented in Table I. Evaluation of the dimensionless flow rate parameter $(C_{pc}/C_{pg})(F/St_o)$ yielded a value of 4.2. Entering Figure 18 at this value yielded an effectiveness ratio of 0.072. The wall temperature of the expandable Airmat nozzle section was then calculated from the effectiveness ratio as shown:

$$T_w = 0.072\ (T_{aw} - T_{ci}) + T_{ci}$$

The wall temperature was calculated to be 967°F. Thus the coolant temperature increases by about 350°F during the transpiration through the porous inner wall. This temperature increase will have an effect on the porosity requirement of the inner wall as shown in Figure 19 . A temperature increase of the coolant gas will tend to shift these design data curves upward and to the left. Thus, for a constant mass velocity, the internal pressure of the Airmat nozzle extension will increase slightly and the porosity requirement at the coolant gas temperature will also increase. Both of these increases appear to be favorable from a design standpoint and when coupled with the predicted temperature level would give the nozzle extension desirable operating characteristics.

E. SUB-SCALE NOZZLE EXTENSION ANALYSIS

The preliminary phase of the nozzle extension development program presented in Reference (1) had recommended the testing of a small scale rocket engine nozzle extension. The results of the analysis presented for the J-2S rocket engine nozzle extension had indicated that a transpiration cooled nozzle extension should operate very effectively within the thermal design criteria specified. A thermal analysis was then conducted to determine the effect of the NASA 4-K test rocket engine operating characteristics on the selection of the point of attachment for a test nozzle extension configuration.

1. Analysis

The initial consideration for selecting the position of the sub-scale nozzle extension was given to establishing the range of heat transfer coefficients along the surface of the extension. These heat transfer coefficients were calculated using Bartz's equation taken from Reference 5 :

$$h_g = \left[\frac{0.026}{(D_*)^{0.2}} \left(\frac{\mu^{0.2} c_p}{Pr^{0.6}}\right)_o \left(\frac{P_c g}{c_*}\right)^{0.8} \left(\frac{D_*}{r_c}\right)^{0.1}\right] \left(\frac{A_*}{A}\right)^{0.9} \sigma \quad (8)$$

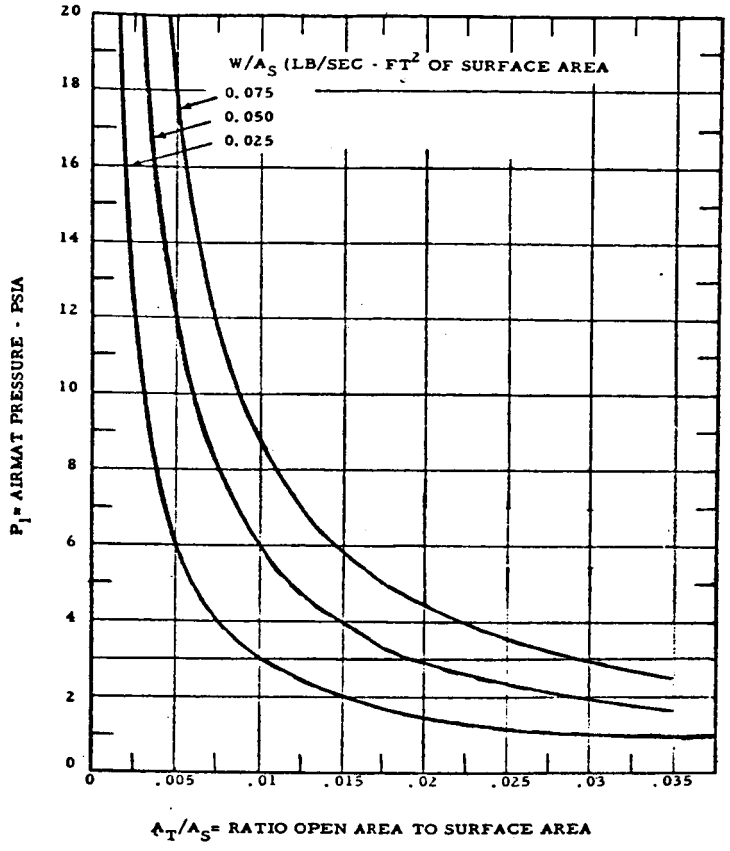

Figure 19. Airmat Pressure vs Porosity J-2S Nozzle Extension Turbine Exhaust Gas

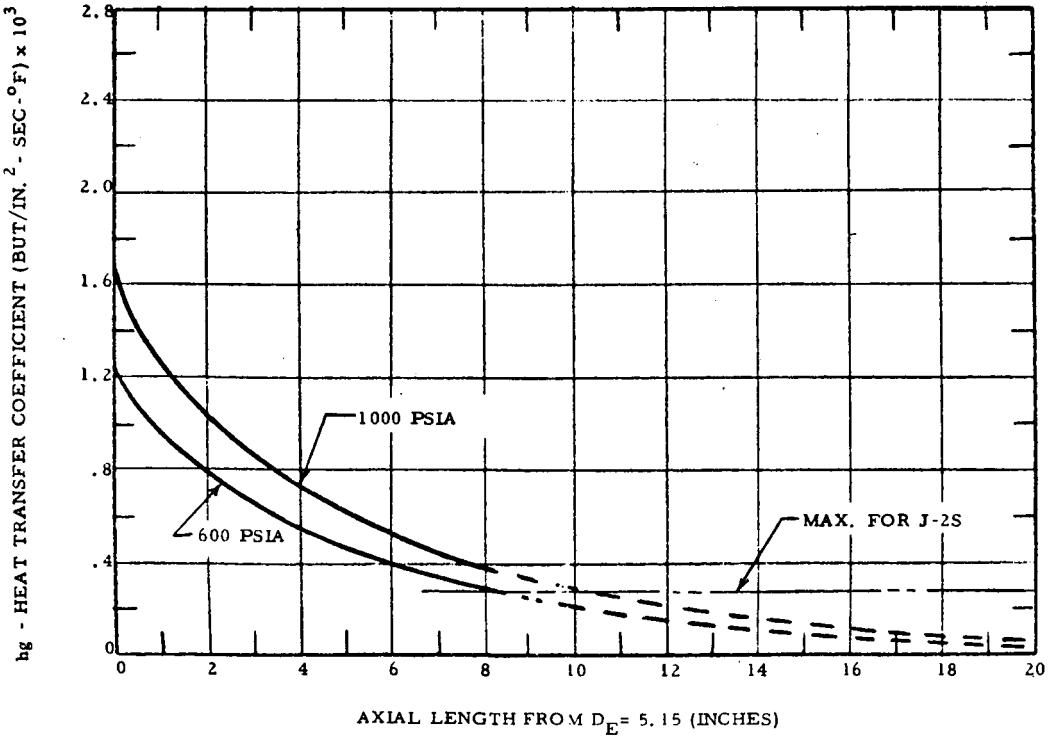

Figure 20. Heat Transfer Coefficient - 4K Engine

The thermal transport properties required for evaluating equation (8) were taken from Reference 6 at the appropriate chamber pressure, combustion temperature and mixture ratio presented in Table IV. The results are shown in Figure (20) for two combustion chamber pressures. The axial distance shown in Figure 20 is referenced from the exit plane of the 4K engine where the exit diameter is 5.15 inches. The heat transfer coefficients vary from a maximum value of 0.0016 Btu/in^2-sec-°F to 0.000038 Btu/in^{-2}-sec-°F for a combustion chamber pressure of 1000 psia and from 0.0012 Btu/in^2-sec-°F to 0.000028 Btu/in^2-sec-°F for a combustion chamber pressure of 600 psia. It appeared that in order to duplicate the J-2S nozzle extension heat transfer coefficients, a point of attachment 8 to 10 inches from the Reference 4K exit plane was required.

The nozzle extension flow rate requirements were examined on the basis of internal Airmat pressure varying from 4.5 psia to 20 psia. The 4.5 psia pressure was predicted to be the maximum static pressure acting on the nozzle extension during the rocket engine operating time while the latter pressure was the maximum pressure at which the turbine exhaust gas would be supplied. A nominal porosity range varying from a 0.5% to 1.5% was examined since it appeared that this porosity goal could be achieved during the weaving of Airmat cloth. The flow rates were calculated using equation (6) using the rocket exhaust gas and coolant gas properties listed in the following table:

	4-K Rocket Engine Exhaust Gas	Hydrogen Coolant Gas
Specific Heat (Btu/lb-°F)	0.92	3.42
Ratio of Specific Heats	1.17	1.40
Molecular Weight (lb/lb-mole)	12.1	2.00
Recovery Temperature	6000°R	- -
Coolant Inlet Temperature	- -	600°F

The results of the computations are shown in Figure 21. The mass velocity of the coolant gas is shown as a function of the internal Airmat pressure for three Airmat porosity values. The mass velocity of the J-2S nozzle extension was expected to be 0.075 lb/sec per square foot of surface area. At this mass velocity and a porosity of 1%, the internal Airmat pressure would be 12 psia. Assuming the surface area of sub-scale nozzle extension to be 3 square feet, a coolant gas flow of 0.225 lb/sec would be required. An increase in porosity to 1.5% for the same

coolant gas flow rate would decrease the internal Airmat pressure to 8 psia.

The inside surface temperature was calculated using the effectiveness ratio given by equation (5). The coolant gas flow rate was obtained from Figure 21 for a porosity of 1%. Using the test rocket engine gas characteristics and the coolant gas properties presented, an inner surface temperature of 620°F was calculated for the assumed transpiration cooling conditions.

2. Test Results

The preceding calculations were based on nominal test rocket engine operating characteristics and tentative nozzle extension geometry. The objective of the study was to establish the test conditions under which the test evaluation of the extendable nozzle extension could support full scale design analysis.

To establish the final design of the test model nozzle extension,a more complete definition of the test rocket engine operating characteristics was desirable. This information was obtained by test firing the test rocket engine with a dummy nozzle extension installed. The dummy nozzle extension was fabricated from steel materials and simulated the geometry of the actual nozzle extension. The following table summarizes the test rocket engine operating characteristics that were obtained.

Engine Combustion Chamber Pressure	=	825 psia
Engine Mixture Ratio	=	4.33
Molecular Weight	=	10.75 lb/lb mole
Specific Heat at Constant Pressure	=	1.3 btu/lb °R
Specific Heat Ratio	=	1.19
Flow Rate	=	8.37 lb/sec
Combustion Chamber Temperature	=	5300°F
Characteristic Velocity	=	7632 ft/sec

These rocket engine characteristics were utilized to obtain a final set of flow parameters required for evaluating the transpiration cooling system.

The zero injection rate heat transfer coefficient is shown as a function of the divergent section area ratio for two wall temperature values in Figure 22. This data was calculated using equation (8) for the rocket engine data presented above, while the wall temperatures were obtained by measurements conducted on the steel wall nozzle extension during rocket engine test firings. At a down-stream area ratio of 27.5, the zero injection rate heat transfer coefficients were predicted to vary from about 0.0003 to

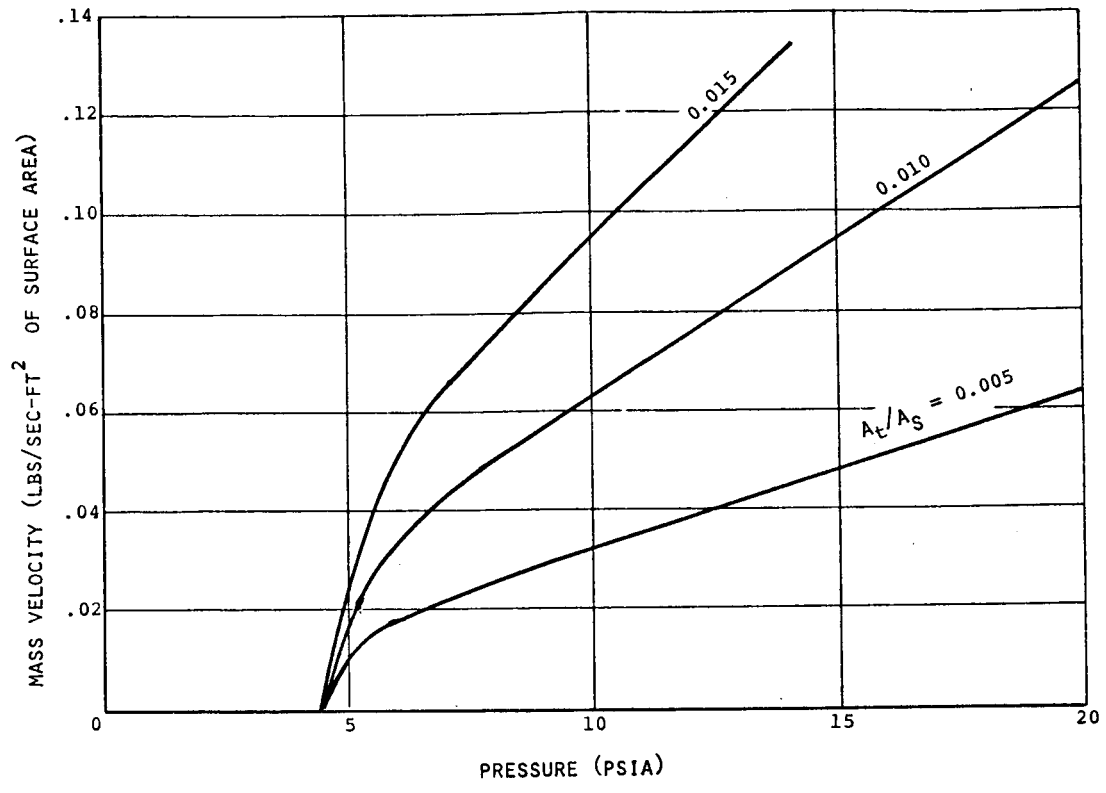

Figure 21. Mass Velocity vs Airmat Pressure - Sub-Scale Nozzle Extension Cooling Gas - Hydrogen

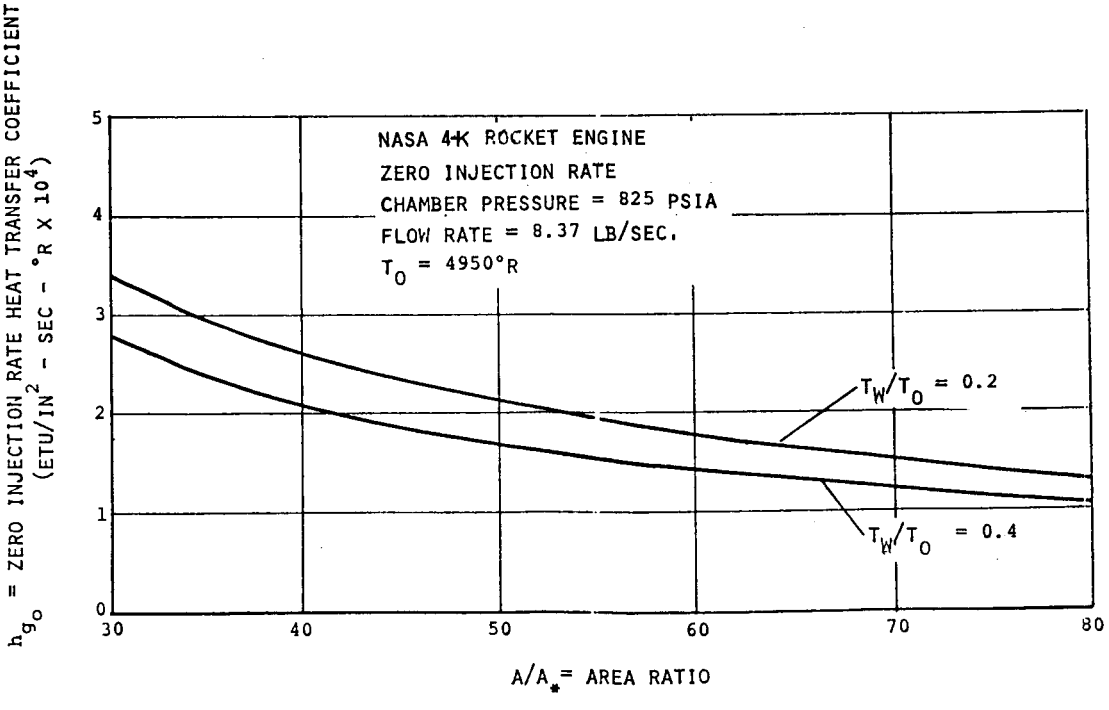

Figure 22. Nozzle Extension Heat Transfer Coefficients

0.00037 Btu/in^2-sec-°R while at an expansion ratio of 80, these values varied from 0.0001 to 0.00013 Btu/in^2-sec-°R. At the forward location, the solid wall heat transfer coefficients are slightly higher than those expected during J-2S extendable nozzle extension operation. However, good simulation can be achieved at an area ratio of about 40.

The static pressure acting on the solid wall nozzle was also measured. These pressures are shown in Figure 23 as a function of the divergent section area ratio. Good agreement with the theoretical pressure distribution which was calculated using the rocket engine data was indicated. This agreement thus supports the validity of the zero injection rate heat transfer coefficients that were presented in Figure 22 .

The mass velocity of the hydrogen coolant gas was calculated using equation (7) as a function of internal Airmat pressure for two porosity levels. These flow rates are shown in Figure 24 and 25 . The Airmat internal pressure is given in absolute units since the diffuser section used in the test set-up was capable of simulating high altitude conditions, i.e. a very low ambient back pressure with respect to the rocket engine. A coolant gas inlet temperature of 60°F was utilized to calculate the mass velocity coolant flow rates since the first series of tests were to be conducted with unheated coolant gas. Superimposed on the theoretical data are seven test points obtained during rocket engine operation of sufficient duration to establish steady state transpiration cooling conditions. The first test point (#12) was purposely conducted at a relatively high coolant flow rate (0.168 lb/sec-ft^2) to check out the transpiration cooling system as well as the instrumentation integrity. The porosity of the expandable nozzle section was established to be slightly higher than 1%. An internal Airmat pressure of 17.8 psia was obtained at the test coolant flow rate. The six other points were obtained during rocket engine steady state operating conditions at much reduced flow rates. The internal Airmat pressure ranged between 10 and 14 psia. The average porosity level resulting from these tests indicate a porosity of about 0.075. The decrease in porosity for these series of test points was evidently due to a cleaning technique used after a repair operation on the expandable nozzle extension conducted after the first test. This repair operation is discussed elsewhere in this report.

Two other porosity test points at an elevated coolant gas inlet temperature obtained during steady state rocket engine firing are shown in Figure 25 . The mass velocity was again calculated using equation (7) as a function of internal Airmat pressure for two porosity levels and three different elevated coolant gas inlet temperatures. The porosity for these two test points appears to be 0.008 for a coolant gas inlet temperature

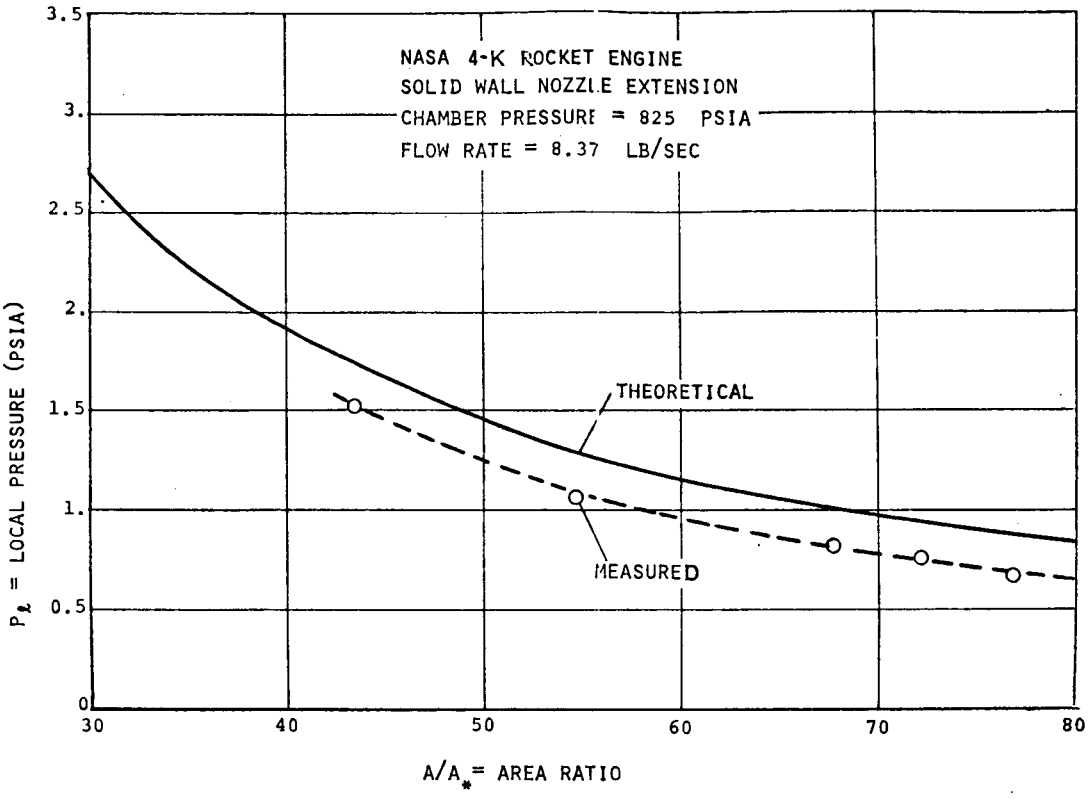

Figure 23. Pressure Distribution

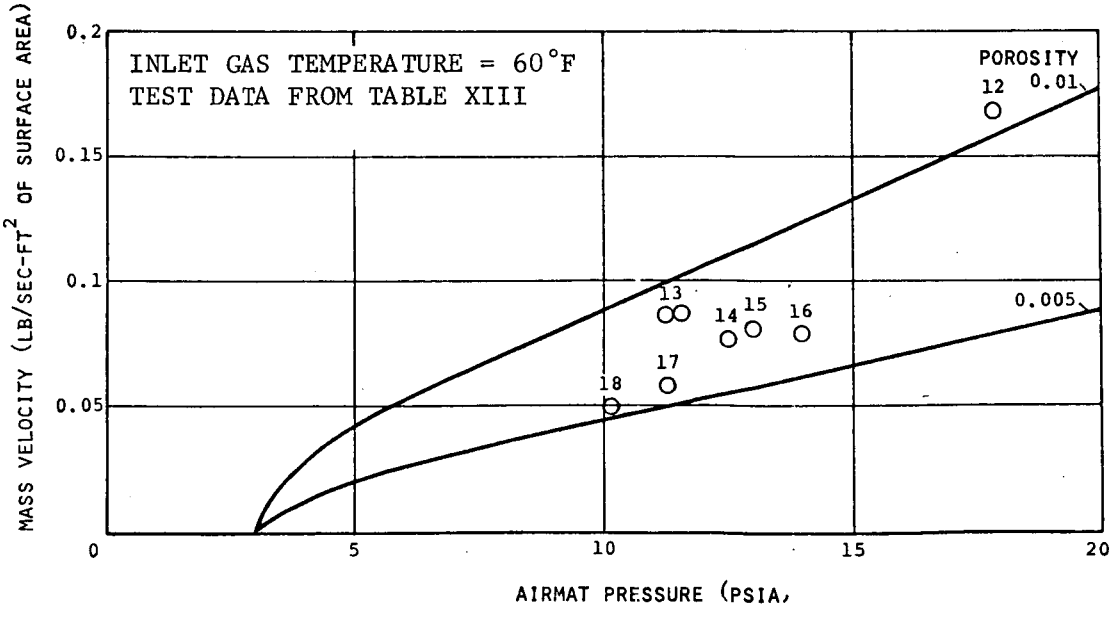

Figure 24. Mass Velocity vs Airmat Pressure

ranging from 200°F to 300°F.

All of the flow data obtained during the test rocket engine firing correlate well with the theoretical flow data generated by equation (7). This equation assumed that sonic flow exists in cloth openings and the coolant gas transpiring through the very low porosity cloth is then a function of the internal coolant gas pressure, temperature as well as the gas physical properties. The gas flow test data obtained on the very thin, very low porosity cloth reinforce the validity of this assumption.

The test flow data was then converted into the dimensionless flow parameter $(c_{pc}/c_{pg})(F/St_o)$ to be plotted against the evaluated effectiveness ratio that was calculated using the measured temperatures. This data presentation is shown in Figure 26 along with the Bartle and Leadon theoretical effectiveness ratio. Most of the data points fall below the Bartle and Leadon data. On the basis of this data comparison it appears that the transpiration cooling system, as utilized in Airmat material, is more effective than the Bartle and Leadon correlation indicates.

A more direct approach toward reducing the test data is shown in Figure 27 and 28 . Utilizing equation (5); the temperature of the inner surface of the Airmat nozzle extension was calculated as a function of the coolant gas flow rate for three different coolant gas inlet temperature straddling the test conditions. These calculations are shown as solid lines in Figures 27 and 28 . The measured temperature extremes are shown as vertical lines. The data shown in Figure 28 was separated from the data shown in Figure 27 for clarity purposes. The test data appear to correlate very well with the theoretical data calculated using equation (5). This is particularly true in the case where the coolant gas flow rate has been decreased to the lowest flow rate values during testing. At these reduced flow rates, the measured surface temperatures reached a maximum level for any of the test conditions.

On the basis of the correlation described above, it was concluded that the measured surface temperatures appeared to be slightly lower than those predicted by using equation (5). Therefore, an attempt was made to develop a modification of the Bartle and Leadon equation for the effectiveness ratio that would fit the test data more closely. The purpose of this effort was to define an effectiveness ratio equation that would account for the observed transpiration cooling technique as used in conjunction with an Airmat expandable nozzle extension. The modification consisted of simply varying the constant which multiplies the dimensionless flow parameter in the effectiveness ratio equation. The results are shown in Figure 29 . In particular, the equation

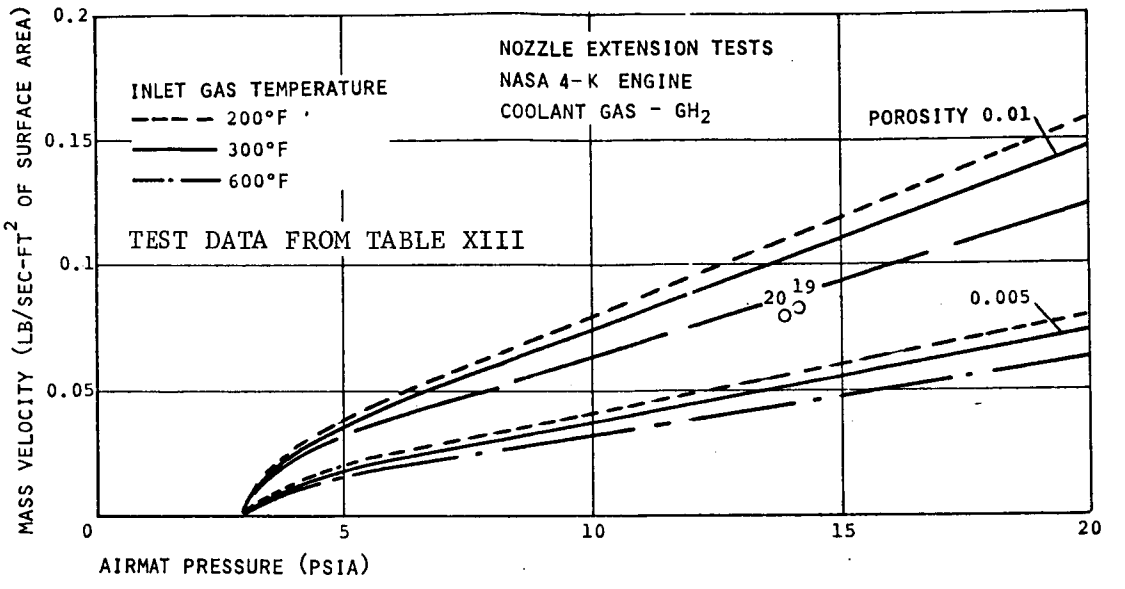

Figure 25. Mass Velocity vs Airmat Pressure (Continued)

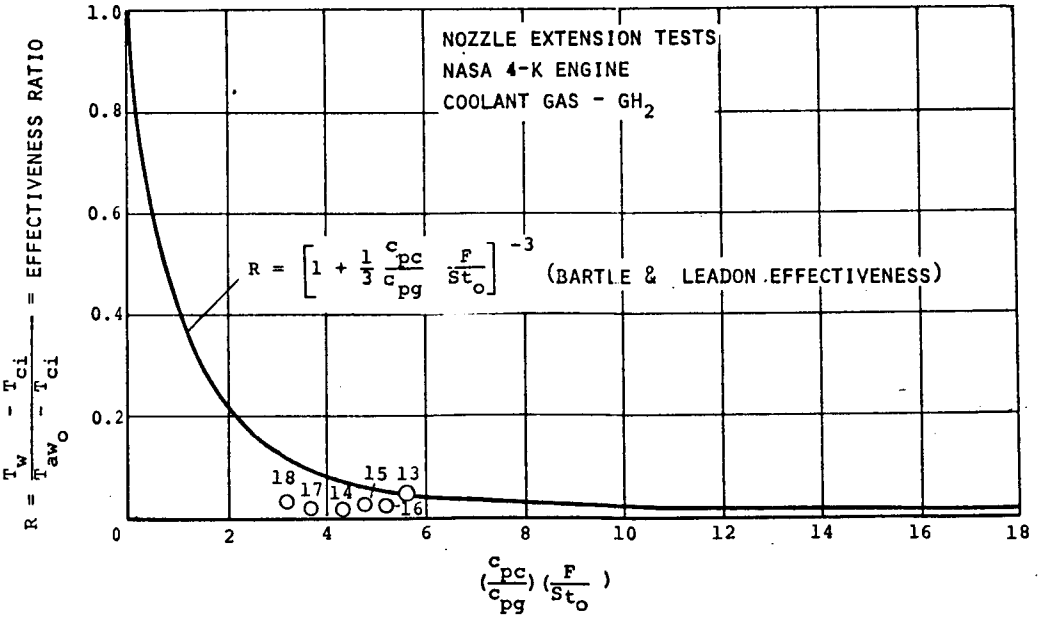

Figure 26. Transpiration Cooling Correlation

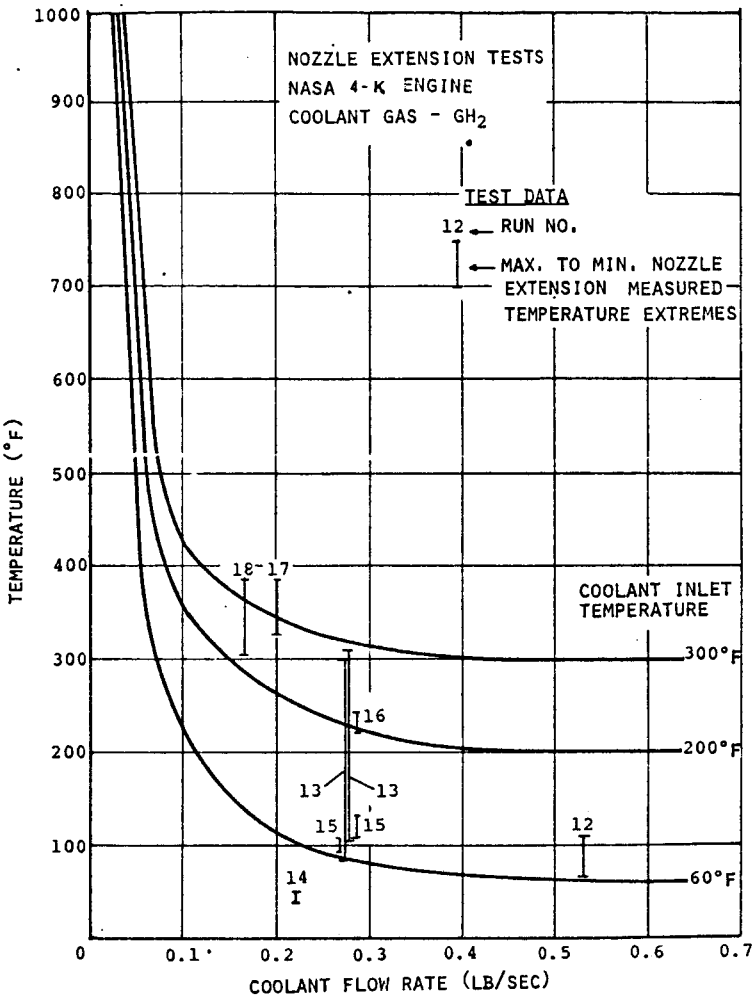

Figure 27. Airmat Temperature vs Coolant Flow Rate

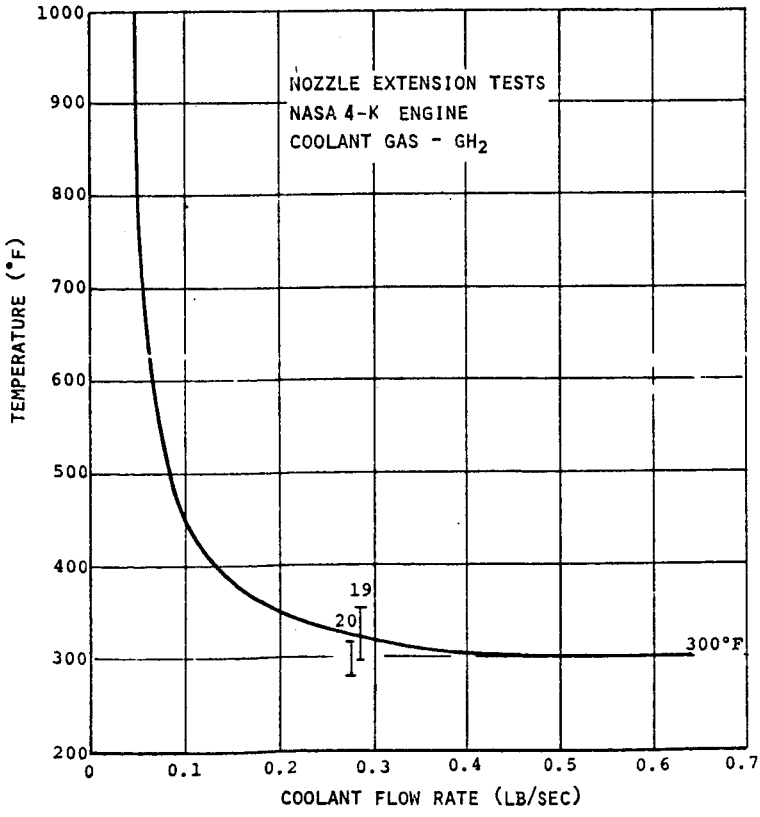

Figure 28. Airmat Temperature vs Coolant Flow Rate (Continued)

$$R = \left[1 + \frac{3}{4}\left(\frac{c_{pc}}{c_{pg}}\right)\left(\frac{F}{St_o}\right)\right]^{-3} \qquad (9)$$

formed an expression that fits the test data satisfactorily.

F. J-2 NOZZLE EXTENSION

On the basis of the positive results obtained from the subscale nozzle extension test program, a decision was made to proceed with the design and fabrication of a full scale J-2 rocket engine nozzle extension. The thermal and flow design criteria are presented here. The design criteria is based on the J-2 rocket engine operating characteristics presented in Table V .

1. Coolant Gas Mass Velocity Criteria

The coolant gas or simply the turbine exhaust gas flow rate has been specified to be 5.22 lb/sec at a supply pressure of 20.9 psia to the nozzle extension manifold. In order to determine the mass velocity of the coolant gas for the nozzle extension the mass velocity as a function of nozzle extension, surface area was calculated by dividing the prescribed coolant gas flow rate by the nozzle extension inside surface area as the area ratio was increased. The results of this computation are shown in Figure 30 . The mass velocity of the coolant gas varies from 0.165 lb/sec-ft^2 for a surface area of 31.4 ft^2 at an area ratio of 35 to 0.04 lb/sec-ft^2 for a surface area of 128.8 ft^2 at an area ratio of 55.

2. Nozzle Extension Pressure Criteria

The internal pressure of the Airmat nozzle extension has been shown to be a function of the mass velocity, the porosity of the inner surface and the coolant gas properties. One of the principle design parameters for defining the geometry of the J-2 nozzle extension is the internal pressure. This pressure was calculated using equation (7) and gas properties presented in Table III for four porosity levels. The results are shown in Figure 31 . Using the mass velocity criteria presented in Figure 30 and assuming a nominal porosity of 1%, the nozzle extension pressure would be 19.3 psia for an area ratio of 35 and 4.7 psia for an area ratio of 55. Increasing the porosity to 1.5% would decrease the internal pressure to 12.9 psia at lower area ratio and drop the internal pressure to 3.3 psia at the upper ratio. Conversly, decreasing the porosity would increase the internal pressure significantly.

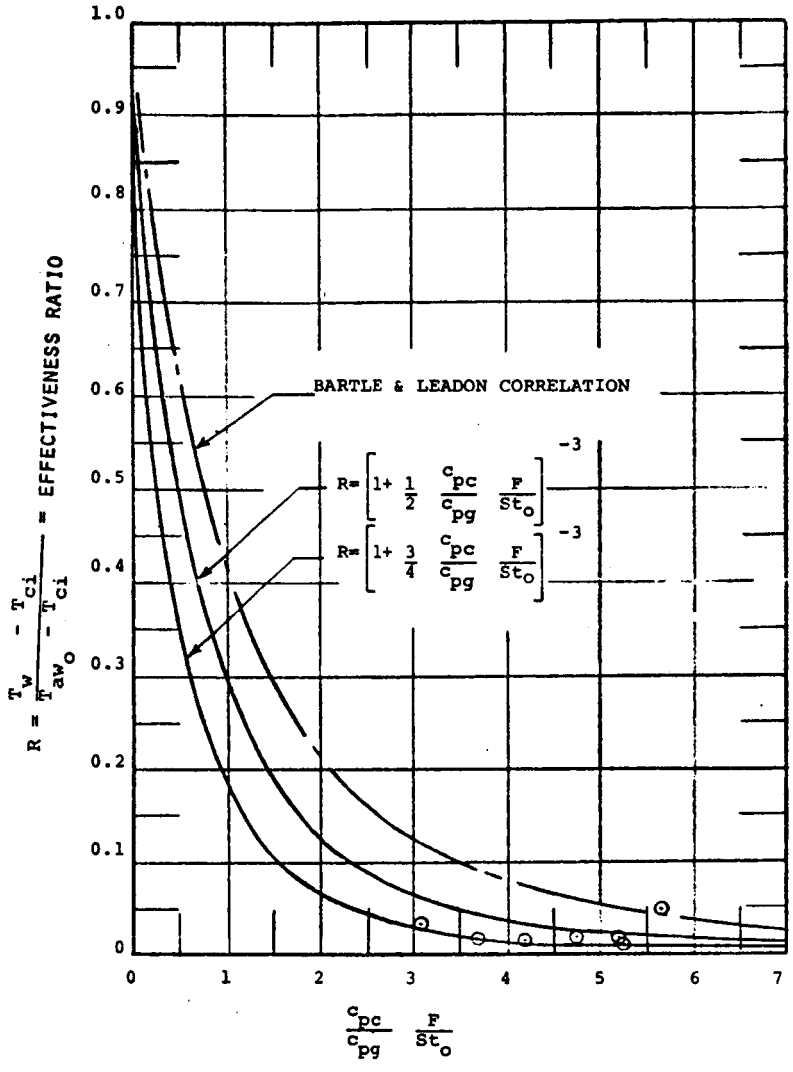

Figure 29. Transpiration Cooling Correlation

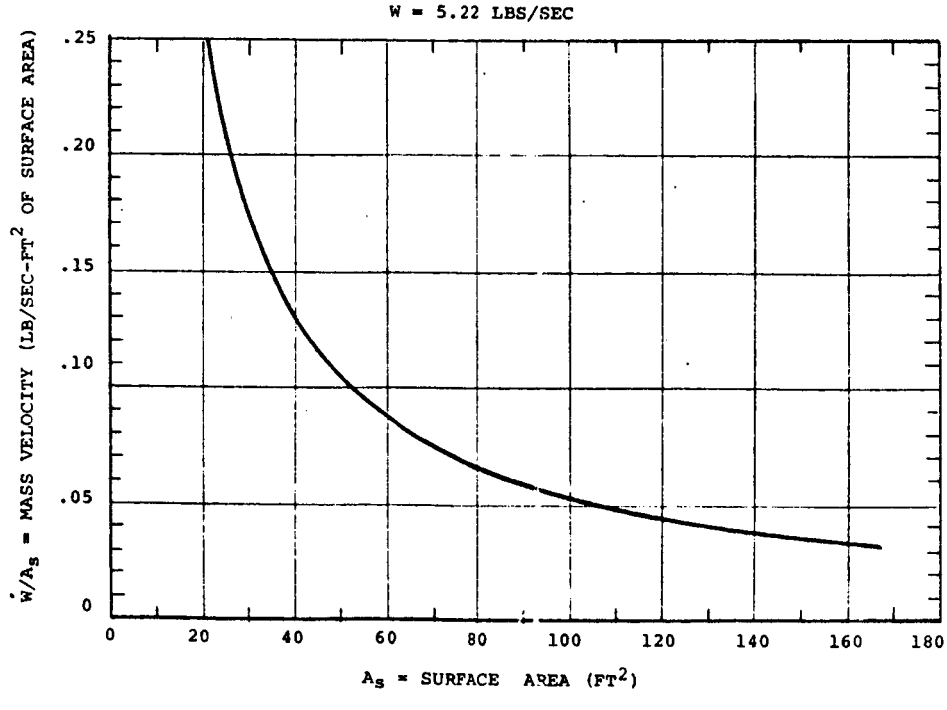

Figure 30. Coolant Mass Velocity vs Nozzle Extension Surface Area

3. Cooling Effectiveness Ratio

The transpiration cooling system effectiveness of the Airmat nozzle extension is primarily a function of the ratio of the specific heat of the coolant gas to the specific heat of the rocket engine exhaust, the mass velocity ratio of the coolant gas to the rocket exhaust gas and the non-dimensionalized heat transfer coefficient. These latter terms form a non-dimensional flow parameter which has been correlated with test data to define an effectiveness ratio for an active transpiration cooling system. The effectiveness ratio has been defined to follow equation (5) on the basis of correlated test data obtained by Bartel and Leadon. However, test results obtained in this program yield an effectiveness ratio that has been correlated to follow the relationship given by equation (9). Since the effectiveness ratio is also a measure of the temperature of the transpiration cooled surface, it is also a design parameter required to define the J-2 nozzle extension geometry. Thus, equation (9) was utilized to obtain the inner surface temperature.

The properties of the coolant gas, the rocket exhaust gas and the heat transfer coefficient are now used to evaluate the dimensionless flow parameter for an expandable nozzle extension out to an area ratio of 55.

$$\frac{c_{pc}}{c_{pg}} = \frac{2.035}{0.92} = 2.21$$

$$F = \frac{(pv)_c}{(pu)_g} = \frac{(5.22/128.8)}{(534/9320)} = \frac{0.0406}{0.572} = 0.071$$

$$St_o = \frac{1.7 \times 10^{-4} \times 144}{(534/9320)(0.92)} = 0.0465$$

Then

$$\frac{c_{pc}}{c_{pg}} \frac{F}{St_o} = \frac{(2.21)(.071)}{(0.0465)} = 3.38$$

Entering Figure 29 at the value of the non-dimensional flow parameter yields and effectiveness ratio of about 0.025. The surface temperature at the attachment point may be calculated from the effectiveness ratio as follows:

$$T_w = R(T_{aw} - T_{ci}) + T_{ci}$$

$$T_w = 0.025\ (5700 - 524) + 524 = 654°F$$

Since the only variable in the non-dimensional flow parameter for a specified set of flow properties and a geometric arrangement is the heat transfer coefficient, the surface temperature along a nozzle extension ray may be calculated. The heat transfer coefficient diminishes along a ray yielding an increasing non-dimensional flow parameters. In turn, the surface temperature of the transpiration cooled surface decreases as the distance along a ray increases. The surface temperature at the exit plane was calculated to 576°F. The surface temperature using equation (5) i.e. the Bartle and Leadon correlation would predict the fore and aft surface temperature variation to range from 1041°F to 784°F.

If it is assumed that the nozzle extension is to be less than for an area ratio of 55, the surface temperature range in the fore and aft direction would decrease. This decrease in the surface temperature range would be due to an increase in the non-dimensional flow parameter which leads to a reduced value of the effectiveness ratio. Hence, a set of lower surface temperature values.

4. System Pressure Drop Analysis

The pressure drop in the turbine exhaust gas ducting system was analyzed to determine if this parameter may compromise the design of the nozzle extension. The analysis was conducted on the basis of a weight flow rate of 5.22 lb/sec being available for transpiration cooling the Airmat nozzle extension section. This flow rate is available at a pressure of 20.9 psia.

The pressure drop in the flow system would be that due to a right angle turn from the exhaust duct into the manifold, expansion from the exhaust duct into the manifold, a right angle turn into the orifices feeding the Airmat section, compression and expansion through the orifices, and finally that pressure drop due to friction forces. These individual pressure drops in the duct system were then estimated in terms of the equivalent duct length of manifold. The Darcy-Weisbach relationship, given as equation (10) was then employed to calculate the pressure drop in the flow system:

$$\Delta p = f\left(\frac{L}{D}\right)_{equi.} \left(\frac{1}{2} \rho v^2\right) \qquad (10)$$

The results of the analysis are shown in Figure 32 . The pressure drop in the duct system has been estimated to be about 5.4 psi at a flow rate of 5.22 lb/sec. The resulting pressure in Airmat nozzle extension would be 15.5 psi. However, the Airmat material porosity is expected to be in the order of 1%. At this porosity level and a flow rate of 5.22 lb/sec., the resulting Airmat pressure is expected to be in the order of 7-8 psia. Thus, the pressure drop in the duct system should not limit the steady state operation of the nozzle extension.

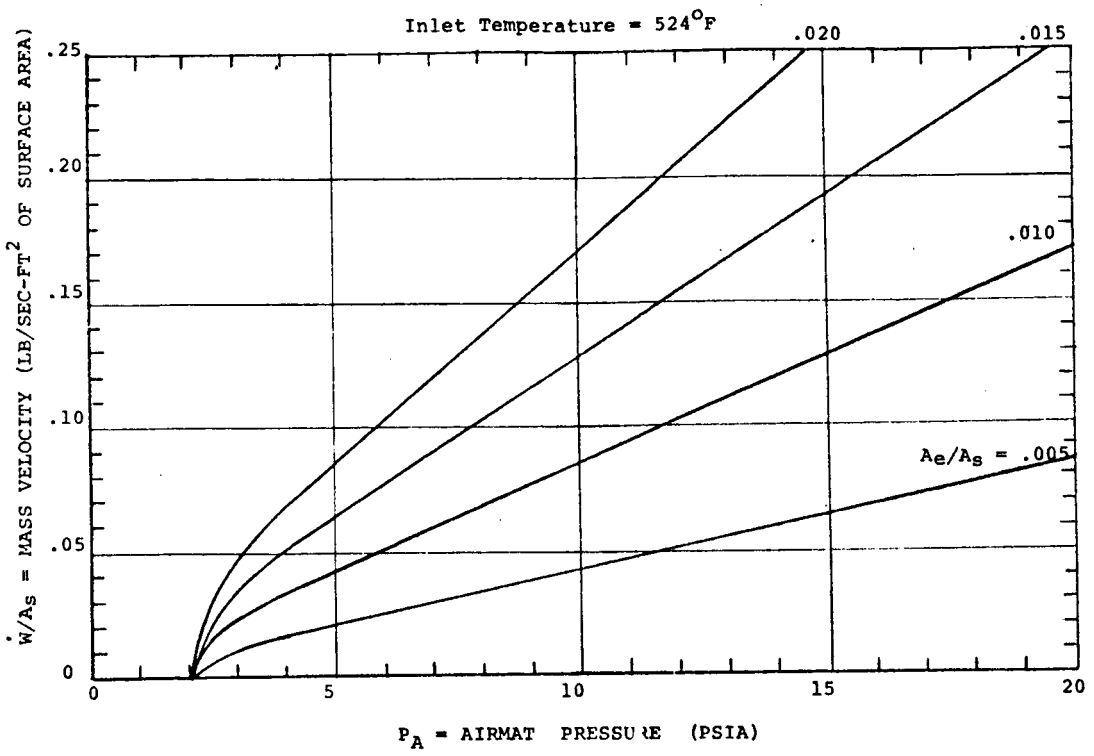

Figure 31. Coolant Mass Velocity vs Airmat Pressure

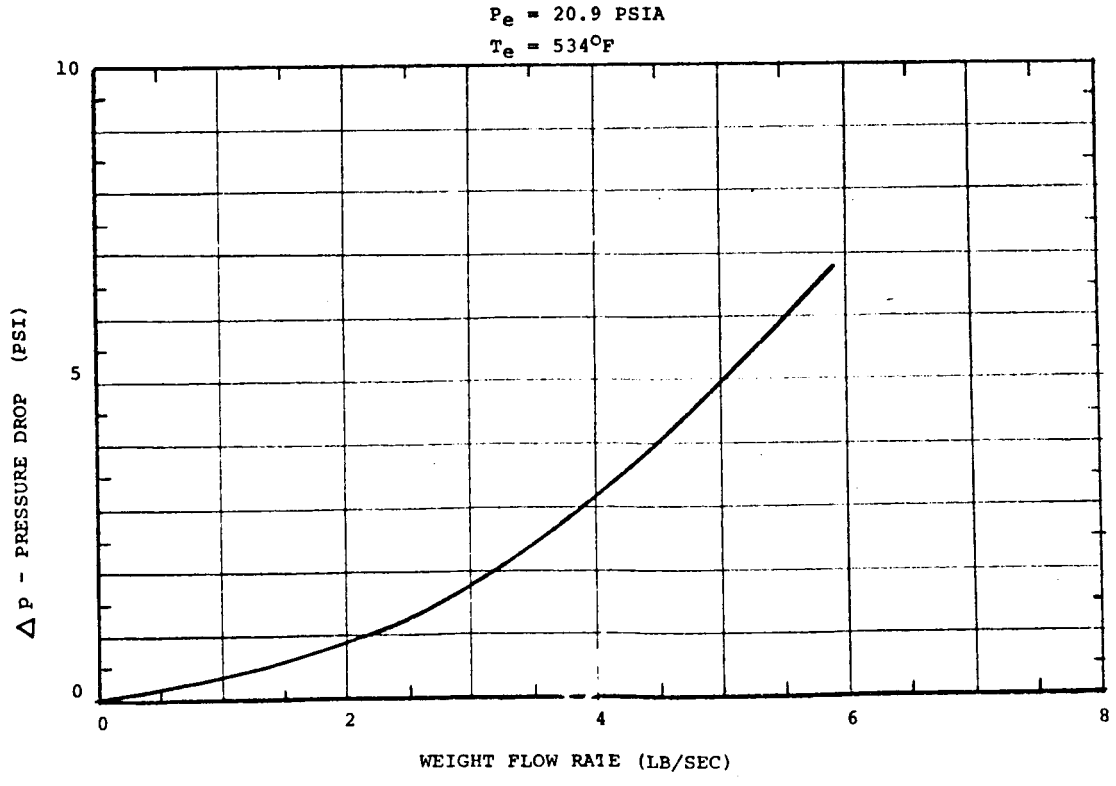

Figure 32. Pressure Drop vs Weight Flow Rate

SECTION V

SUBSCALE NOZZLE EXTENSION TESTING

A. NOZZLE EXTENSION DIMENSIONAL CHECK

Prior to shipping of the test model extension to NASA, a flow or pressure test was conducted on the extension. The purpose of this test was to obtain porosity measurements on the extension to ascertain the effects of fabrication on the Airmat porosity, to check the leak tightness of the extension coating, and to check the general nozzle shape characteristics. Figure 33 shows the test setup.

The nozzle extension was bolted to a piece of three-quarter inch plywood which had cut in it, six equally spaced slots with an O.D. of 14.25 inches and an I.D. of 11.25 inches, with 1.5 inches between slots, giving a total inlet area of 43.65 square inches. A one-half inch thick piece of plywood, 11.20 inches in diameter was used as a spacer between the inner ring of the specimen and the mounting panel. A six-inch diameter hole was also cut in the mounting panel as a bypass. This hole could be closed by means of a slide gate recessed in the forward face of the panel.

The panel with extension installed was bolted to the outlet side of a Buffalo Forge blower. Surgical tubing, one-quarter inch in diameter,was run from the four pressure measurement fittings on the specimen to four water manometers in order to obtain the Airmat pressure.

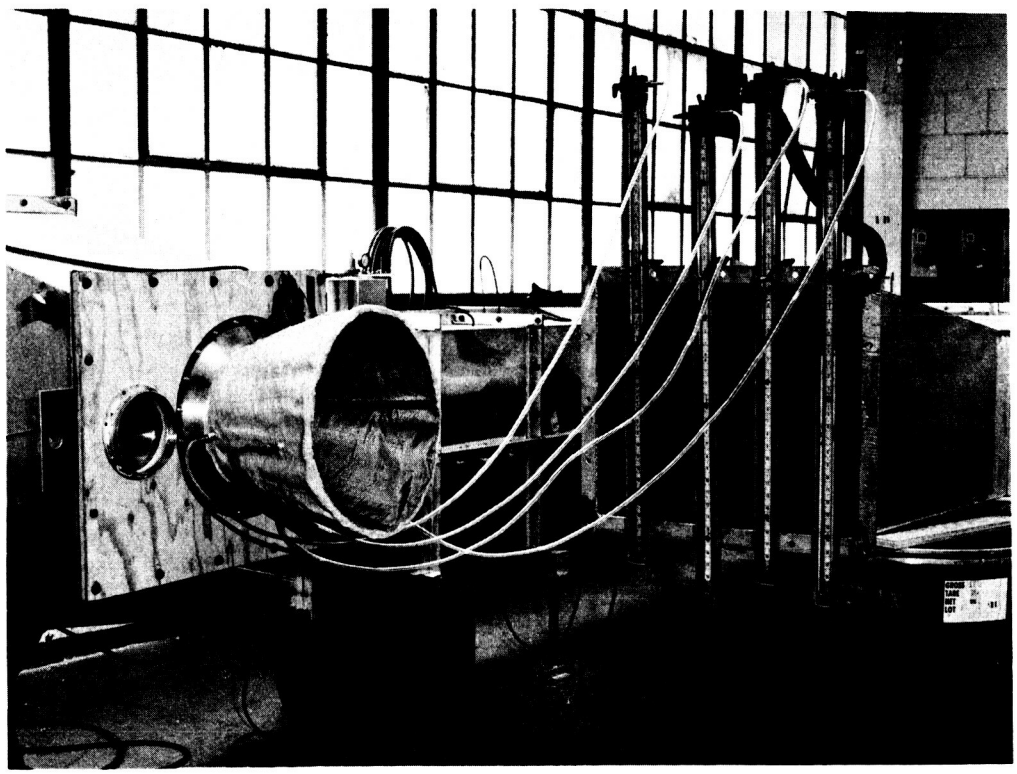

Figure 33. Subscale Model Nozzle Extension Flow Test Setup

Air velocity readings were obtained from a mechanical anemometer which was centered in a hole with an area of one square foot in another three-quarter inch plywood panel which was bolted to the inlet side of the blower.

The blower was turned on with the slide gate in the mounting panel open. The slide gate was gradually closed and the Airmat nozzle extension was inflated.

Two series of test readings were taken, each for approximately two minutes. Air velocity was read on the anemometer at the inlet of the wind tunnel. Static pressure in the nozzle was read on each of four water manometers, while pressure upstream of the specimen was read on a fifth water manometer.

The test readings are presented in Table XII.

Table XII. Test Measurements - Subscale Model Nozzle Extension

Dial Reading	Time.	Velocity	Inlet Area	Volume Flow Rate	Upstream Static Press.	Airmat Pressure Pa - Inches Water				Air Temp. T_a	Amb.Press. P - In/Hg.
N(ft)	t(min)	V = N/T	A	Q = AV	Psi-In. Water	1	2	3	4		
814	2:00.10	406.99	1 Ft^2	407	9.7	9.8	9.6	10.2	9.2	71°	28.94
772	1:59.87	386.42	1 Ft^2	386	9.6	9.6	9.6	10.0	9.0	71°	28.94

The purpose of conducting a few tests on the fabricated model nozzle extension was to confirm the 1 percent porosity obtained earlier from fabric specimen tests. Since the total pressure capability of the test facility was limited to a relatively low value of total pressure when compared to the pressure range available from the J-2S turbine exhaust gas, the experimental evaluation was limited to evaluating porosity of the nozzle extension at a very low pressure differential. Inserting the experimentally obtained values of air flow rate ($\sim$ 400 CFM), at an Airmat pressure of 735 mm of Hg and a temperature of 71°F into the mass flow rate equation for less than sonic velocity at the porous surface, yields a porosity of less than 1 percent. This confirmed the specimen porosity evaluation tests which indicated that a porosity of 1 percent should be expected.

B. SUBSCALE MODEL TESTING

The subscale model nozzle extension testing was conducted at the NASA, George C. Marshall Space Flight Center, facility at Huntsville, Alabama. Several cold flow tests were performed to evaluate the nozzle porosity and to check for any leakage. The major test program consisted of ten hot-firing tests with the nozzle installed on a 4-K Rocket Engine test facility. These tests were conducted at coolant flow rates varying from 0.53 lbs/sec to 0.17 lbs/sec with the engine operating at chamber pressures ranging from 823 psia to 1000 psia. These tests have shown feasibility of the nozzle transpiration cooling concept.

The test setup is shown in Figure 34.

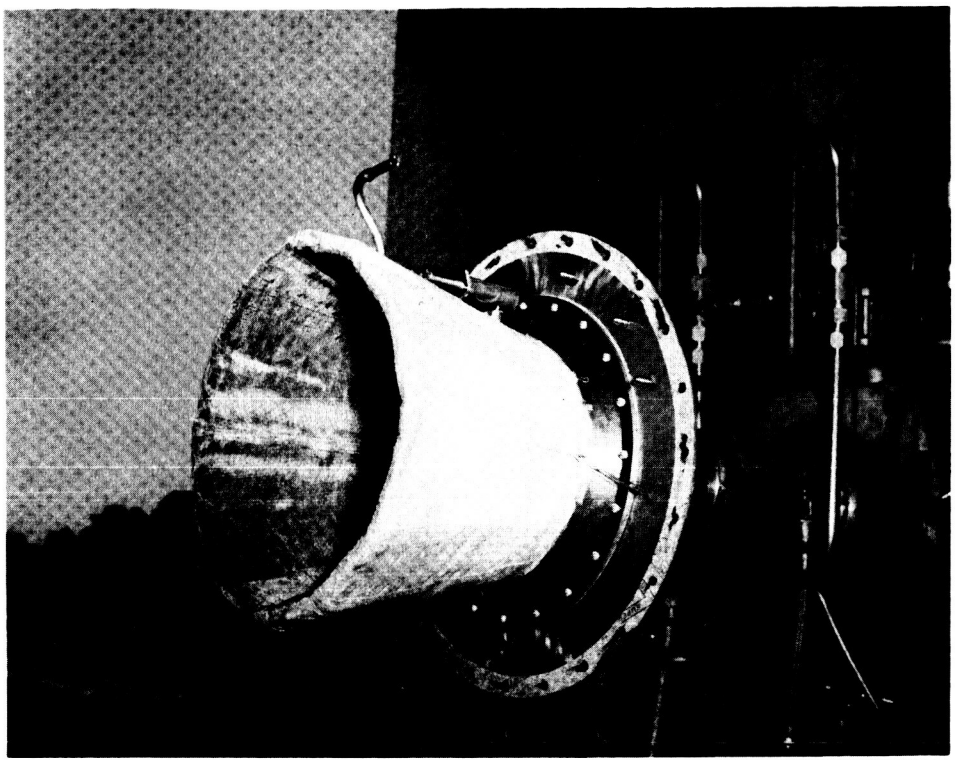

Figure 34. NASA 4-K Engine Test Setup

1. First Test Series

Upon receipt of the subscale test model from GAC, NASA installed it on the 4-K engine test facility. Cold flow tests were first conducted to verify the Airmat inner wall porosity, and second to check the test setup for leakage. These tests confirmed that the inner wall porosity was approximately one percent and that the test model was acceptable for hot-firing tests.

The first test was conducted on 30 April 1970 with coolant flow rates larger than available on the J-2S Rocket Engine. The nozzle extension wall pressure was established at 20 psia using nitrogen as the coolant gas. The 4-K engine was started and the coolant switched to hydrogen. Measurements of Airmat pressure, Airmat inside face temperature, Airmat outside face temperature, coolant supply temperature, and coolant flow rate were recorded.

The test data shows that the Airmat pressure stabilized at approximately 18 psia. The maximum inside wall temperature was 107°F, the outside wall temperature was approximately 80°F, the coolant flow rate was approximately 0.53 lbs per second, and the coolant in temperature was approximately 80°F. This data agreed well with predicted values.

The second hot firing test was conducted on 1 May 1970. For this test the coolant flow rate was established at 0.25 lbs per second. This setting, by prediction, would result in an extension Airmat pressure of 10 psia. The

duration of this test was 45 seconds. The test data appeared to be satisfactory except that a higher inner wall temperature than expected resulted.

At the conclusion of the second test firing, it was found that an inner wall burn-through had occurred. The area affected was adjacent to the aft edge of the inner attachment ring. It was concluded that this burn-through was the cause of the higher inner-wall temperature measurements. As a result, the test model was returned to GAC for rework.

2. Test Model Rework

Examination of the test nozzle, after the second test discussed above, showed that a hot spot had resulted along the aft edge of the inner attachment ring. A redesign of the attachment ring and the attachment of the Airmat to this ring was initiated. Figure 35 shows the original design along with the new design.

Basically the metal ring was extended aft by addition of an adapter ring. The metal ring was also reduced in thickness. The Airmat was attached on the outside of the adapter ring rather than on the inside of the metal ring on the original design. Coolant holes were also provided in both the metal ring and in the adapter ring. The net intent of the several detail design changes was to reduce the temperature of the nozzle inner face at the forward attachment area.

The test nozzle was reworked accordingly. Subsequently, a pressure test of the test nozzle was conducted. This test was conducted to check the smoothness

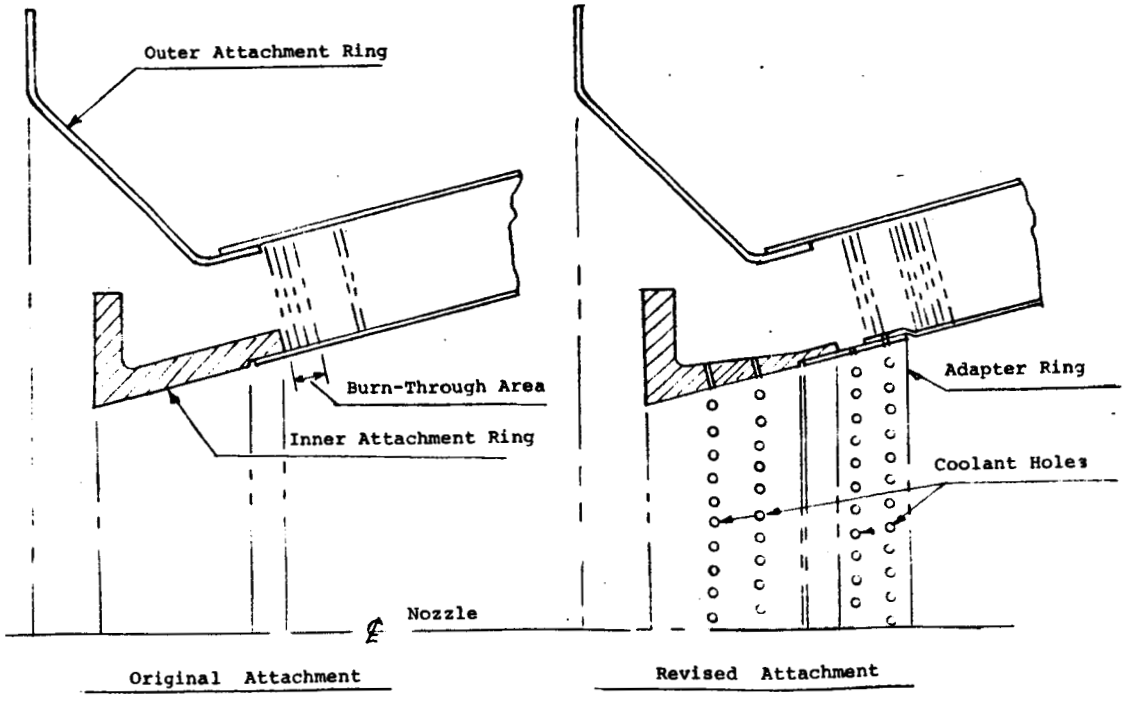

Figure 35. Test Model Rework Details

of the test nozzle Airmat inner surface. During the test, an adjustment of the outer Airmat wall longitudinal tension was conducted by varying the shims between the upper attachment ring and the diffuser bulkhead. By lengthening the outer wall, tension in the inner wall was increased. At the conclusion of this test, the corner wall was smooth and without wrinkles or discontinuities.

In order to pressurize the test model in the above test, the porous inner wall was first coated with PVA. This sealer coat of poly-vinyl-alcohol is water soluble. At the conclusion of the above tests the PVA was removed with hot water and the test model was returned to NASA for further hot-firing tests.

Upon receipt of the nozzle extension, NASA performed a cold-flow test to redetermine the porosity of the Airmat inner wall and to determine the effect on coolant flow rate caused by the addition of the cooling holes in the lower attachment ring and adapter. Upon analyzing the flow test data, it was found that the porosity was approximately 0.25 percent instead of the original 1.00 percent. Therefore, it was apparent that complete removal of the PVA sealer coat had not been accomplished and this coating residue was reducing the inner wall porosity.

As a result, a steam line was connected to the nozzle extension and the steam allowed to flow through the extension wall for several hours. A second flow test was then conducted. The resultant porosity calculations showed the porosity to be 0.75 percent. This indicated that the PVA had been essentially removed and that hot fire testing could proceed.

During the steaming operation, the extension was inadvertently over-pressurized and a local failure in one of the Airmat gore joints occurred. This was repaired using a woven stainless steel patch which was bonded to the Airmat outer wall using Silastic No. 140 cement.

3. Second Test Series

Seven additional hot firing tests were conducted. The total test time for all nine hot-fire tests was 253 seconds. The test variables were coolant flow rate coolant temperature and chamber pressure. The nozzle extension performed satisfactorily during this test series and was in good condition at the completion of the tests.

Table XIII presents the complete data measured during the testing. Figure 36 shows the location of the instrumentation.

C. ANALYSIS OF TEST RESULTS

The test results from Table XIII were plotted on the predicted data curves of coolant flow rate vs temperature and mass velocity vs Airmat pressure to assess the effectiveness and feasibility of the transpiration cooling concept. Since six temperature readings were taken for each test, the data was plotted as a spread between the highest and lowest temperature recorded during each run. See Subsection IV-E of this report for the thermal and flow analysis.

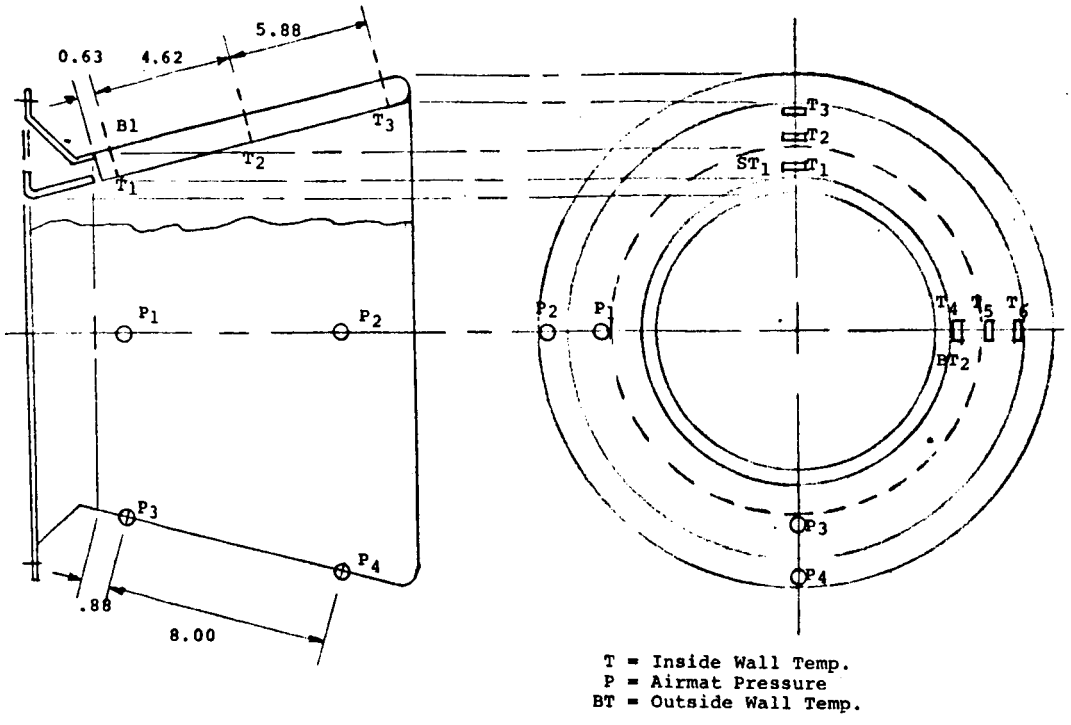

Figure 36 . Test Model Instrumentation

Figures 27 and 28 are plots of the predicted inner wall temperature versus the coolant flow rate at various coolant inlet temperatures with data points plotted on the graph. These data show that the nozzle extension performed as predicted within reasonable limits of calculation and data measurement accuracy.

Figures 24 and 25 are plots of the predicted mass velocity versus Airmat wall pressures for various Airmat wall porosities with the data points plotted on the graphs. These data point-up several conclusions which are:

(1) The nominal inner wall porosity was very close to the 1.0 percent porosity as fabricated.

(2) That at Airmat wall pressures between 10 and 15 psia, the predicted J-2S engine available turbine exhaust flow would effectively pressurize and cool the nozzle extension.

(3) The predicted pressures for the various mass velocities were in good agreement with the actual data.

(4) From the plotted test data, it appears that as the Airmat wall pressures increase the wall porosity increases. This can be explained by the fact that as the pressure increases, the relative relation between yarns in the Airmat changes due to shifting of the individual yarns.

From the tests performed, it was concluded that the transpiration cooled nozzle extension is highly feasible and that it's operation can be predicted.

Table XIII. Test Data

TEST NO. (22S-)	DATE (MONTH/DAY/69)	DURATION (SEC)	ENGINE DATA										DIFFUSER PRESS. (PSIA) AVERAGE	DIFFUSER TEMP. °F	NOZZLE DATA																		MOUNTING RING TEMP. °F	COMMENTS
			LOX INJECTION PRESS. PSIG	GH_2 INJECTION PRESS. PSIG	GH_2 RUN PRESS. PSIG	LOX FLOW (#/SEC)	GH_2 FLOW (#/SEC)	TOTAL FLOW (#/SEC)	O/F RATIO	CHAMBER PRESS. PSIA	CHARACTERISTIC VELOCITY (FT/SEC)				COOLANT CONTROL PRESS. PSIG	COOLANT FLOW (GH_2) (#/SEC)	COOLANT INLET PRESS. PSIG	COOLANT INLET TEMP. °F	COOLANT MANIFOLD TEMP. °F	INTERNAL NOZZLE PRESSURE PSIA				INTERNAL WALL TEMPERATURE °F						BACKWALL TEMP. °F			
																				1	2	3	4	1	2	3	4	5	6	1	2		
12	4-30	10.0	918	1145	1425	7.06	1.46	8.52	4.8	840	7635	1.38	----	755	0.530	108	----	----	17.8	17.8	17.8	17.6	107.0	66.0	66.0	92.0	75.0	84.0	78.5	81.0		
13	5-1	45.0	930	1134	1530	7.32	1.42	8.74	5.2	838	7475	1.20	49.8	348	0.272	48.0	81.0	44	11.3	11.0	11.0	11.1	298.0	81.0	71.0	118.0	84.0	75.0	78.9	69.5		@ 9 sec
	5-1	45.0	930	1160	1528	7.26	1.45	8.71	5.0	845	7513	1.30	89.6	350	0.277	49.5	61.8	98	11.6	11.5	11.4	11.5	308.0	102.0	126.0	199.0	148.0	138.0	153.8	125.5		@ 44 sec
14	6-5	3.6	919	1118	1525	7.14	1.42	8.56	5.0	823	7445	1.16	59.7	351.0	0.271	46.5	----	38.5	----	12.1	11.6	12.3	37.5	39.0	37.0	48.0	37.0	35.0	35.3	122.0	79	
15	6-5	45.0	919	1134	1523	7.25	1.40	8.65	5.2	835	7475	1.18	62.0	347.0	0.267	48.3	70.5	52.0	----	11.8	11.7	12.5	93.0	106.0	71.0	92.0	92.0	55.0	90.5	165.0	97	@ 9 sec
	6-5	45.0	919	1146	1520	7.20	1.46	8.66	4.9	836	7476	1.37	65.2	348.0	0.284	50.0	65.5	108.0	----	13.1	12.0	13.0	116.5	126.0	114.0	127.0	130.0	106.0	113.0	208.0	168	@ 40 sec
16	6-9	30.0	920	1145	1520	7.25	1.39	8.64	5.2	837	7502	1.80	145.2	365.0	0.287	58.5	208.0	217.0	----	14.0	13.2	13.5	219.5	244.3	232.7	242.5	242.5	201.5	246.0	296.0	299.4	
17	6-11	30.0	920	1145	1520	7.19	1.41	8.60	5.1	825	7479	1.20	110.0	254.0	0.203	41.0	306.0	308.3	11.3	11.2	11.3	11.3	385.0	323.6	302.7	336.5	324.8	228.0	329.0	277.5	407.3	
18	6-12	30.0	908	1138	1508	7.15	1.41	8.56	5.1	828	7491	1.20	141.2	210.0	0.170	33.0	296.5	316.8	10.2	9.3	10.0	10.2	331.0	301.0	271.4	326.5	315.5	223.5	298.0	293.5	410.0	
19	6-13	30.0	1025	1245	1645	8.07	1.52	9.59	5.3	915	7389	1.50	158.7	365.0	0.287	63.5	286.4	271.1	14.2	14.1	13.9	14.1	353.0	329.8	298.7	316.6	315.0	295.5	298.5	302.5	376.0	
20	6-16	30.0	1135	1390	1812	8.69	1.72	10.41	5.1	1005	7476	1.60	159.1	352.0	0.277	60.5	270.7	267.0	13.9	15.2	13.5	14.1	316.0	294.5	281.0	301.0	296.0	279.0	295.0	275.0	361.7	

SECTION VI

SUPPLEMENTAL TASKS

A. GENERAL

The program plan included four supplemental tasks which were directed to support the design and the fabrication of the nozzle extensions. In general these tasks were conducted and reported as individual items. A summary of each task is presented in this report for information purposes. For detail information the applicable detail task reports can be consulted.

The four Tasks and their applicable Goodyear Engineering Reports are as follows:

Task b - Coating Investigation, Reference 7

Task c - Design Refinement Investigations, Reference 8

Task d - Heat Transfer Investigation, Reference 9

Task g - Gas Generator Investigation, Reference 10

B. COATING INVESTIGATION

The Task b Coating Investigation was performed to determine the best elastomeric coating material available for sealing of the outer surface of the extendable nozzles.

A survey of candidate coating materials was first conducted. The candidate materials were evaluated for their application characteristics and for their ability to seal the nozzle under applicable environmental conditions. The survey recommended two materials as the most promising. They were Dow Corning silicone materials S-2288 and 92-009.

An evaluation of the coating application characteristics of each material was next conducted followed by a test evaluation of the two materials.

The coating procedures required for the application of either material were found to be practical and are considered to be standard procedures at GAC. The main difference in the coating procedures of the two materials is that the S-2288 elastomer requires an oven cure, while the 92-009 material cures at room temperature. Thus, the curing procedures of the 92-009 material are less complex than for the S-2288 material.

The test evaluation included pressure tests at ambient, elevated, and cold temperatures. Elevated temperature cycling tests, as well as elevated temperature pressure tests after cold temperature flexing of the test specimens, were also conducted. The ambient and cold temperature pressure tests resulted in failure of the Airmat material rather than the coating material. Thus for these conditions,the coating is not the critical material. The three test conditions involving elevated temperatures, in general, showed that the coating becomes the critical material at temperatures of 500°F and above.

The type of coating deterioration at elevated temperature was quite different for the two elastomers. The S-2288 elastomer tends to craze until cracks or leaks result. After cooling the test specimens to ambient temperature, the coating becomes brittle and light flexing will produce many more cracks. The 92-009 material tends to blister and flake off in layers leaving a portion of the coating on the Airmat material. After cooling,the material remains flexible although a portion of the remaining material can be removed by scraping. Analysis of the test results along with inspection of the tested specimens indicates that at temperatures over 500°F deterioration of the coatings may occur. The severity of the resultant leakage depends upon the test condition. In one test condition leakage was not evident at 700°F. The test results indicate that the 92-009 coating material, in general, is more reliable than the S-2288 coating material at temperatures higher than 500°F.

The 92-009 coating material has been shown to be easier to apply and appears to perform more reliably at temperatures higher than 500°F. Consequently it was recommended as the best available coating material for the nozzle extension application.

This task is reported in detail in Reference 7.

C. DESIGN REFINEMENT INVESTIGATION

The Task c Design Refinement Investigation was conducted to fully evaluate the structural characteristics of a nozzle extension. The analysis was applied to the J-2S extendable nozzle. The nozzle extension considered had an expansion ratio of 40 to 1 at its forward end and 73.6 to 1 at its aft end.

The load analysis, the stability analysis, and the stress analysis of the nozzle extension are presented. Loads and stresses in the Airmat are caused by the pressure of the nozzle exhaust gases and by the internal pressure in the Airmat. The internal pressure in the Airmat must be sufficient to ensure that the resultant stresses are tension stresses rather than compression stresses for the stability criteria. The stresses resulting must not exceed the strength properties of the Airmat material.

Investigations were also conducted on analysis refinements. These included an analysis to determine the effect of differential temperatures on the stress distribution in the Airmat. Orthotropic theories were also investigated as the Airmat has different axial and circumferential properties.

A study was also conducted to investigate methods and to predict the natural frequencies and modes of vibration of the J-2S extendable nozzle.

Two special analyses were also conducted. The first investigation involved determination of the deployment loads that might be encountered in deploying the nozzle extension. The second investigation analyzed the nozzle extension for a one-sided sine load distribution.

The most significant results of this design refinement task are summarized below. This task is reported in detail in GER-14913, Reference 8.

(1) The total thrust load on the J-2S, 73.6 to 1 expansion ratio, nozzle extension is calculated to be 6716 pounds.

(2) The Airmat internal pressure requirement for this nozzle extension is 10 psi. This includes a 1.5 safety factor.

(3) The Airmat stresses were calculated using a minimum Airmat pressure of 10 psi and a maximum Airmat pressure of 20 psi.

(4) For a 20 psi inflation pressure, the axial stresses in each surface are approximately 40 pounds per inch. The circumferential stresses are 103 pounds per inch on the inside surface and 93.5 pounds per inch on the outside surface when the Airmat is pressurized to 20 psi and also subjected to nozzle gas pressure.

(5) The axial strength of the Airmat faces are 260 pounds per inch and the circumferential strength is 731 pounds per inch. The strength across the welds is 148 pounds per inch in the axial direction and 312 pounds per inch in the circumferential direction.

(6) The axial and circumferential inflation stresses in the Airmat are just a little different from ph/2 where p equals pressure and h equals Airmat depth. Orthotropic properties and drop yarn extensions do not affect the fabric stresses appreciably.

(7) If the inside surface temperature is 700°F and the outside surface temperature is 600°F, the circumferential stresses become 127 pounds per inch on the outside surface and 70 pounds per inch on the inside surface.

(8) A one-sided sine-load distribution will not cause axial buckling unless the peak pressure is greater than 2 psi. The beam bending deflection may be almost six inches unless shear stiffness is derived from the Airmat material. Some out-of-round buckling will occur in the aft portion unless the pressure is raised to 27 psi.

(9) A dynamic model was used to simulate deployment of the nozzle extension. If the nozzle extension is deployed in two seconds, the axial deployment load on the existing nozzle will be 7500 pounds. If deployment is accomplished in less than two seconds, the deployment load will be higher.

(10) Several approaches or methods of predicting the natural frequency of the J-2S nozzle extension were reviewed. Published approaches to nozzle dynamic analysis, test model data, and GAC experiences in the dynamic analysis of similar structures were considered. It was concluded that the most practical approach would be to obtain dynamic data from tests of scale models and to scale the results up to obtain predicted values for full-scale nozzles.

D. HEAT TRANSFER INVESTIGATION

The Task d Heat Transfer Investigation was conducted to evaluate the basic nozzle extension material heat transfer coefficient.

The transpiration cooling concept used in the design of the extendable nozzles involves a nozzle fabricated of Airmat material. This material is woven from multifilament stainless steel yarns. The outer surface of the Airmat is coated with a silicone elastomer. The inner surface of the Airmat is woven to a controlled porosity, approximately one percent. The rocket engine turbine exhaust gases are used to pressurize the Airmat nozzle extension. As these gases escape through the porous inner wall,they cool the inner wall material which is exposed to the hot engine gases.

Two heat transfer mechanisms are involved in the transpiration cooling process through which heat energy is transferred. The coolant gas absorbs heat energy from the face cloth material, as it passes through this material, because of the temperature differential between the coolant gas and the face cloth material. Secondly, the coolant gas is injected into the boundary layer of the hot rocket exhaust gas flowing parallel to the face cloth. The coolant gas transpiring into this boundary layer thereby decreases the potential of the hot exhaust gas boundary layer to transfer heat energy into the face cloth.

This investigation concerns only the first heat transfer mechanism, to evaluate the amount of heat energy transferred during the passage of the coolant gas through the face cloth material. The investigation involved a test program followed by an evaluation of the test data.

A preliminary test procedure outline, using electrical energy to heat the test specimens, and an alternate test procedure outline, using radiant energy quartz lamps to heat the test specimen, were both prepared by GAC and submitted to the Marshall Space Flight Center, Huntsville, Alabama. NASA selected the test procedure using electrical energy for heating and prepared a final test outline. GAC prepared the test specimens. The testing program was conducted at NASA and the test data was reported by NASA, GAC performed the analysis of the test results and prepared the final test report.

It was concluded, for the range of conditions covered by the tests, that the temperature of the gas after passing through the heated face cloth was equal to the resultant face cloth temperature. Thus the coolant gas temperatures and the face cloth temperatures equalized.

A comparison of test data with published heat transfer coefficient data for flow normal to a cylinder is also presented.

This task is reported in detail in Reference 9.

E. GAS GENERATOR INVESTIGATION

The Task g Gas Generator Investigation was conducted to survey, evaluate and recommend a gas generator which could supply pressurized gas for rapid deployment of the extendable nozzle under development. This concept was considered a back-up to the turbine exhaust deployment gas supply and could be utilized if that source of deployment gas was determined by test to be inadequate.

A gas generator specification was prepared and used as a basis for requesting proposals from five vendors. Three vendors submitted proposals with two vendors declining. Each concept is described in Reference 10. A tradeoff analysis was conducted showing a comparison and evaluation of the concepts. One concept stands out as the best system on the basis of the tradeoff criteria.

This task is reported in detail in Reference 10.

SECTION VII

CONICAL AIRMAT WEAVING DEVELOPMENT

A. GENERAL

Airmat material consists of two simultaneously woven face cloths attached together by a number of drop yarns. The drop yarns are similar to the warp yarns except that they are woven alternately in each face cloth. The drop yarns may be programmed as to their spacing, the frequency of cross-over between face cloths, and their length to achieve design requirements.

Ordinarily, a flat Airmat is woven with identical face cloths. Thus to form a conical surface, as in a nozzle extension, the outer face cloth must be slit and opened up at several locations around the outer periphery of the nozzle extension to allow for the larger circumference of the outer face cloth in relation to the inner face cloth. The opened slits are subsequently joined together by welding a tape across the slits. This requires a considerable amount of welding time in the nozzle extension fabrication procedures. It also produces a discontinuity in the material as the drop yarns are absent in the opened up area.

Consequently, the major development area for this contract involved development of a weaving process to weave conical Airmat. By weaving the Airmat at a programmed differential weaving rate, both across the loom width and between the two face cloths, a true conical nozzle could be formed and tailoring after weaving would not be required. It was also desirable to weave the conical Airmat so that one piece would be sufficient to form a complete nozzle extension.

To achieve the capability to perform conical weaving on the GAC experimental loom, several modifications of the loom were required. The major change involved incorporation of the differential rate of weaving. To achieve the capability to weave the nozzle extension Airmat in one piece required a reversal of the warp and fill directions. The flat Airmat woven during the initial portion of this program utilized the fill direction in the loom as the hoop direction of the nozzle extension. To achieve a one-piece nozzle extension, the warp direction in the loom must become the hoop direction of the nozzle extension.

The program plan for development of the conical Airmat weaving capability included four steps as follows.

(1) GAC Experimental Loom Modification

(2) Loom Setup

(3) Experimental Weaving

(4) Porosity Testing

The experimental weaving and porosity testing was performed to evaluate the qualities of the conical Airmat that could be woven. Two major criteria

were that the face cloth porosity should be in the 1.0 percent range and the dimensional accuracy of the Airmat should be sufficient so that a satisfactorily shaped nozzle would result.

B. LOOM MODIFICATION

This task involved modification of the GAC Experimental Loom to provide a capability to perform conical weaving. The modifications are subdivided as follows:

(1) Take-off System

(2) Let-off System

(3) Selvage Cutter

(4) Gage Blocks

(5) Warping Equipment

1. Take-off System

The major loom modification involved the design, fabrication, and installation, of a new take-off system. The system used for flat Airmat weaving advanced all warp yarns uniformly. To perform conical weaving, the warp yarns must be advanced at a differential rate across the loom. The top and bottom cloths also require a different advancement rate.

To accomplish the conical weaving, the warp yarns were advanced by two tapered pin rolls which were installed in the take-off system. One roll advanced the lower face cloth and the other roll the upper face cloth. The two pin rolls were similar but not identical in diameter. Their diameters were programmed to achieve the proper advancement per revolution of the rolls.

The take-off modification also required the design, fabrication, and installation of a drive system for the pin rolls. This system rotated the two pin rolls at the same rate. The take-off system modification is shown in Figure 37 .

2. Let-off System

Ordinarily,the warp spools are locked-in on a continuous shaft which is geared to rotate and let off yarn a programmed amount as the weaving progresses. This system advances all warp yarns at the same rate. To accomplish conical weaving, all warp yarns must be let-off at different rates. Thus, a redesign of the let-off system was required.

The warp spools were installed on the shaft as before; however, they were not locked to the shaft. The shaft was also fixed. Thus, the spools were free to rotate individually on the shaft. Their degree of rotation was dependent on the tensioning of the warp wires in the loom setup. To provide for a programmed warp tension during weaving, a set of brakes was installed on the loom applicable to the warp spools. Each spool had an individual brake.

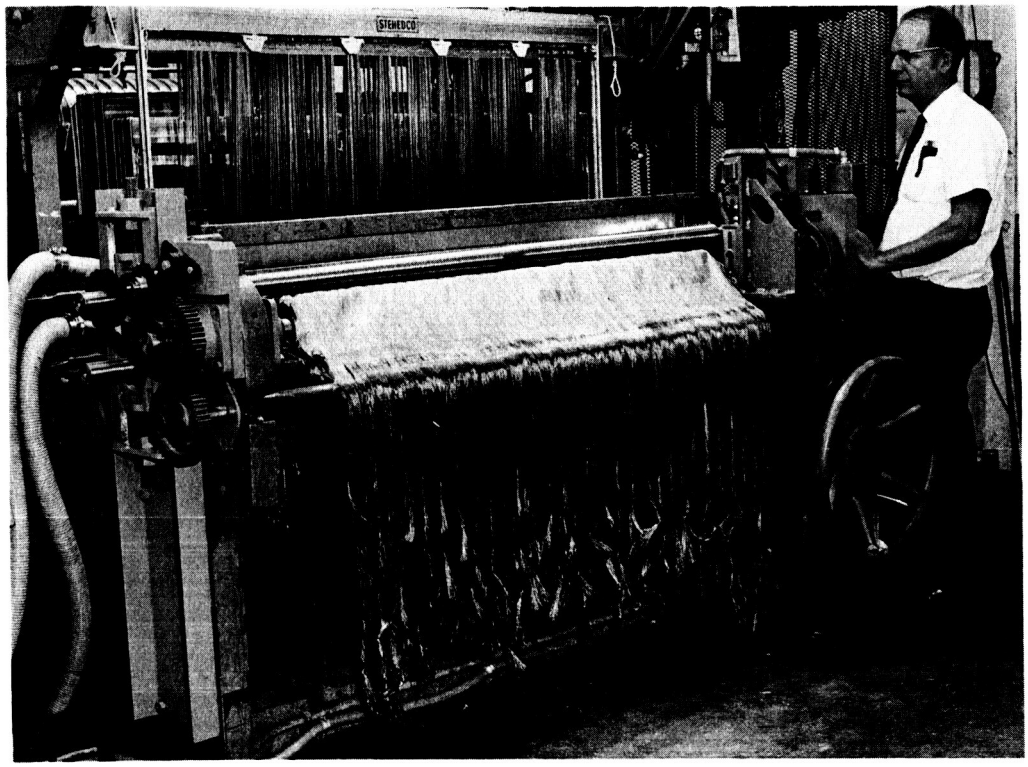

Figure 37. Pin Roll Installation

The brakes were a mechanical device in which a rubber pad was installed on one end of a pivoted arm. Weights were added to the other end of the arm. By adjusting the weights and their lever arm distance, the friction of the rubber pad against the warp spool could be adjusted to regulate the warp yarn weaving tensions.

3. Selvage Cutter

During the weaving process, the fill yarns must be cut during each yarn insertion. The installation of the pin rolls for the new take-off system required that a new selvage cutter be designed, fabricated and installed in the loom. An automatic device was designed to cut both fill yarns identically. This device was fabricated and installed in the loom as a removable unit.

4. Gage Blocks

In order to hold the woven material close to the pin rolls, thin metal gage blocks were added to the weaving system between the pin rolls. These spacers aided in programming the four-inch Airmat depth.

5. Warping Equipment

During previous weaving operations, warping of the warp spools was performed by manually rotating the spools. This setup did not result in the warping quality desired. This affected the weaving operation. Consequently,

a new warping setup was designed and this equipment was fabricated. The equipment was power driven and allowed for a uniform spool rotation during warping. A variable speed drive, an adjustable fan reed, and a leasing reed were also added to the setup. This equipment produced a good quality warp.

C. LOOM SETUP

The loom setup involved preparation and installation of the yarns in the loom. This included yarn procurement, warping of the warp yarns, drawing-in of the warp yarns into the loom, and installation of the drop yarns in the loom.

Multifilament Type 304 stainless steel yarn was purchased from the Brunswick Corporation. These yarns had been multi-drawn and were in a hard condition. All yarns were obtained with a twist of two turns per inch. Warp yarns and drop yarns were 300 filament yarn and the fill yarns were 90 filament yarn. Each filament was approximately one-half mil in diameter.

To prevent fraying during the weaving operation, all warp and drop yarns were given a protective coating of a water soluble PVA material. This coating was removed after weaving.

The warping operation was accomplished using the new warping equipment described in Section VII-B-5. Sixty, two-inch, spools were warped with 168 yarns on each spool.

The warp spools were then installed in the loom, and each yarn, 10,080 in number, was drawn individually through the proper harness heddle and between the proper reed dents. The drop yarn spools, 420 in number, were installed on creels located at the rear of the loom, and the drop yarns were drawn into the loom similarly to the warp yarns.

Tensile and loop tensile strength tests were performed on the two types of yarn procured. The two types of yarn are described as follows.

Fill Yarn - Number 22-12/90/2Z Type 304 Stainless Steel,
No Coating

Warp Yarn - Number 23-12/300/2Z Type 304 Stainless Steel,
1% PVA Coating

Fifteen tensile and fifteen loop tensile tests were performed. The following average results were obtained.

Number 22 yarn = 5.26 pounds ultimate tension
1.31% elongation at failure
4.40 pounds ultimate loop tension

Number 23 yarn = 11.8 pounds ultimate tension
1.20% elongation at failure
5.20 pounds ultimate loop tension

D. EXPERIMENTAL WEAVING

The basic experimental weaving criteria was to weave conical Airmat with sufficient dimensional accuracy so that a conical nozzle extension would result and to weave conical Airmat with an interface porosity of one percent or less.

Five different experimental panels were woven and evaluated for dimensional accuracy and for porosity. The weaving criteria used on the fifth experimental panel was recommended for weaving of the actual nozzle extension. The Panel 5 dimensional checks showed that a satisfactory dimensional weaving accuracy could be achieved. The Panel 5 porosity evaluation showed that a porosity of approximately 1.0 percent could be expected.

The dimensional checks were performed by dividing the Airmat faces into grids. These grids were set up during weaving by inserting colored textile yarns in the weaving process. Red yarns were added in both the warp and fill directions. After removal of the woven panels from the loom, the grid dimensions were measured and compared with the calculated dimensions required to form the desired conical surface.

The porosity evaluation was performed by testing specimens cut from the experimental weaving panels. The test procedures and test results are reported in Section VII-E.

One preliminary weaving experiment was first conducted to adjust the tension of the warp yarns. Approximately three feet of double-face cloth material was woven. Drop yarns were not included in this experiment. During the weaving experimentation, the warp tensions along each side of the Airmat were increased as they were weaving slack causing a buildup of the fill along each side.

The buildup was also found to be a function of the fill yarn count. It was found that when weaving 90 fill yarns per inch, the buildup, even with increased warp tensions, was excessive for good dimensional control. Consequently, the fill count was reduced to 80 yarns per inch.

1. Experimental Panel No. 1

Panel No. 1 was woven approximately two feet long. The fill yarn count woven was 80 yarns per inch. Approximately sixty percent of the drop yarns were incorporated into this weaving experiment. The side of the Airmat that corresponds with the forward end of the nozzle extension was woven along the left hand side of the loom for this panel only.

The dimensional accuracy,particularly along the left hand side of the Airmat,was not considered to be satisfactory.

The porosity evaluation of the Airmat showed that the porosity along the left hand side of the Airmat was high and also unsatisfactory.

2. Experimental Panel No. 2

Panel No. 2 was woven approximately two feet long. The fill yarn count woven and the drop yarns woven were the same as for Panel No. 1. The pin rolls were reversed however so that the forward end of the extendable nozzle Airmat was woven along the right hand side of the loom.

The evaluation of the first panel woven had indicated that the better dimensional control was obtained on the right-hand side of the loom. Because of the nature of the loom, the fill yarns are considered to be held tighter during beat-up on the right side. The pin rolls were then reversed as dimensional accuracy at the forward end of the nozzle extension Airmat was considered to be the more critical.

The best dimensional accuracy was obtained across the center of the Airmat while both sides were weaving short. Improvement in the dimensional accuracy of the right side of the Airmat was noted in comparison with the left side of the Airmat for Panel No. 1.

The porosity evaluation of Panel No. 2 yielded about the same results as for Panel No. 1. It should be noted that the lower porosity values obtained at the 30 and 70 percent station were from specimens that did not contain drop yarns.

3. Experimental Panel No. 3

Panel No. 3 was woven approximately one foot long. The fill yarn count was reduced to 70 yarns per inch to determine if this would improve the dimensional accuracy. The remainder of the drop yarns were also installed so that drop yarns were woven across the full Airmat width. The forward end of the nozzle extension Airmat was woven along the right hand side of the loom.

The dimensional accuracy of the outer Airmat face cloth for this panel was good except for a short length along the left side. The inner face cloth dimensional accuracy was improved although deviations were noted along both sides of the Airmat.

The porosity tests of Panel No. 3 showed that the porosity along both sides of the Airmat was unsatisfactory.

4. Experimental Panel No. 4

Panel No. 4 was woven approximately two feet long. The fill yarn count was 70 yarns per inch and drop yarns were woven across the full width of the Airmat. The forward end of the nozzle extension was woven along the right hand side of the loom.

Two changes in weaving criteria were incorporated as follows.

First the upper and lower pin rolls were reversed in their relative position on the loom. During previous weaving the upper pin roll controlled the outer face cloth of the Airmat and the inner pin roll controlled the inner face cloth of the Airmat. The upper surface, outer surface of the

Airmat, had previously shown the best dimensional accuracy. As the inner surface accuracy is considered more critical for both dimensional and porosity considerations,it appeared desirable to change the pin rolls.

An experiment was also conducted to reduce the porosity of the inner face cloth at the large end of the nozzle extension Airmat. Extra warp yarns were drawn into the loom over a width of twelve inches along the left hand side of the loom for the inner Airmat face only. The extra warp yarns were intended to decrease the porosity along the large end of the Airmat where the fill yarns are spaced wider apart as a result of conical weaving.

The dimensional checks of this panel showed that the dimensional accuracy of the Airmat along the left hand side of the inner face of the Airmat was much improved.

The porosity checks of this panel showed that the porosity of the right hand side of the inner Airmat face was decreased by the addition of the additional warp yarns.

5. Experimental Panel No. 5

Panel No. 5 was woven approximately two feet long. The weaving criteria was the same as for Panel No. 4 except that the additional warp yarns were woven in across the full width of the Airmat. The distribution of the extra warp yarns were programmed so that 8 warp yarns per inch were added at the large end of the Airmat and tapering to 0 warp yarns per inch at the small end.

Porosity checks were conducted on this panel after weaving. Tests showed that a more uniform porosity was achieved on this panel than on the others.

E. POROSITY TESTING

This task was conducted in parallel with Section VII-D, Experimental Weaving, and involved the porosity testing and evaluation of the experimental panels.

1. Test Setup

The test setup was similar to that used by GAC during the J-2X Program as reported in Reference 1. Nitrogen gas was used for testing. The test setup is described in detail in this reference. Other porosity tests using hydrogen gas were performed in the early part of this program and are reported in Section III-A-5-d of this report.

The test setup utilized six bottles of nitrogen, connected together to a common feed line, as the pressure gas source. Each bottle was equipped with a pressure regulator. The feed line was equipped with a shut-off valve and a flowmeter. This flowmeter measured the gas flow. The test specimen which had a test area of 16 square inches, four inches by four inches square, was mounted on one side of the test chamber. The feed line was connected to this chamber. The chamber contained a thermocouple and lead to a temperature gage and a pressure tap to a pressure gage.

The tests were conducted at chamber pressures up to 20 psig. Flow, temperature, and pressure readings were recorded at 5, 10, 13, 17, and 20 psig pressure points. The flow meter readings were then converted to cubic feet per minute and with the use of the temperature readings and gas constants to mass flow in terms of pounds per square foot per second.

2. Airmat Porosity Determination

To obtain porosity values, a set of curves were derived for nitrogen gas flow through the Airmat face material at ambient back pressure conditions. These curves for porosities ranging from 0.005 to 0.020 were plotted with mass velocity in terms of pounds per second per square foot of surface area and Airmat pressure as variables. The test mass flow value was plotted at the applicable pressure and a corresponding porosity obtained.

3. Presentation of Data

The five panels tested are described in Table XIV and the test data for each are tabulated in Tables XV thru XIX . The test specimen locations are shown in Figure 38 . This data in terms of gas flow or mass velocity is plotted on Figures 39 thru 43 for the applicable pressures. Figures 44 thru 48 are plots of porosity across the loom width for each pressure. Figure 49 is a plot of porosity across the loom width for all panels at 10 psig pressure. Figures 50 and 51 are plots of the porosity across the loom width for Panel No. 5 only at 10 psig pressure and 7 psig pressure respectively.

The Figure 49 plots are included for information purposes. Actually Panels No. 1 and No. 2 are not representative of the final Airmat weaving criteria. Panels No. 3 and No. 4 are not as representative of the final Airmat weaving criteria as is Panel No. 5 which has added warp yarns across the entire nozzle length.

4. Summary of Data

The results of the porosity tests on Panel No. 5, shown in Figure 50 indicate that a nominal porosity of 1.10 percent was obtained at an Airmat pressure of 10 psig. The scatter range was 0.15 percent. Thus, the porosity range at 10 psig is from 0.95 percent to 1.25 percent or 1.10 $\pm$0.015 percent.

The results of the porosity tests on Panel No. 5 shown in Figure 50 indicate that a nominal porosity of 0.95 percent was obtained at an Airmat pressure of 7 psig. The scatter was plus 0.15 percent and minus 0.10 percent. Thus, the porosity range at 7 psig is from 0.85 to 1.10 percent.

Table XIV. Test Panel Description

Panel 1:	Fill count 80 yarns per inch Small end of rolls on L.H. side of loom Airmat inner surface - lower roll Drop yarns at 10, 50, and 90% stations
Panel 2:	Fill count 80 yarns per inch Small end of rolls on R.H. Side of loom Airmat inner surface - lower roll Drop yarn at 10, 50, and 90% station
Panel 3:	Fill count 70 yarns per inch Small end of rolls on R.H. side of loom Airmat inner surface - lower roll Drop yarns at all stations
Panel 4:	Fill count 70 yarns per inch Small end of rolls on R.H. side of loom Airmat inner surface - upper roll Drop yarns at all stations Extra warp yarns at 90% station only
Panel 5:	Fill count 70 yarns per inch Small end of rolls on R.H. side of loom Airmat inner surface - upper roll Drop yarns at all stations Extra warp yarns at all stations

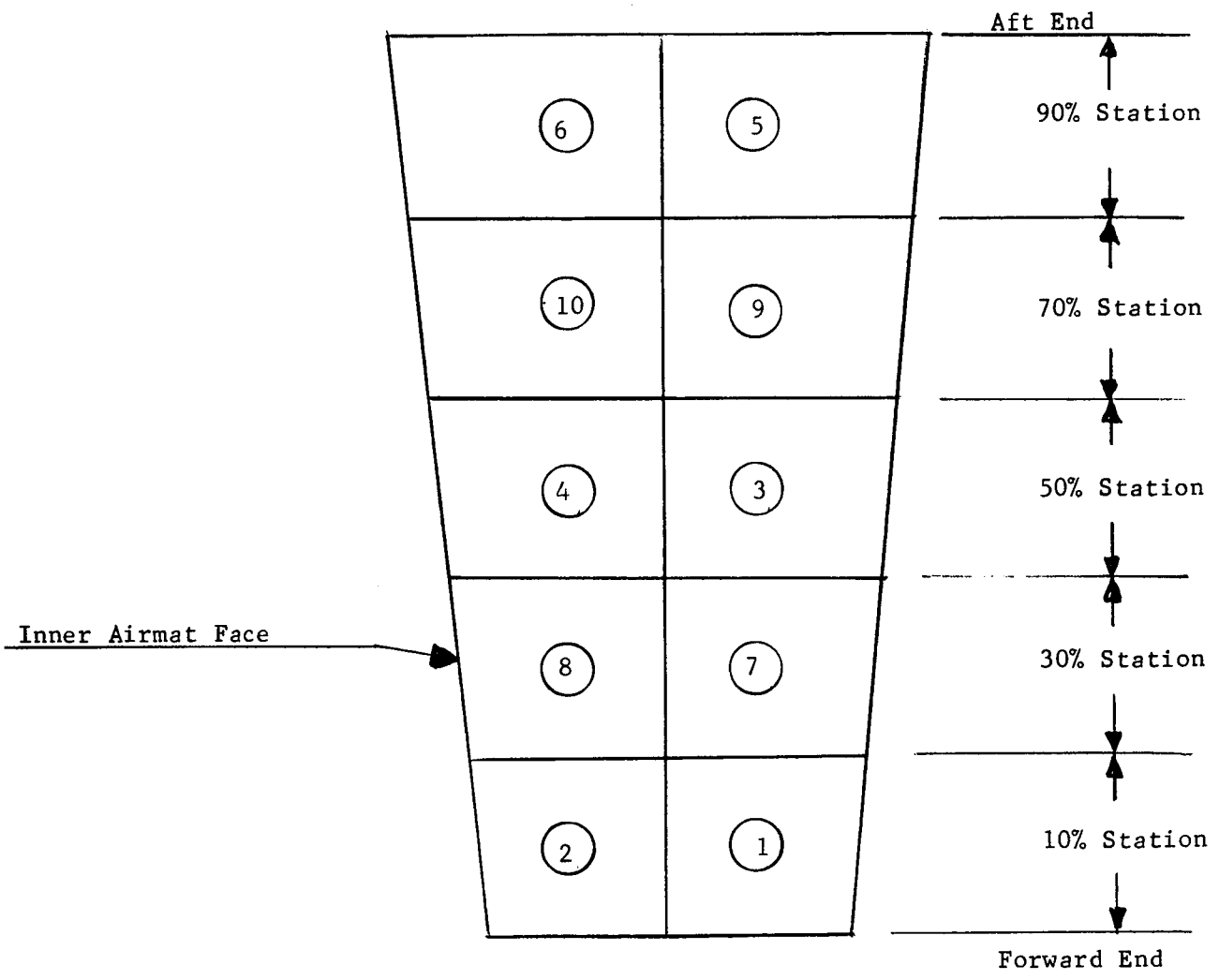

Figure 38. Test Specimen Locations

Table XV. Porosity Test Results - Panel Number 1

Test Value	Specimen No.	Test Pressure psig				
		5	10	13	17	20
Flow, cu ft/sec-ft^2	1	247	382	454	535	594
	2	265	423	495	594	661
	3	175	283	326	389	423
	4	207	310	351	423	472
	5	238	373	436	504	549
	6	225	337	400	450	504
	7	157	234	274	292	360
	8	157	234	274	292	360
	9	171	292	337	405	481
	10	207	306	360	423	472
Gas Temp. ^{o}F	1	68	67	66	63	60
	2	62	62	61	60	60
	3	63	63	62	61	60
	4	63	63	62	62	62
	5	68	67	67	66	65
	6	66	65	65	64	64
	7	65	65	64	64	64
	8	66	66	65	65	66
	9	66	65	65	65	64
	10	65	65	65	64	64
Flow, lbs/sec-ft^2	1	0.40	0.78	1.04	1.41	1.73
	2	0.42	0.87	1.14	1.57	1.91
	3	0.29	0.58	0.75	1.10	1.32
	4	0.34	0.64	0.81	1.12	1.38
	5	0.39	0.76	1.00	1.16	1.58
	6	0.37	0.69	0.92	1.18	1.45
	7	0.26	0.48	0.63	0.77	1.04
	8	0.26	0.48	0.63	0.77	1.04
	9	0.28	0.60	0.78	1.07	1.39
	10	0.34	0.63	0.83	1.11	1.38

Table XVI. Porosity Test Results - Panel Number 2

Test Value	Specimen No.	Test Pressure psig				
		5	10	13	17	20
Flow, cu ft/min-ft^2	1	270	472	549	648	729
	2	292	468	544	648	702
	3	238	355	414	486	535
	4	216	319	373	432	472
	5	234	337	405	472	513
	6	252	373	445	517	562
	7	189	292	337	391	432
	8	157	252	306	355	387
	9	198	291	337	391	432
	10	157	252	292	337	373
Gas Temp, F^o	1	71	71	70	70	69
	2	71	70	70	70	69
	3	70	70	70	70	69
	4	70	70	70	70	70
	5	71	70	70	70	70
	6	71	71	71	71	70
	7	72	71	71	71	71
	8	71	71	71	71	71
	9	72	72	72	72	72
	10	72	72	72	72	72
Flow, lbs/sec-ft^2	1	0.44	0.95	1.24	1.69	2.08
	2	0.47	0.94	1.23	1.69	2.00
	3	0.39	0.72	0.94	1.26	1.53
	4	0.35	0.64	0.85	1.12	1.35
	5	0.38	0.58	0.92	1.23	1.46
	6	0.41	0.75	1.01	1.35	1.60
	7	0.31	0.59	0.76	1.02	1.23
	8	0.25	0.51	0.69	0.92	1.10
	9	0.32	0.59	0.76	1.02	1.23
	10	0.25	0.51	0.66	0.88	1.06

Table XVII. Porosity Test Results - Panel Number 3

Test Value	Specimen No.	Test Pressure psig				
		5	10	13	17	20
Flow, cu ft/min-ft^2	1	342	526	634	707	833
	3	245	373	436	508	562
	5	315	468	540	634	693
	7	261	393	456	531	585
	9	290	400	495	585	645
Gas Temp, F^o	1	79	79	80	80	71
	3	78	78	78	78	78
	5	75	75	74	74	73
	7	76	75	75	75	74
	9	78	76	76	76	76
Flow, lbs/sec-ft^2	1	.55	1.06	1.42	1.82	2.35
	3	.39	.75	.97	1.30	1.58
	5	.50	.96	1.21	1.63	1.95
	7	.42	.79	1.02	1.36	1.65
	9	.46	.80	1.11	1.50	1.82

Table XVIII. Porosity Test Results - Panel Number 4

Test Value	Specimen No.	Test Pressure psig				
		5	10	13	17	20
Flow, cu ft/min-ft^2	1	235	351	400	468	513
	2	261	391	450	526	585
	3	279	418	486	562	625
	4	297	441	508	585	648
	5	316	463	531	616	675
	6	324	486	558	657	706
	7	211	373	444	508	562
	8	270	400	468	558	607
	9	373	553	648	751	828
	10	355	526	666	738	792
Gas Temp, F^o	1	68	68	68	68	68
	2	68	68	68	68	68
	3	69	69	69	69	69
	4	69	69	69	68	68
	5	70	69	68	68	67
	6	70	69	69	69	69
	7	72	72	70	70	69
	8	72	72	72	70	70
	9	71	70	70	69	69
	10	71	70	70	69	68
Flow, lbs/sec-ft^2	1	0.38	0.71	0.92	1.22	1.46
	2	0.42	0.80	1.03	1.37	1.70
	3	0.45	0.85	1.26	1.46	1.78
	4	0.48	0.90	1.16	1.52	1.85
	5	0.51	0.94	1.28	1.71	1.92
	6	0.53	0.99	1.27	1.71	2.01
	7	0.31	0.76	1.02	1.32	1.60
	8	0.44	0.81	1.01	1.22	1.73
	9	0.60	1.12	1.48	1.95	2.36
	10	0.57	1.07	1.52	1.92	2.26

Table XIX. Porosity Test Results - Panel Number 5

Test Value	Specimen No.	Test Pressure psig				
		5	10	13	17	20
Flow, cu ft/min-ft^2	1	252	372	438	508	562
	2	263	401	472	552	609
	3	357	538	626	778	810
	4	339	512	601	708	770
	5	303	446	512	594	655
	6	286	430	490	569	626
	7	286	423	480	569	666
	8	293	430	498	585	643
	9	323	478	562	646	708
	10	310	450	523	638	679
Gas Temp, F^o	1	78	78	78	76	76
	2	78	78	77	77	77
	3	78	78	77	76	76
	4	76	76	75	74	72
	5	74	74	74	74	73
	6	76	76	76	75	74
	7	80	80	80	79	77
	8	78	77	76	75	74
	9	78	76	76	76	74
	10	76	76	75	74	73
Flow, lbs/sec-ft^2	1	.40	.74	.98	1.30	1.58
	2	.42	.80	1.06	1.42	1.71
	3	.57	1.08	1.40	2.00	2.28
	4	.54	1.03	1.34	1.82	2.16
	5	.48	.89	1.15	1.53	1.81
	6	.46	.86	1.10	1.46	1.76
	7	.46	.85	1.07	1.46	1.87
	8	.47	.86	1.11	1.50	1.81
	9	.52	.96	1.26	1.66	1.99
	10	.50	.90	1.18	1.65	1.91

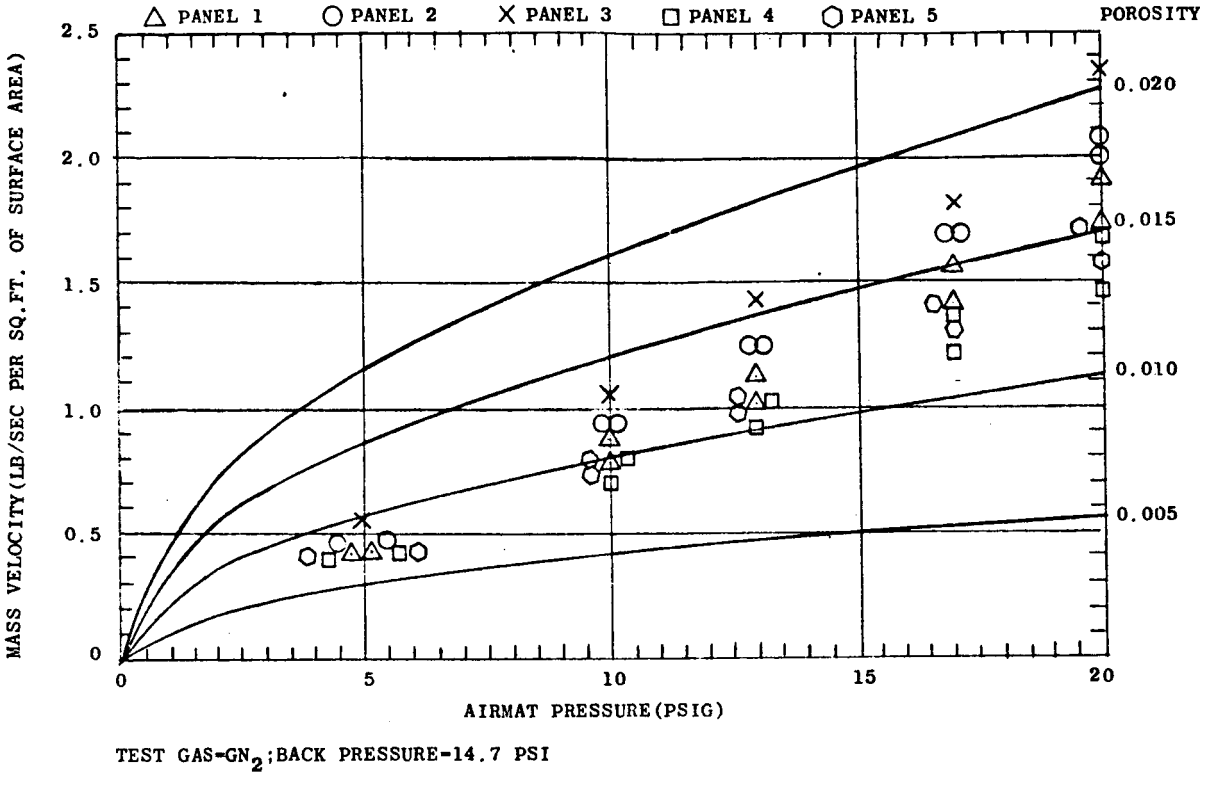

Figure 39. Mass Velocity vs Airmat Pressure - 10% Station - Specimens 1 & 2

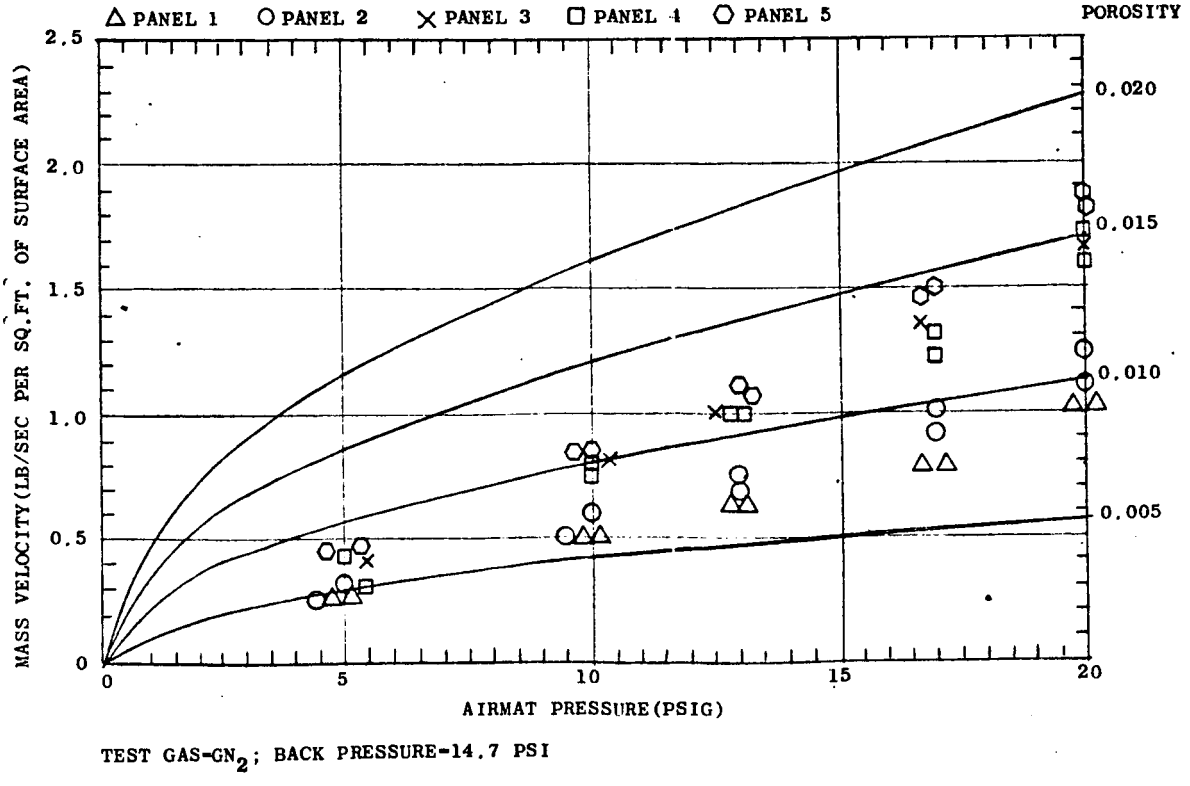

Figure 40. Mass Velocity vs Airmat Pressure - 30% Station - Specimens 7 & 8

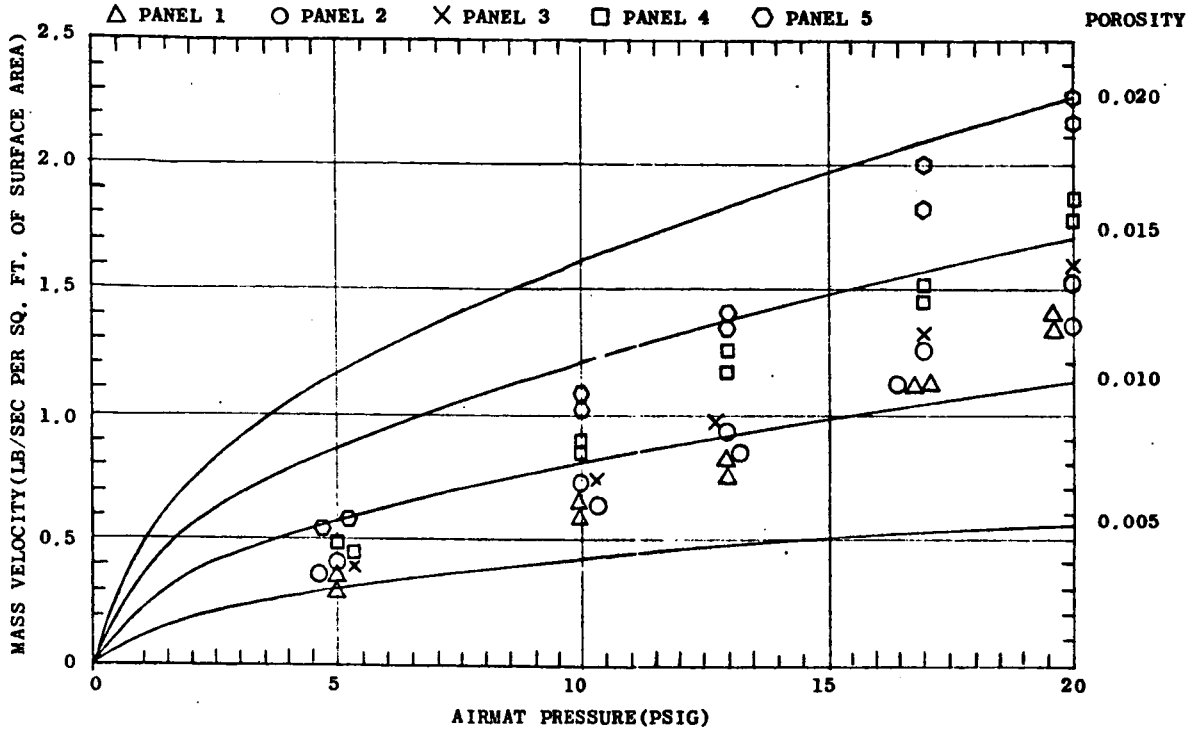

TEST GAS=GN_2; BACK PRESSURE=14.7 PSI

Figure 41. Mass Velocity vs Airmat Pressure - 50% Station - Specimens 3 & 4

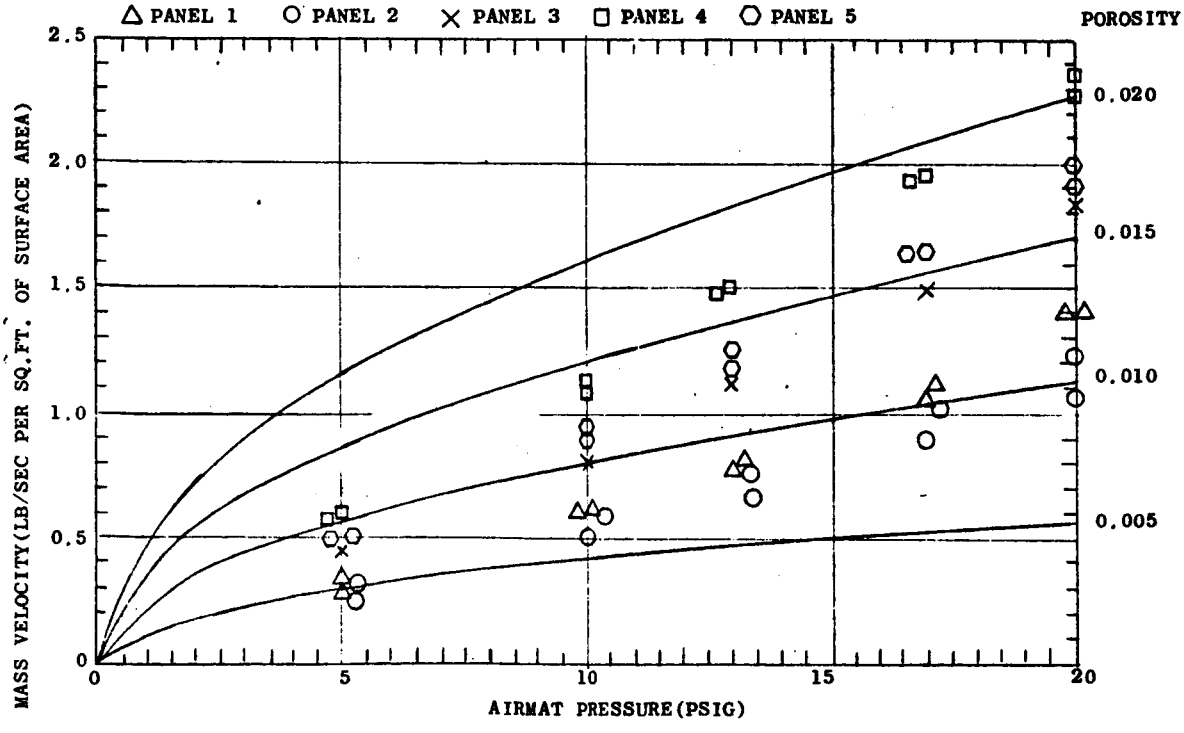

TEST GAS=GN_2; BACK PRESSURE=14.7 PSI

Figure 42. Mass Velocity vs Airmat Pressure - 70% Station - Specimens 9 & 10

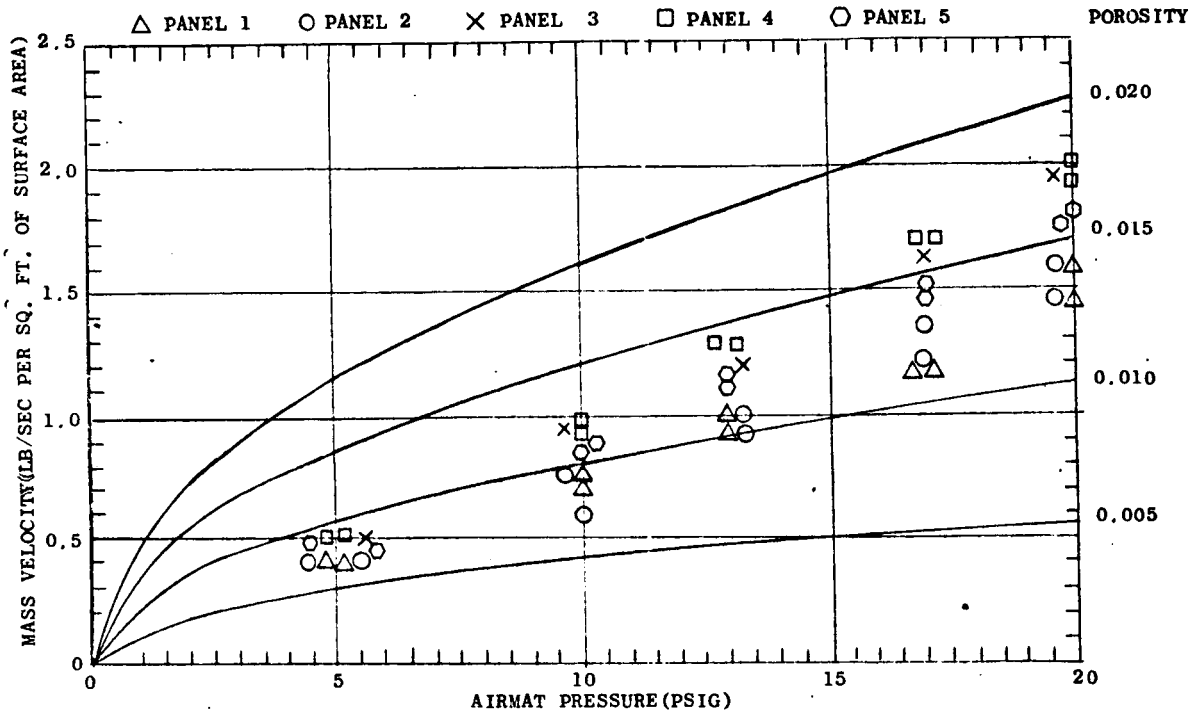

TEST GAS=GN_2; BACK PRESSURE = 14.7 PSI

Figure 43. Mass Velocity vs Airmat Pressure - 90% Station - Specimens 5 & 6

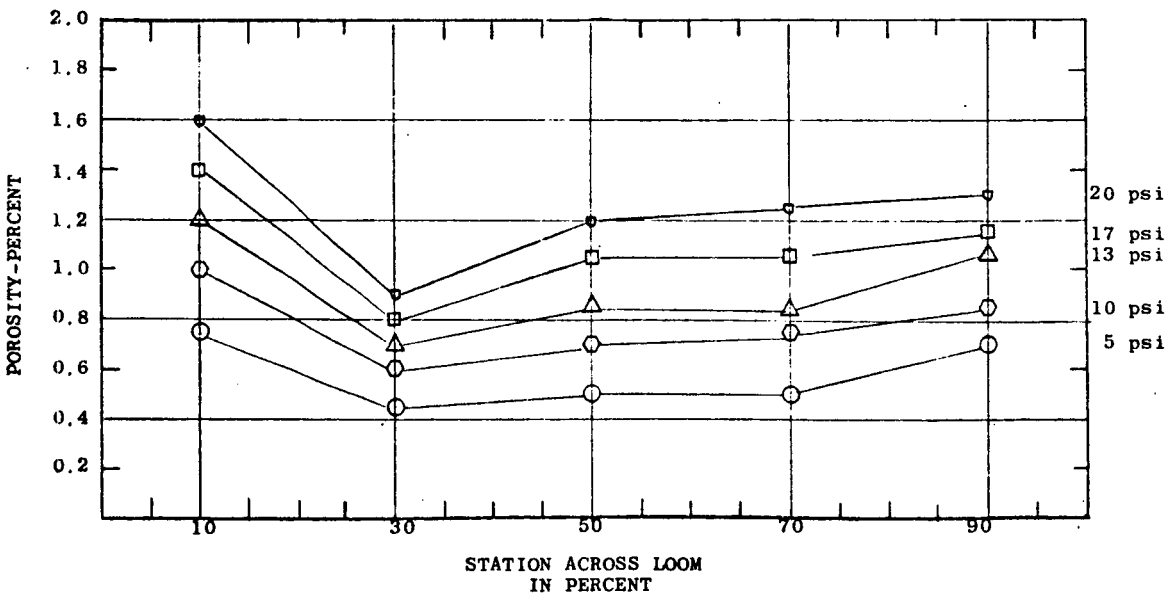

Figure 44. Panel 1 Porosity

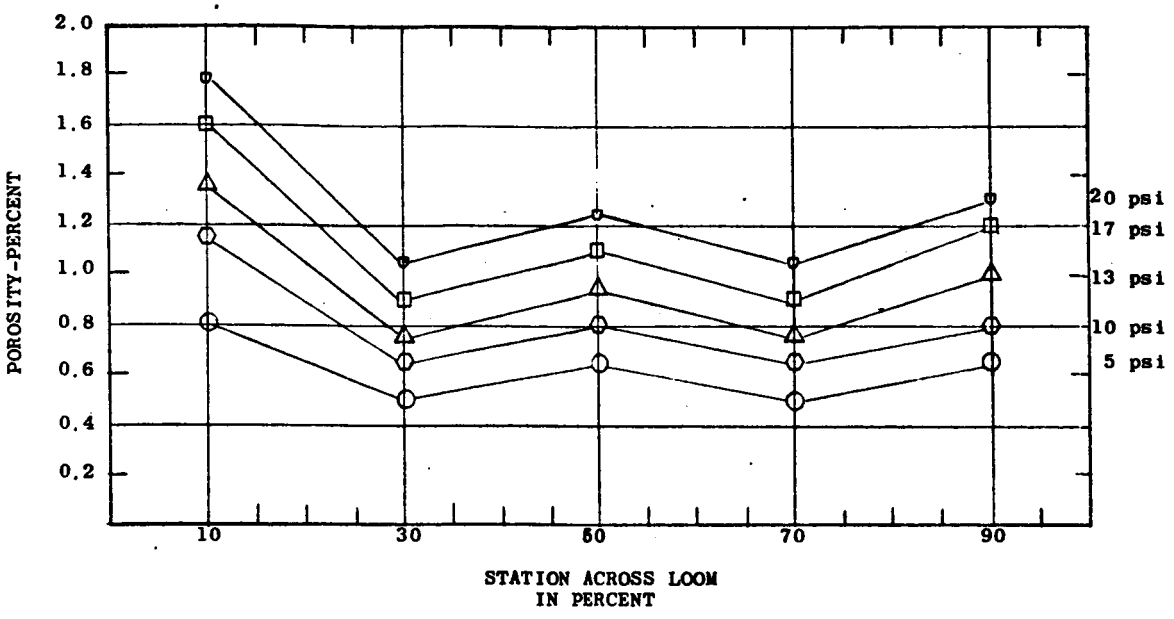

Figure 45. Panel 2 Porosity

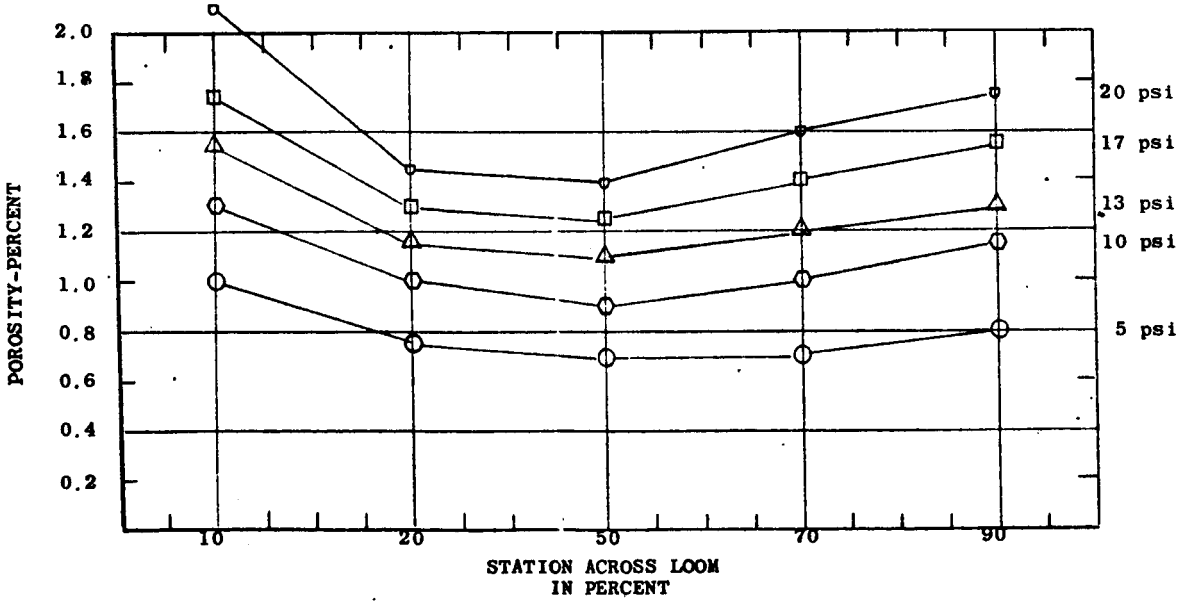

Figure 46. Panel 3 Porosity

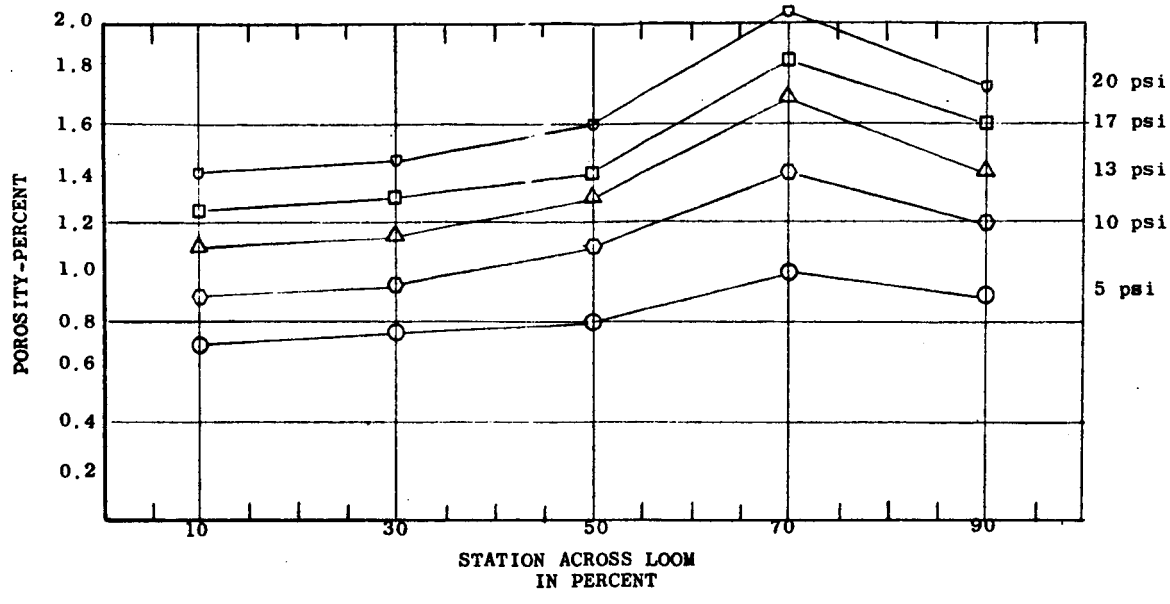

Figure 47. Panel 4 Porosity

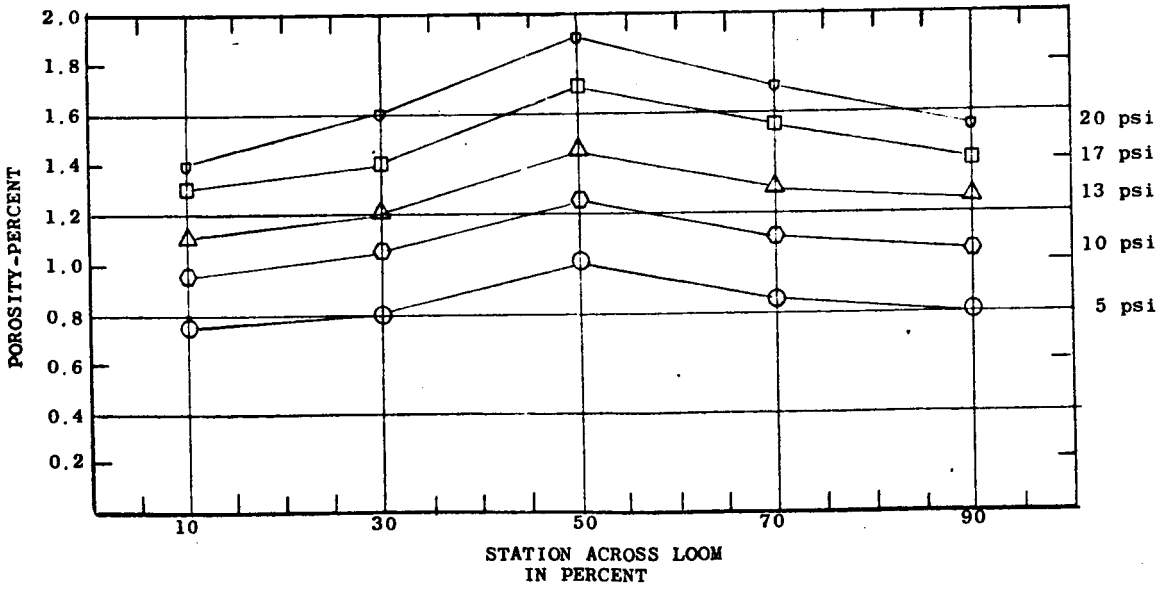

Figure 48. Panel 5 Porosity

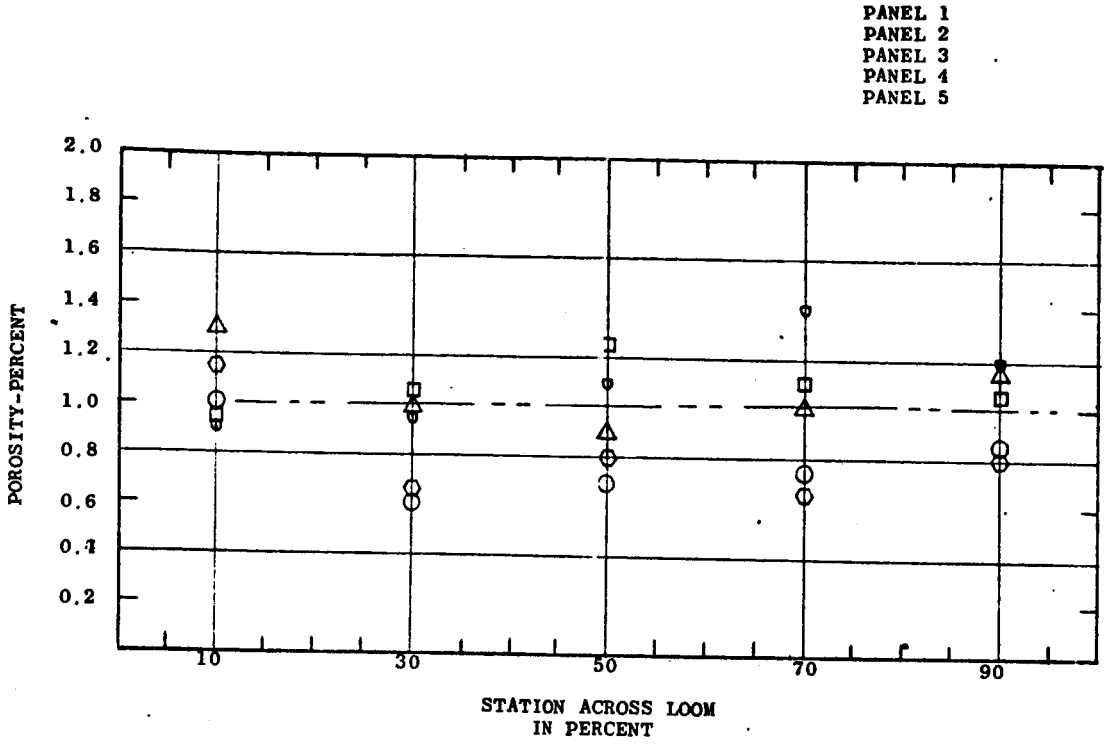

Figure 49. Porosity - 10 PSIG

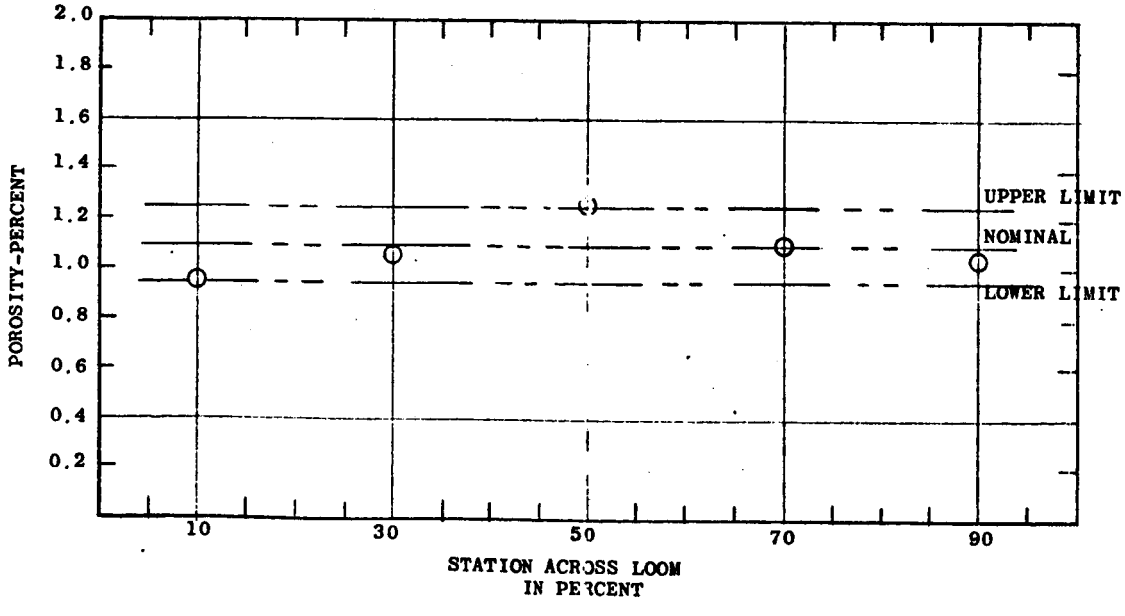

Figure 50. Panel 5 Porosity - 10 PSIG

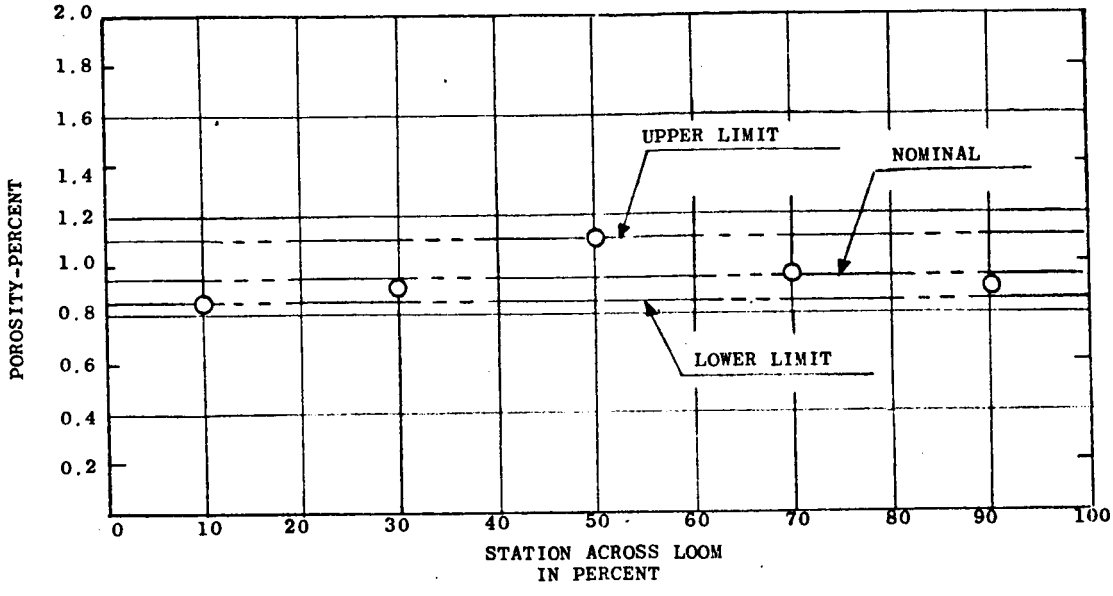

Figure 51. Panel 5 Porosity - 7 PSIG

SECTION VIII

FABRICATION

A. GENERAL

This task effort involved the fabrication of two nozzle extension assemblies and one manifold assembly. The fabrication of the nozzle extension assemblies included Airmat weaving, fabrication of metal parts, fabrication of the Airmat subassemblies, final assembly of the Airmat and the metal parts, and coating of the outer surface of the Airmat with a silicone elastomer. The manifold fabrication included fabrication of metal parts, fabrication of the fabric torus subassembly, final assembly of the fabric torus and the metal parts, and coating of the fabric torus with a silicone elastomer.

The basic completed assemblies were identified by their GAC Drawing Numbers as follows:

EA 2211-013-103	Number 1 Nozzle Extension Assembly
EA 2211-013-101	Number 2 Nozzle Extension Assembly
EA 2211-016-101	Manifold Assembly

The -103 nozzle extension assembly was the shorter of the two nozzles. Its expansion ratio was 27.5 to 1 at the small end and 41.3 to 1 at the larger end. The -101 nozzle extension assembly had an expansion ratio of 27.5 to 1 at the small end and 48 to 1 at the large end.

Test instrumentation requirements were added to the nozzle extension in accordance with Drawing EA-2211-019. Test instrumentation requirements were added to the manifold in accordance with Drawing EA-2211-020. Installation bolts that are required to attach the outer nozzle extension ring, EA-2211-011, to the manifold which are called out on the EA-2211-018 installation drawing were included with the manifold assembly. This completed all of the fabrication requirements.

Following final inspection the three assemblies were packaged and shipped to the George C. Marshall Space Flight Center, Huntsville, Alabama.

B. WEAVING - NUMBER 1 NOZZLE EXTENSION

Weaving of the Airmat for the first nozzle extension was initiated and completed in two months. The length of conical Airmat woven was 250 inches.

During the weaving program, and with the woven material attached to the loom, spot dimensional checks were performed. These checks in general indicated that good dimensional accuracy was being obtained over the forward portions of the nozzle extension and that the loom was weaving short over the aft portion of the nozzle extension. Consequently,a series of adjustments in warp tensions were made as the weaving progressed to reduce the warp tension in the short area. This procedure reduced the tendency to weave short but did

not completely eliminate the problem. After weaving of 210 inches, an additional reduction in warp tension was made which later proved to be too large a reduction. The subsequent weaving resulted in material that appeared to be marginal from quality, porosity, and dimensional control criteria. Buildup at the fill line was also evident. Additional weights were added as soon as the problem was determined. As the 250-inch mark was reached, the weaving was returning to normal. Forty inches of the material were thus considered to be marginal. The woven material was subsequently removed from the loom and spread out on the floor as shown in Figure 52.

A dimensional check was performed over the total length of the 250 inches of woven material. Dimensions were measured in six-inch length increments and at seven stations across the Airmat width. Both Airmat faces were measured. Averages were computed for the first 210 inches of Airmat and compared with theoretical values calculated for the seven stations.

Over the forward portion of the Airmat, the actual dimensions were within three percent of the theoretical. The actual dimensions were within six percent of the theoretical over the aft nine inches. At Station 0, the forward end, and Station 27, the center of the Airmat, the actual dimensions were within three tenths of one percent of the theoretical. The dimensions of the last 40 inches of weaving were quite erratic. Thus, they were not included in the averages.

The woven material, particularly the last 40 inches, was also evaluated for quality and, secondarily, porosity by visual inspection. The material from length 210 to 250 inches showed a different color and texture than the

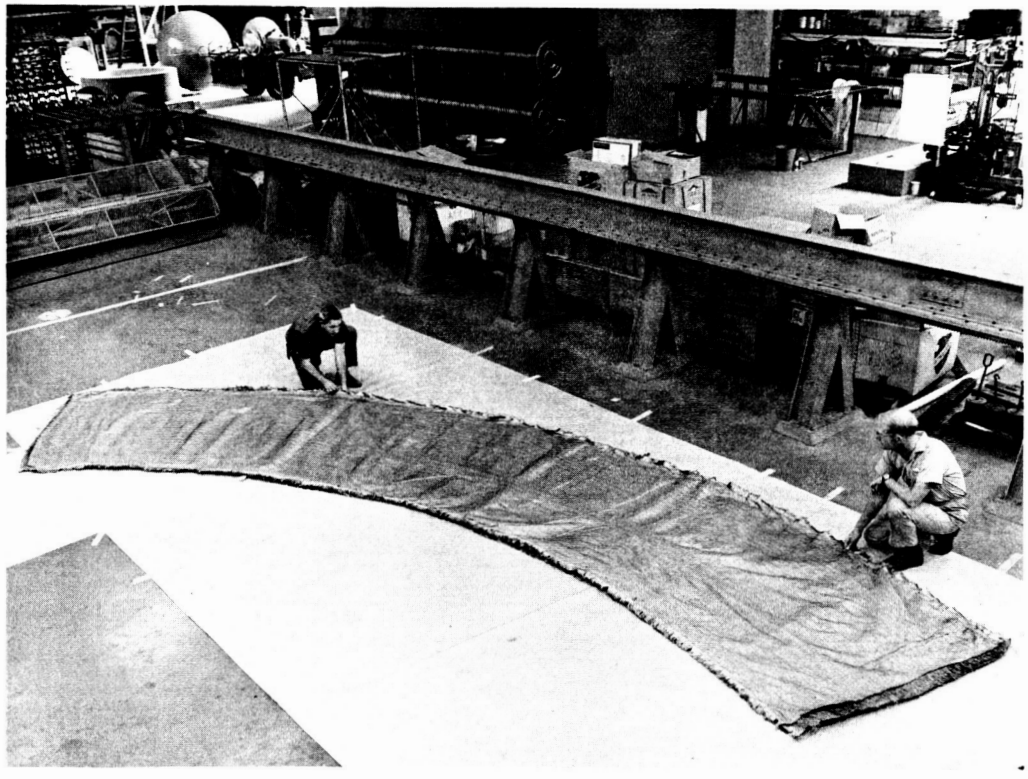

Figure 52. Conical Airmat Woven for Number 1 Nozzle Extension

other material. Inspection with a magnifying glass showed that the warp yarns were woven in a slack condition and that an irregular weave pattern resulted. The material woven first showed the warp yarns to be tighter and that a uniform pattern between warp and fill yarns resulted. Small gaps between fill yarns at several places in the last 40 inches of material were noted.

It was thus concluded that the first 210 inches of material woven was an acceptable material for use in fabrication of the first nozzle extension. It was also concluded that the quality, dimensional accuracy, and the porosity of the last 40 inches woven was marginal and this material was not recommended for use.

Based on the weaving evaluation, a revised fabrication plan for the first nozzle extension, which is the short nozzle extension, was adapted. The only basic change in the nozzle extension design involved changing from a one gore plan to a four gore plan. Figure 53 presents a sketch showing the difference between the two fabrication methods.

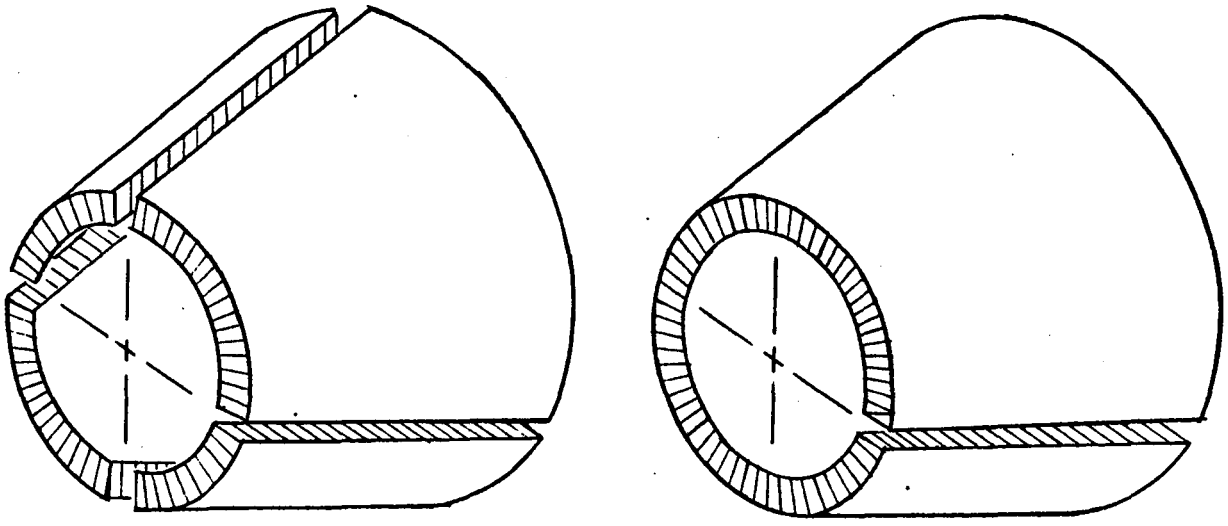

Four-Gore Fabrication Technique

One-Gore Fabrication Technique

Figure 53. Sketch of One and Four Gore Fabrication Methods

The original weaving approach was to weave one piece of conical Airmat long enough so that the nozzle extension could be fabricated from one piece or gore. This material when wrapped around would form a truncated cone and only one longitudinal seam would be required. This approach provides the minimum amount of seaming.

The revised approach involves fabrication of the nozzle extension from four identical pieces or gores. Each gore represents one-fourth of the one gore pattern. In this case, four longitudinal seams are required.

Three of the four gores were patterned from the first 120 inches of Airmat woven. One additional piece of Airmat 66 inches long was subsequently woven. This material was used to pattern the fourth gore. This completed the weaving for the first nozzle extension.

The second piece of Airmat woven was removed from the loom and checked dimensionally similarily to the first piece. This material was accepted for fabrication.

C. WEAVING - NUMBER 2 NOZZLE EXTENSION

Weaving of the Airmat for the second nozzle extension completed the weaving task.

The second nozzle extension weaving operation produced one piece of conical Airmat 264 inches long. This material was used to fabricate a one piece nozzle extension requiring only one longitudinal seam. Dimensional checks were performed on this material both during the weaving process and after removal of the material from the loom.

In general, the dimensional accuracy of the material woven for the second nozzle extension was considerably improved over that obtained during weaving of the first nozzle extension. The weaving short problem that was encountered during the weaving of the first nozzle over the aft portion of the inner face of the Airmat was essentially eliminated.

The dimensional checks included measuring the Airmat length in six-inch increments over the Airmat length of 264 inches. These measurements were performed at seven points along the Airmat width. The measured lengths were then compared with theoretical or programmed lengths at the seven locations. The maximum variation between actual and theoretical dimensions for the inner face cloth was 1.0 percent. The maximum variation between actual and theoretical dimensions for the outer face cloth was 2.0 percent.

D. FABRICATION - NUMBER 1 NOZZLE EXTENSION

The No. 1 nozzle extension was fabricated in accordance with GAC Drawing EA 2211-013-103. This nozzle is commonly known as the short nozzle.

The nozzle extension fabrication procedure included fabrication of metal parts, fabrication of the Airmat subassembly, final assembly which joined the forward mounting rings to the Airmat subassembly, and coating of the outer surface of the Airmat.

The metal part assembly consisted of the fabrication of the forward mounting rings. These rings were fabricated from Type 316 stainless steel angles which were machined, rolled, and welded into rings. Attachment holes were drilled to match the manifold assembly holes using a common drill template.

The Airmat subassembly was fabricated from the material woven for the Number 1 nozzle as described in Section VIII - B. Actually,the subassembly deviated from the design in that it was fabricated as a four-gore assembly rather than as a one-gore assembly. This required four longitudinal seams rather than one. Three gores were obtained from the first piece of Airmat woven and the fourth gore from the short replacement piece of Airmat.

The first procedure in fabrication of the Airmat subassembly involved establishment of the final trim lines for each of the four gores. To accomplish this procedure,two metal templates were fabricated, one for each face cloth. The templates represented the flat pattern of each face cloth. These templates were located and centered on the Airmat. The Airmat was then stretched out under the template to establish a smooth surface. The edges of the template were then marked on the Airmat. This procedure was repeated four times for each face cloth.

The resultant gore end lines did not follow a specific fill yarn over the width of the Airmat. The deviations were measured and analyzed. As a result,corrections were programmed in the gore trim lines. The general, philosophy followed in making the corrections was to use the template lines for trimming the inner face cloth. The drop yarns at the inner face cloth were then projected to the outer face cloth and a new outer face cloth trim line was established. In general this extended the outside face trim line. This procedure avoided cutting of any drop yarns. It did, however, program cutting of fill yarns. The intent of this procedure was to obtain a smooth inner face cloth and to allow weaving tolerances to be absorbed by the outer face cloth whose smoothness is not as critical in operation.

After locating all trim lines, a seam weld was run along all edges to prevent ravelling after trimming. The drop yarns were then trimmed to the trim lines and the face cloths were cut along these trim lines. The face cloths were doubled back at the forward edge to provide a double thickness for attachment to the mounting rings.

The next assembly procedure involved closure of the aft end of each nozzle extension. This involved joining of the inner and outer face cloths. As their woven lengths are different,the lengths were equated by removing material from the outer face and opening of the inner face. This slitting and slotting operation was performed at six locations along the aft edge of each gore. The slits and slots were closed by a common welded strap at each location. The joining of the two face cloths was next accomplished using a butt joint with a welded strap.

Instrumentation provisions were next added to the Airmat in accordance with Drawing EA 2211-019 Nozzle Test Assembly. This included six thermocouple installations and attachment of six ports for installation of pressure taps during future testing.

The final Airmat assembly procedure was to attach the four Airmat gores together to form a cone. This was accomplished using a butt joint with a welded strap. Four longitudinal seams were required for each face cloth. This completed the Airmat subassembly.

The nozzle extension final assembly procedure involved attachment of the two attachment rings to the Airmat subassembly and coating of the outer surface of the nozzle extension.

The inner face cloth of the Airmat was attached to its corresponding attachment ring by resistance spot welding. This resulted in a fixed attachment. The outer face cloth was attached to its corresponding attachment ring by a clamping arrangement. This allows for future adjustment if desired in the radial and longitudinal positioning of the outer face cloth.

The coating applied to the outer Airmat surface was Dow Corning 92009 silicone elastomer. This is a room temperature cure material. The coating was applied by brushing. Approximately 0.10 pounds per square foot dry weight of coating was applied. This completed the nozzle extension assembly.

The completed nozzle extension assembly is presented in Figure 54.

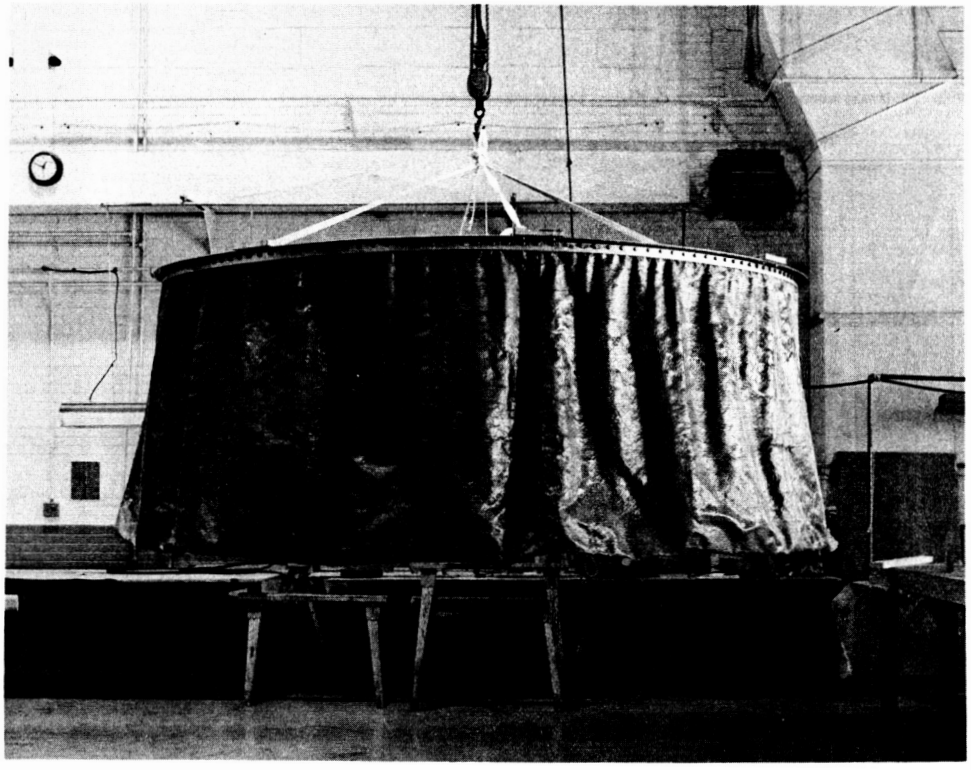

Figure 54. Number 1 Nozzle Extension Assembly

E. FABRICATION - NUMBER 2 NOZZLE EXTENSION

The Number 2 nozzle extension was fabricated in accordance with GAC Drawing EA 2211-013-101. This nozzle is commonly known as the long nozzle extension.

The nozzle extension fabrication procedure included fabrication of metal parts, fabrication of the Airmat subassembly, final assembly which joined the forward mounting rings to the Airmat subassembly, and coating of the outer surface of the Airmat.

The metal part assembly consisted of the fabrication of the forward mounting rings. These rings were identical to the rings fabricated for the Number 1 nozzle extension.

The Airmat subassembly was fabricated from the material woven for the Number 2 nozzle as described in Section VIII - C. The Airmat subassembly was fabricated from one piece of Airmat requiring only one longitudinal seam to form the Airmat into a cone.

The first procedure in fabrication of the Airmat subassembly involved establishment of the final trim lines along all sides of the one-piece of Airmat. The general philosophy adapted in establishing these trim lines was to lay out the inside forward circumference accurately as this is the most critical dimension in obtaining a smooth surface for the inside surface of the nozzle. All trim lines were then located to follow corresponding station lines. This procedure did not provide for corrections for weaving tolerance other than at the one point. It did, however, eliminate cutting of any drop or fill yarns as in the first nozzle extension where fill yarns were cut to correct for weaving tolerances.

The Airmat was woven 264 inches long at the inner forward corner. Red fill yarns were inserted at approximately one inch spacings on each face cloth. Red warp yarns were also woven-in at the forward edge of each face cloth. These yarns were used to establish station lines. Thus length wise stations 0 through 264 were established. Width wise Station 0 was established.

The calculated circumference at the forward inner point was 246.77 inches. One end of the Airmat was fixed at Station 1. Thus,the other end was tentatively located at Station 247.77. To determine this end accurately,the inner face cloth template used in fabricating the first nozzle were employed. This template was positioned on the Airmat four times starting at Station 1. The resulting end point was at Station 248.50. This showed that the Station lines were 0.73 inch short over the total length. The second end trim line was thus fixed at Station 248.50.

The forward and aft edge trim lines were established by measurements from the red warp yarn locating Station 0.

After locating the trim lines,a seam weld was run along all edges to prevent ravelling after trimming. The drop yarns were then trimmed to the trim lines and the face cloths were cut along these trim lines. At the forward edge,the face cloths were doubled back to provide a double thickness for attachment to the mounting rings.

Instrumentation provisions were next added to the Airmat in accordance with Drawing EA 2211-019 Nozzle Test Assembly. This included ten thermocouple installations and attachment of ten ports for installation of pressure taps during future testing.

The next Airmat assembly procedure involved closure of the aft end of the nozzle extension. This involved joining of the inner and outer face cloth. As their woven lengths are different,the lengths were equated by removing material from the outer face and slitting and opening up the inner face.

This procedure was programmed at twenty-four locations around the nozzle extension circumference. The cuts made in the Airmat were closed by a common welded strap at each location. The joining of the two face cloths was accomplished using a butt joint with a strap welded around the entire circumference.

The final Airmat assembly procedure was to attach the two ends of the Airmat together to form a cone. This was accomplished using a butt joint and a welded strap. One longitudinal seam was required for each face cloth. This completed the Airmat subassembly.

The nozzle extension final assembly procedure involved attachment of the two attachment rings to the Airmat subassembly and coating of the outer surface of the nozzle.

The inner face cloth of the Airmat was attached to its corresponding attachment ring by resistance spot welding. This resulted in a fixed attachment. The outer face cloth was attached to its corresponding attachment ring by a clamping arrangement. This allows for future adjustments, if desirable, in the radial and longitudinal positioning of the outer face cloth.

The coating applied to the outer Airmat surface was Dow Corning 92009 silicone elastomer. This is a room temperature cure material. The coating was applied by brushing. Approximately 0.10 pounds per square foot, dry weight, of coating was applied. This completed the nozzle extension assembly.

The completed nozzle extension assembly is shown in Figures 55 and 56.

F. FABRICATION - MANIFOLD

One manifold was fabricated in accordance with GAC Drawing EA 2211-016-101 Manifold Assembly. The fabrication procedure included fabrication of metal parts, fabrication of a fabric torus subassembly, final assembly which joined the metal and fabric parts together, and coating of the fabric portion of the final assembly.

The basic metal parts included one EA 2211-014-101 Manifold Ring Welded Assembly, one EA 2211-015-101 Load Ring Assembly, and one EA 2211-016-105 Inlet Assembly. These parts were all fabricated of Type 316 stainless steel material. The major fabrication effort involved the welded Manifold Ring Assembly.

The EA 2211-016-103 Torus Assembly was fabricated using Type 304 woven stainless steel cloth. This material was purchased from the Unique Wire Weaving Company. The material designation was 100 x 100 x 0.0045. This means that there are 100 wires per inch in both the warp and fill directions. The wire diameter was 4.5 mils.

Figure 55. Number 2 Nozzle Extension Assembly

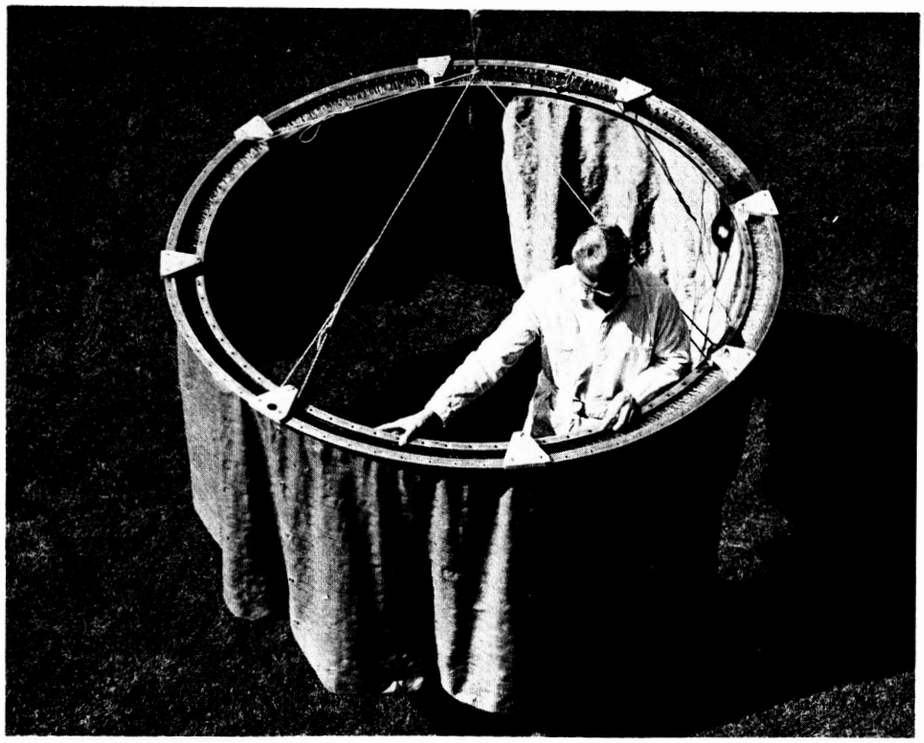

Figure 56. Number 2 Nozzle Extension Assembly

Forty-eight patterned gores were used to form the fabric assembly. These gores were welded together to form a torus. The gores were first tack welded together using a Weldmatic, 45 watt-second power supply, Capacitor Discharge Resistance Welder with a light duty hand piece. The permanent seams were made using a Thomson, 50 KVA-AC, roll-spot Resistance Seam Welder.

The metal parts and the fabric assembly were next joined together to form the final assembly. The Weldmatic welding equipment was used for this operation. Five ports for attachment of pressure taps during testing were added to the manifold assembly in accordance with drawing number EA 2211-020 Manifold Test Assembly.

The final fabrication procedure involved coating of the fabric portion of the manifold assembly with Dow Corning 92009 silicone elastomer. This material cures at ambient temperatures. Both sides of the manifold cloth were coated by brushing. A total dry coating weight of approximately 0.08 pounds per square foot was applied.

The completed manifold assembly is shown in Figure 57 . This photograph shows the aft side of the manifold and the openings through which the coolant gas enters the Airmat nozzle extension. The inner bolt hole circle provides for attachment to the existing J-2 Rocket Engine Nozzle and also attaches the inner nozzle extension mounting ring. The outer bolt circle provides for attachment of the outer nozzle extension mounting ring.

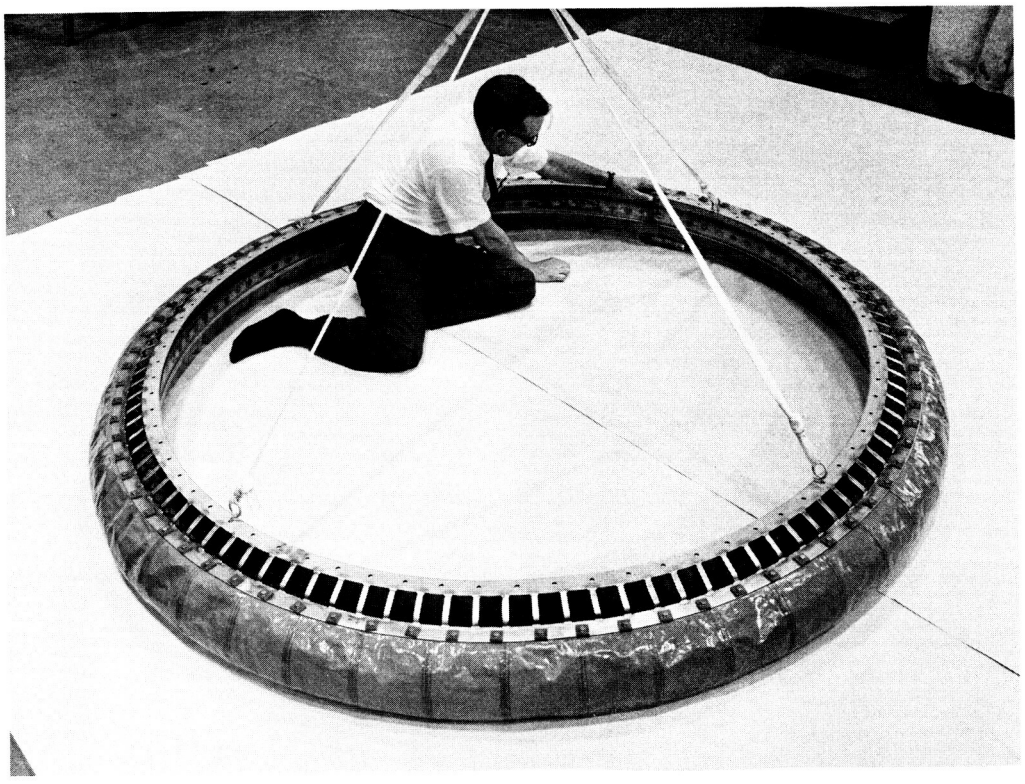

Figure 57. Manifold - Assembly

SECTION IX

FULL-SCALE NOZZLE EXTENSION TESTS

A. INTRODUCTION

It was originally planned to conduct actual hot firing demonstrations of the J-2 engine nozzle extensions at the altitude facilities of the Arnold Engineering Development Center (AEDC), Tullahoma, Tennessee. This testing was to be accomplished as a part of existing J-2 experimental activity being conducted at that time. Due to changes in J-2 program plans, the altitude test series at AEDC was cancelled and it was not considered economic to carry out additional testing with the demonstration of the inflatable nozzle extension as a sole objective.

As a compromise to the desired hot fiting demonstration, a series of cold flow deployment tests were conducted at the Marshall Space Flight Center with the 48 to 1 nozzle extension attached to an inactive J-2 engine.

B. FLOW TESTS

1. General

The primary objective of the flow tests was to evaluate the Airmat internal pressure and the porosity of the nozzle extension inner wall under steady state flow conditions using several flow rates of nitrogen gas.

The second objective was to evaluate the dimensional shape of the nozzle extension when pressurized.

2. Test Setup

The number two nozzle extension assembly, ϵ = 48 to 1, was mounted on a J-2 nozzle at the NASA test facility. The first two tests in the series of flow tests utilized the GAC fabricated nonrigid manifold assembly, while the remaining tests in the series utilized a rigid manifold assembly.

A piping schematic of the test setup for the nitrogen gas supply to the manifold is shown in Figure 58.

The location of the pressure tap instrumentation for the nozzle extension and for the manifold is shown in Figure 59.

3. Test Procedures

All flow tests were initiated with the nozzle extension in a deployed condition. Six separate tests were conducted using different flow rates ranging from 26 to 46 pounds per second. The latter flow rate represented the maximum flow available with the test setup. Flow data, manifold pressure at two locations, and Airmat pressure at ten locations were recorded during the tests.

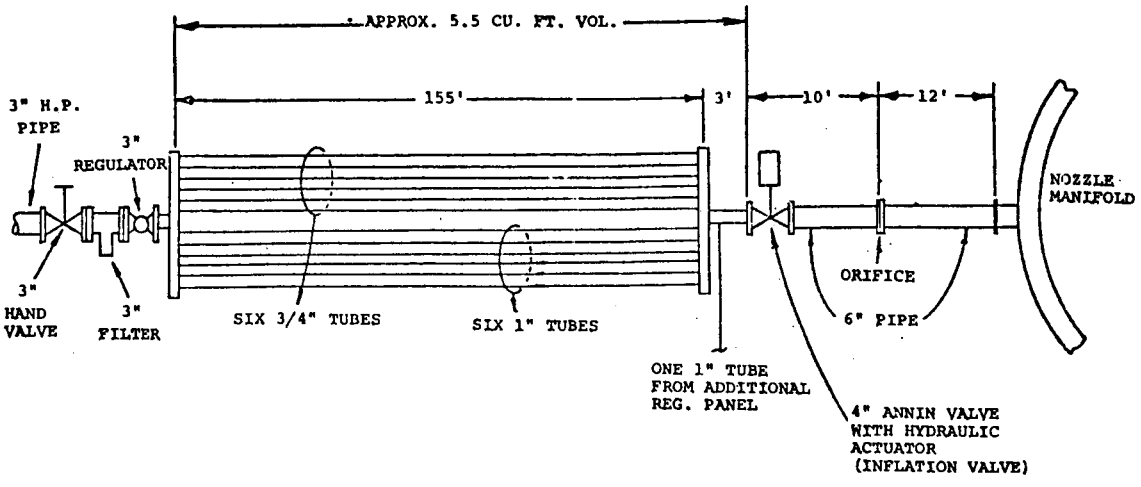

Figure 58. Piping Schematic for Extendible Nozzle Tests

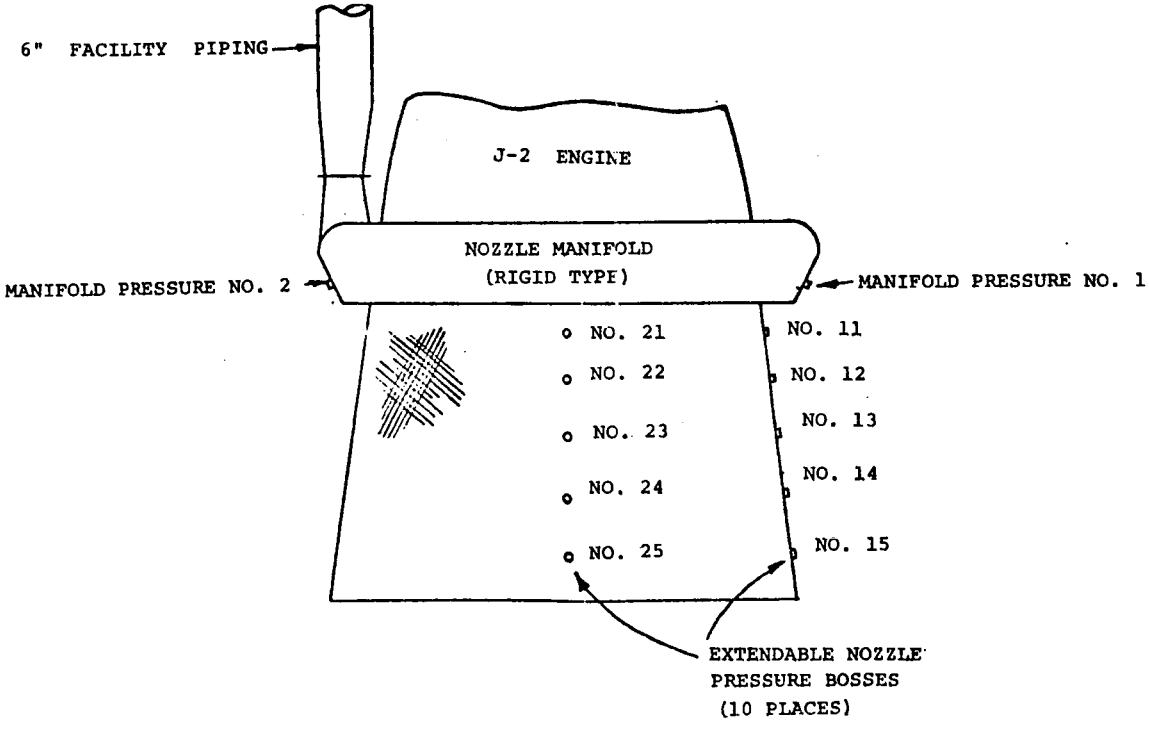

Figure 59. Instrumentation Locations for Extendible Nozzle Tests

The last four tests were conducted by opening the nozzle extension inflation valve prior to starting the flow. The flow was then adjusted to a predetermined value.

4. Test Data

The flow and pressure data for the six tests are summarized in Table XX. The highest pressures obtained during the tests are tabulated.

During the flow tests the dimensional shape of the nozzle extension was visually inspected. It was concluded that when pressurized the nozzle extension had a true conical shape.

During the tests the diameter of the nozzle extension exit plane was measured at four locations each 45° apart. The measurements were accurate to approximately plus or minus one-half inch. The first and third measurement was one inch different from the second and fourth measurement. It was concluded that the nozzle extension at its exit was round.

Table XX. Extendible Nozzle Flow Test Data
Steady State Conditions

Ambient Pressure 14.37 PSI

Test No. *	Flow	Manifold Pressures (PSIG)	Nozzle Pressures (PSIG)										
	lbs/sec	No. 1	No. 2	No. 11	No. 12	No. 13	No. 14	No. 15	No. 21	No. 22	No. 23	No. 24	No. 25
EN06	16.8	0.57	0.80	0.88	0.69	0.60	0.56	0.57	0.52	-	0.52	0.46	0.45
EN07	26.0	0.99	1.00	1.62	1.25	1.00	0.99	1.00	0.83	0.85	0.80	0.75	0.72
EN08	24.5	2.50	2.63	-	0.95	0.90	0.90	1.06	-	1.05	1.00	0.98	0.90
EN11	28.5	3.00	3.13	1.20	1.19	1.13	1.00	1.25	-	1.19	1.25	1.13	1.08
EN12	38.0	4.40	4.75	1.75	1.56	-	1.38	1.75	-	1.69	1.90	1.75	1.53
EN13	46.0	5.50	6.25	2.25	2.00	2.25	1.88	2.25	-	2.18	2.43	2.25	2.00

*Peak values given to show maximum pressure obtained in nozzle during flow

5. Test Analysis

The individual readings of the Airmat internal pressure was averaged for each test. The flow rates were converted from pounds per second to pounds per second per square foot of surface area. The surface area of the nozzle extension was 94.8 square feet.

The unit flow and the average pressure readings were plotted on Figure 60. This figure contains a plot of calculations of unit flow versus Airmat pressure for different porosity values for nitrogen gas and with a backup pressure of one atmosphere.

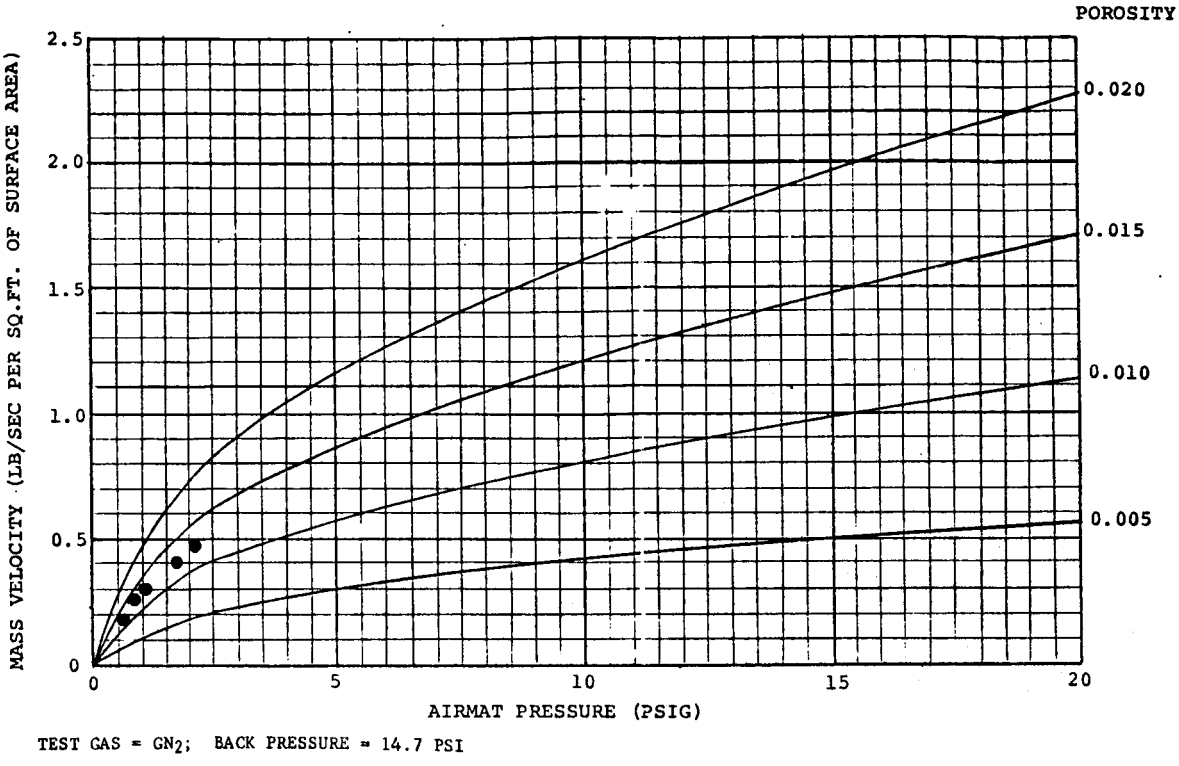

Figure 60. Mass Velocity vs Airmat Pressure - Extendable Nozzle Flow Tests

Figure 60 plots show that the porosity obtained was approximately 1.2 percent which correlates with porosity data obtained from laboratory tests during the development efforts.

It is noted that the flow rates used in the flow testing produced Airmat pressures up to 2.2 psi. This is considerably less than the Airmat operating pressures of 7 to 10 psi. The capacity of the test setup was however limited to a flow of 46 pounds per second. This flow rate produced the 2.2 Airmat pressure. This gas supply would have produced higher Airmat pressures under space environment operation.

6. Replacement of the Fabric Manifold

During the second test the fabric manifold failed in its fabric area. This manifold was replaced with a rigid manifold for the remaining tests. The replacement manifold had been designed and fabricated during the J-2X program which is summarized in Reference 1. The manifold was originally designed and fabricated by the North American Rockwell Corporation, Rocketdyne Division. Modification of this manifold to match the J-2 nozzle extension design was performed by NASA.

The failure of the non-rigid manifold occurred in the fabric area and the failure was extensive. The failure apparently was initiated in the area

where the fabric is cutout and attached to the manifold inlet fitting. After the manifold was originally fabricated it was determined that the manifold inlet fitting was too small. A larger inlet fitting was subsequently designed fabricated, and installed. This required rework of the fabric in this area. As the fabric was already coated with a silicone elastomer, it could not be resistance welded to the inlet fitting. Thus, a clamping arrangement was used to attach the fabric to the fitting for the rework.

It was concluded that three different reasons or combinations of these reasons caused the manifold failure.

(1) The clamping attachment of the fabric to the fitting may not have been as reliable as a welded attachment.

(2) The fabric may have been damaged during the installation of the larger inlet fitting.

(3) The fabric used was a commercial stainless steel cloth material which has a low tear strength.

It is recommended that in any future non-rigid manifold design that commercial stainless steel fabric not be used because of its low tear strength. A stainless steel fabric similar to textile rip-stop fabrics could be developed or a stainless steel fabric could be woven using multi-filament yarns similar to the face cloths of the Airmat woven for the nozzle extensions. These materials would have a higher tear strength.

C. DEPLOYMENT TESTS

1. Introduction

The objectives of the deployment tests were to evaluate the ability of the nozzle extension to deploy from a packaged condition and to evaluate the deployment gas pressure, flow rate, and inflation time, that would produce the optimum deployment characteristics.

2. Test Setup

The Number 2, ϵ = 48 to 1, nozzle extension was mounted on a J-2 nozzle at the NASA test facility. The rigid manifold was utilized for all of the deployment tests. The piping schematic was the same as used for the cold flow tests. See Figure 58.

The location of the pressure tap instrumentation for the manifold was the same as used for the flow tests (see Figure 59). Pressure taps were not used on the nozzle extension during the deployment tests.

3. Test Procedures

The nozzle extension was packaged by rolling up the Airmat material starting at the exit end and restraining it in place around the engine exit with adhesive tape. While the restraining method was not considered to be a desirable flight design, it was an expedient approach which if successful, would serve as a worst case guide for future restraining technique designs.

A total of eleven deployment tests were conducted. During the first six tests, EN15-1, EN15-2, EN15-3, EN17-1, EN17-2 and EN17-3, a predetermined pressure was set upstream of the inflation valve and then the inflation valve was opened to deploy the nozzle. Different valve opening times were used to evaluate the optimum deployment procedure.

During the last five tests EN20, EN21, EN22, EN23, and EN24, the inflation valve was opened as fast as possible. Only the amount of gas stored between the pressure regulator and the inflation valve was used to deploy the nozzle extension. The volume of this gas was approximately 5.5 cubic feet (see Figure 58).

4. Test Data

The test data recorded during the deployment tests are presented in Table XXI.

Table XXI. Extendable Nozzle Deployment Test Data

Test No.	Pressure	Valve Opening		Flow		Manifold Pressure #1		Manifold Pressure #2	
		Max %	Time	Max	Time	Max	Time	Max	Time
EN15-1	385	100	7.0	7.6	21.0	0.4	21.0	0.6	21.0
EN15-2	735	100	5.0	19.0	9.5	1.3	10.0	1.5	10.0
EN15-3	1225	100	4.2	34.0	5.5	3.3	5.5	3.8	5.5
EN17-1	770	100	3.0	20.0	2.0	1.5	2.0	1.7	2.0
EN17-2	1245	100	3.0	33.0	2.0	3.3	2.5	3.7	2.5
EN17-3	1590	100	2.5	46.0	1.5	5.0	1.5	6.0	1.7
EN20	1514	100	1.0	43.0	0.9	5.8	0.85	6.8	0.80
EN21	1601	100	1.25	46.0	0.9	6.2	0.88	7.3	0.90
EN22	1575	100	1.0	45.0	0.92	6.0	0.75	7.0	0.75
EN23	1540	100	1.25	44.0	0.90	5.8	0.88	6.8	0.80
EN24	1523	100	1.0	44.5	0.85	6.0	0.80	6.9	0.85

Time = seconds Pressure = psig Flow = lbs/sec

5. Test Analysis

The nozzle extension deployed satisfactorily from a rolled-up position. Photographs of the deployment sequence are presented in Figure 61. Figure 61 View A shows the nozzle extension in the rolled-up position and restrained with adhesive tape. Figure 61, Views B, C and D show the nozzle extension at several stages in deployment. Figure 61, View E shows the nozzle extension fully deployed and pressurized.

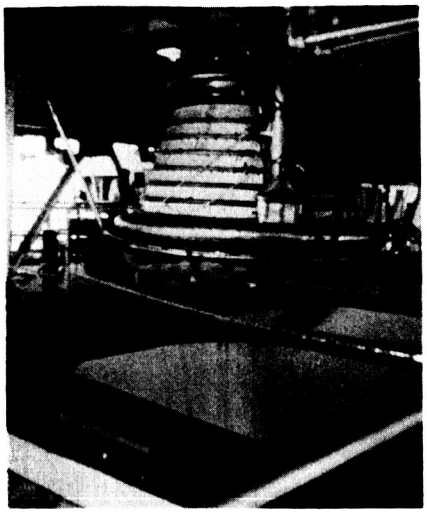

A. ROLLED-UP AND RESTRAINED POSITION

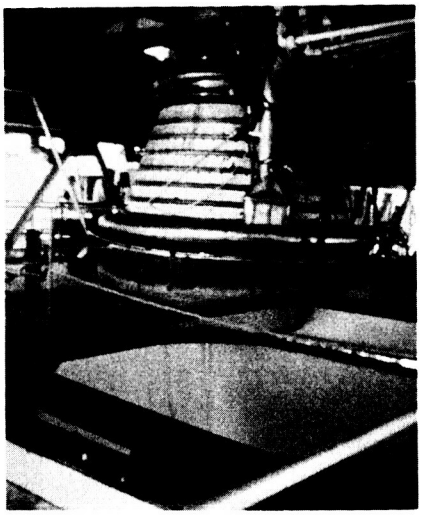

B. DEPLOYMENT SEQUENCE NO. 1

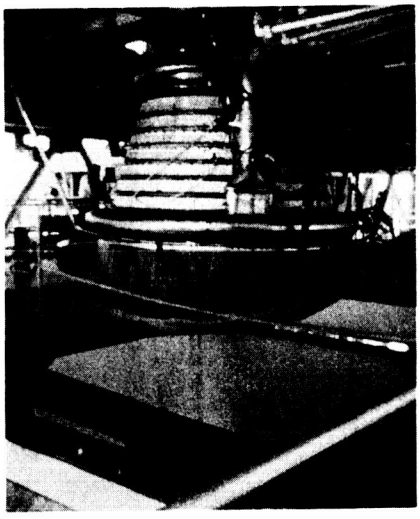

C. DEPLOYMENT SEQUENCE NO. 2

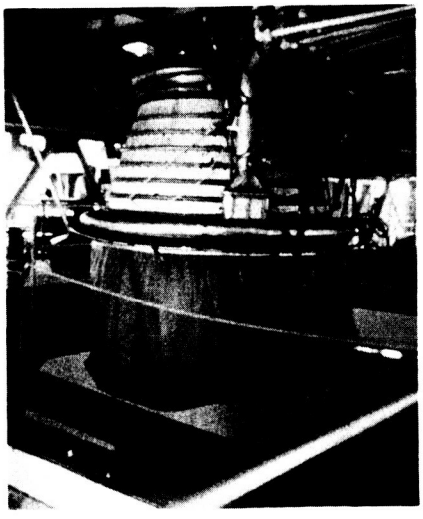

D. DEPLOYMENT SEQUENCE NO. 3

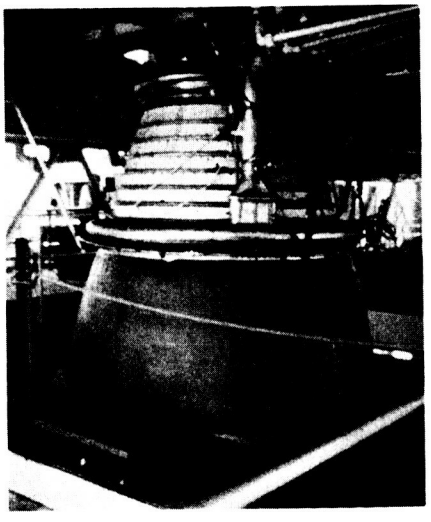

E. FULLY DEPLOYED AND PRESSURIZED

Figure 61. Nozzle Extension Deployment Test

Test Number EN17-3 was considered to have exhibited the most even deployment characteristics. Irregularities were observed in several deployments where the initial downward movement was not evenly distributed around the entire 360° of the packaged nozzle extension. This was definitely attributed to the inconsistency of the adhesive tape restraining method and a more sophisticated restraining technique should eliminate any irregular deployment.

Even with the non-optimum restraining methods utilized, there was never a case of incomplete deployment. In all cases the nozzle deployed and achieved a fully pressurized shape in less than three seconds.

SECTION X

CONCLUSIONS

The objectives of this program were several. However, the major one was to prove the feasibility of fabricating full-scale nozzle extensions for improving the altitude performance of rocket engines. These extensions had as their major requirements:

(1) The extension structure to be Airmat woven from stainless steel multifilament yarn.

(2) The rocket engine exhaust gas side or face of the Airmat extension to be transpiration cooled using the pump drive turbine exhaust gas as the coolant.

(3) The extensions to be packageable and deploy automatically upon pressurization.

(4) To demonstrate through thermal analysis and subsequent testing that the performance of the nozzle extensions is predictable.

The effort completed on the program has established the feasibility of these objectives and all design goals have been met.

The results of the extendable nozzle concept investigation allows the following additional conclusions to be drawn:

(1) The Phase I preliminary design and analysis effort established the feasibility of J-2S rocket engine nozzle extension having an expansion ratio of 40 to 1 at the forward end and 80 to 1 at the exit. The J-2S coolant gas supply flow rate availability of 9 pounds per second was sufficient for the nozzle extension operation. The weaving investigation performed established that the Airmat face porosity of one percent or less could be achieved.

(2) By sub-scale testing on an oxygen-hydrogen rocket engine, the feasibility of the nozzle extension transpiration cooling concept was proven. These test results also proved the validity of the thermal and flow analysis methods and that extension performance could be predicted.

(3) The objectives of the contract were further expanded by the Phase II Program. Modification of the loom to weave conical Airmat was accomplished. This effort resulted in the following conclusions:

(a) Conical Airmat can be woven. The ability to weave conical Airmat in sufficient length to form a conical nozzle from one-piece of Airmat was demonstrated.

(b) The dimensional control achieved in conical Airmat weaving was good; however, closer control is desirable for very long Airmat panels. This close control could be achieved by the use of a loom designed for the specific purpose.

(c) The conical Airmat was woven to a one percent porosity. To obtain lower porosities, additional loom modifications and experimental weaving would be required.

(d) The width of the loom limits the length of the nozzle extensions. The greater the expansion ratio, the longer the length of the extension and therefore the wider the loom that would be required.

(4) Additional testing was accomplished in the Phase II program which further proved the validity of the assumptions made in the performance of the thermal analysis. By tests conducted, a satisfactory sealing coating was selected.

(5) An investigation of a deployment gas generator was conducted. This investigation showed that after development, deployment gas generators could be procured for relatively low cost.

(6) A cold flow test on a J-2 nozzle extension with an expansion ratio of 48 to 1 was successfully accomplished. Airmat porosity values calculated from test data showed that the porosity was in the 1.2 percent range.

(7) Deployment tests were conducted on the same J-2 nozzle extension. The nozzle deployed successfully from a rolled-up position.

REFERENCES

1. Goodyear Engineering Report GER-13641, Inflatable Transpiration Cooled Nozzle - Final Summary Report, 22 January 1968.

2. Goodyear Aerospace Proposal GAP 4972, Proposal for Investigation of Extendable Nozzle Concepts, 22 May 1968.

3. Friedman, J.: "A Theoretical and Experimental Investigation of Rocket Motor Sweat Cooling," ARS Journal, No. 79, pp 147-154, 1949.

4. Bartle, E. R. and Leadon, B. M.: "The Effectiveness as a Universal Measure of Mass Transfer Cooling for a Turbulent Boundry Layer," Proceedings of the 1962 Heat Transfer and Fluid Mechanics Institute, pp 27-41.

5. Bartz, D. R., "A Simple Equation for Rapid Estimation of Rocket Nozzle Convective Heat Transfer Coefficients," Jet Propulsion, January 1947.

6. NASA SP-3011, Thermodynamic and Transport Properties for the Hydrogen-Oxygen System, R. A. Suehla, 1964.

7. Goodyear Engineering Report GER-15203 - Investigation of Extendable Nozzle Concepts, Coating Investigation, Task b, February 1971.

8. Goodyear Engineering Report, GER-14913, Investigation of Extendable Nozzle Concepts, Design Refinement Investigation, Task c, July 1970.

9. Goodyear Engineering Report, GER-15306, Investigation of Extendable Nozzle Concepts, Heat Transfer Investigation, Task d, March 1971.

10. Goodyear Engineering Report, GER-14879, Investigation of Extendable Nozzle Concepts, Deployment Gas Generator Investigation, Task g, May 1970.